

**Emplacement Mechanisms and Magmatic
Differentiation Induced by Magma Flow in Sill
Intrusions in Sedimentary Basins**

Christophe Galerne



**Dissertation for the degree of Doctor Scientiarum
Physics of Geological Processes
Faculty of Mathematics and Natural Sciences
University of Oslo
January 2009**

© **Christophe Galerne, 2009**

*Series of dissertations submitted to the
Faculty of Mathematics and Natural Sciences, University of Oslo
Nr. 853*

ISSN 1501-7710

All rights reserved. No part of this publication may be reproduced or transmitted, in any form or by any means, without permission.

Cover: Inger Sandved Anfinsen.
Printed in Norway: AiT e-dit AS, Oslo, 2009.

Produced in co-operation with Unipub AS.
The thesis is produced by Unipub AS merely in connection with the thesis defence. Kindly direct all inquiries regarding the thesis to the copyright holder or the unit which grants the doctorate.

*Unipub AS is owned by
The University Foundation for Student Life (SiO)*

Acknowledgements

The work presented in this thesis was carried out at Physics of Geological Processes (Department of Physics), University of Oslo from 2004 through 2008. The research was financially support by the Norwegian Research Council (NFR) through the project 159824/V30 “Emplacement mechanisms and magma flow in sheet intrusions in sedimentary basins”. This study was also supported by a Centre of Excellence grant from the Norwegian Research Council to PGP.

I am indebted to my principal supervisor Professor Else-Ragnhild Neumann for her guidance and teaching that I received in my studies. I am equally grateful to my second supervisor Sverre Planke for assistance and help I received. To both, thank you for the encouragement that helped me to bring this work to completion and make this Ph.D possible.

I am also grateful to all the people involved in the project including Anders Malthe-Sørenssen and the project collaborators that helped to initiate this project. Thanks are due also to Henrik Svensen, Julian Marsh and Luc Chevallier for their introductions to the field work and the project problematic. I also thank my collaborators in the field that helped me to accomplish the early stage of this work.

This project would not have been complete in this way without the insight and directions from Yuri Podladchikov, who I thank for his patient teaching and collaboration. I would like to thank all the PGP’ans of Yuri’s courses that supported me and Evgeni Tantserev through the suffering of learning thermodynamics and geomodelling.

Special thanks go to Olivier Galland, Timm John and Magali Rossi for their concerns and help to keep me in the right direction. Also I would like to thank Nina Simon for her moral support, that also goes equally to Olivier, Timm and Magali.

To my flat- and office-mates, and to those with whom friendships started at PGP, thank you. Also to all my friends back in France, thank you for your moral support and your infallible friendship.

Finally, I would like to thank my family for their constant support. For all you gave to me and the love that is in this family, to understand me and believing in me, Merci.

Oslo, June 2008

Christophe Galerne

Scientific advisers:

Prof. Else-Ragnild Neumann

Dr. Sverre Planke

Prof. Anders Malthe Sørensen

List of Scientific Manuscripts

- I. **Galerne, C.Y.**, Neumann, E.R. and Planke, S., 2008. Emplacement mechanisms of sill complexes: Information from the geochemical architecture of the Golden Valley Sill Complex, South Africa. *Journal of Volcanology and Geothermal Research*, 177(2): 425-440.

- II. **Galerne, C.Y.**, Galland, O., Neumann, E.R. and Planke, S., 2008. The shapes of the feeders control the 3D shapes of sills. *Terra Nova*. (in review).

- III. **Galerne, C.Y.**, Neumann, E.R., Aarnes, I., Planke, S., 2008. Magmatic Differentiation Processes in Saucer-Shaped Sills: Evidence from the Golden Valley Sill in the Karoo Basin, South Africa. *Geosphere, Special issue LASI III Conference*. (in review).

Contents

Acknowledgements	i
List of Scientific Manuscripts	iii
Contents	v
1. General Introduction.....	1
2. Geological setting.....	6
2.1. The Karoo Basin.....	6
2.2. The volcanic basin of the Karoo.....	7
2.3. Sill Complex and saucer-shaped sills: example of the Golden Valley Sill Complex....	11
3. Emplacement mechanisms	14
3.1. The laterally-fed sills model.....	15
3.1.1. Model a: Francis (1982)	15
3.1.2. Model b: Chevallier and Woodford (1999)	15
3.2. The centrally-fed sills model.....	16
3.2.1 Model c: Malthe-Sørenssen et al. (2004).....	16
3.2.2. The nested sill complex model.....	16
3.3. The geochemical test on emplacement mechanisms of sill complexes in sedimentary basins	17
3.4. Case study: the Golden Valley Sill Complex	19
4. Differentiation of tholeiitic magma	21
4.1. Physics of magmatic differentiation in tholeiitic magma.....	21
4.2. The concept of melt fractionation inducing magma differentiation in tholeiitic sills ...	22
4.2.1. Thermal stresses related to melt fractionation.....	22
4.2.2. Buoyancy related melt fractionation	23
5. On the quantification and validity of post-emplacement melt flow differentiation	24
6. Authorship statement.....	26
7. References	28
8. Papers	35
Paper I: Emplacement mechanisms of sill complexes: Information from the geochemical architecture of the Golden Valley Sill Complex, South Africa.....	37
Paper II: The shapes of feeders control the 3D shapes of sills.....	55
Paper III: Magmatic Differentiation Processes in Saucer-Shaped Sills: Evidence from the Golden Valley Sill in the Karoo Basin, South Africa	69
Appendix	127
Appendix A: Sampling locations.....	129
Appendix B. Complementary data Table 2; Galerne et al. (2008).	133

1. General Introduction

Large Igneous Provinces (LIPs) are continental scale eruptions of mafic magma that occur intermittently on the Earth. Despite the discussion on the LIP definition (Sheth, 2007) numbers of common properties of the LIPs are envisaged: rapid eruption (< 5 Ma), high rate ($0.1 - > 1 \text{ km}^3/\text{yr}$) and large voluminous ($\sim 10^6 \text{ km}^3$; Bryan and Ernst, 2008). The occurrence of picrite magmas amongst the volcanics (e.g., Sweeney et al., 1991) indicates high temperature anomalies. Most of the on-land LIPs named Continental Flood basalts (CFBs) are on or near a boundary involving a thick Achaean lithosphere (Anderson, 1995). Finally, their geochemical signatures often show negative Nb-Ta anomalies and strongly positive Pb anomalies which indicate a significant interaction of the melt with the lithospheric mantle (or crust) containing a significant arc or backarc component (Puffer, 2001). These studies give insight into the generation of melts and are important to understanding their geodynamic significance.

The volcanic basins associated with LIPs commonly present sill complexes dominated by saucer-shaped sills (Fig. 1). They have been found in the Vøring and Møre basins offshore Norway, in the Karoo Basin in South Africa, in the Parana Basin in Brazil and on the NW Australian shelf (Symonds et al., 1998; Chevallier and Woodford, 1999; Svensen and Planke, 2003). The saucers and dykes forming sill complexes occur through the whole stratigraphy of these volcanic basins. Although saucer-shaped sills are common, little is known about the processes related to their emplacement mechanisms: 1) what is the relationship between saucer-shaped sills and their feeders? Are saucer-shaped sills feeding each other or are they fed by vertical dykes or by narrow channels? 2) Is there a specific mechanism of magmatic differentiation associated with their shallow emplacement? These are the topics addressed in the present thesis.

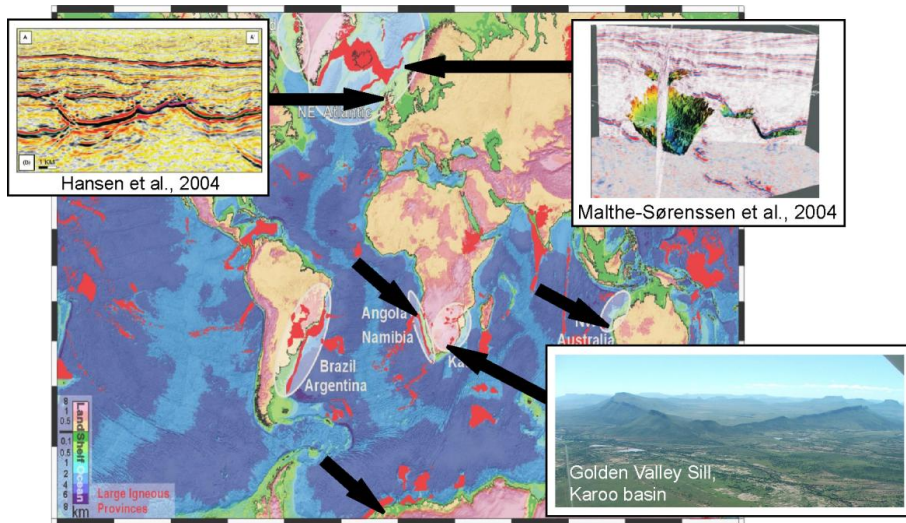


Figure 1: Worldwide distribution of saucer-shaped sills in sedimentary basins. The black arrows indicate occurrences of saucer-shaped sills and sill complexes. These sill complexes represent the intrusive or plumbing system associated with Large Igneous Provinces marked in red (Coffin and Eldholm, 1994; see LIPs definitions therein). Examples inserted from the Vøring offshore mid-Norway (Malthe-Sørenssen et al., 2004), and British island inferred from seismic images (Hansen et al., 2004a) and from the Karoo Basin, South Africa (Galerne et al., 2008).

The worldwide occurrence of saucer-shaped sills in volcanic basins suggests that they represent a fundamental way for the magma to intrude in the shallow crust. Yet the mechanisms governing their emplacement are still not clear. This comes partly from the fact that the relationships between sills and their feeders are rarely exposed (Hyndman and Alt, 1987) and are difficult to image on the basis of seismic data (Hansen et al., 2004b; Thomson and Hutton, 2004). Also, the feeding relationships between various structures in sill complexes are poorly constrained. However, the relationship between sills and their feeders are essential factors in existing models of sill emplacement. For example, some models propose that saucer-shaped sills intrude along the level of neutral buoyancy of the magma (e.g., Bradley, 1965; Francis, 1982; Chevallier and Woodford, 1999). In such models, saucer-shaped sills are fed laterally and the magma is expected to flow downward and from one side of the sill to the other. Other models propose that saucer-shaped sills are fed from a central feeder, and the magma flows radially outward and upward (Pollard and Johnson, 1973; Hansen et al., 2004b; Malthe-Sørenssen et al., 2004; Thomson and Hutton, 2004; Hansen and Cartwright, 2006; Galerne et al., 2008; Polteau et al., 2008; Galland et al., 2009; Polteau et al., submitted).

Additionally, the magmatic differentiation processes related to sills and saucer-shaped sills are unclear. Most recurrent geochemical profiles observed in these relatively thin sills (~100 m thick) are I-, D- and S-shaped profiles (Fig. 2; e.g., Gibb and Henderson, 1992; Latypov, 2003a; Latypov, 2003b). The nomenclature is based on the variations in the whole-rock $Mg\#$ (cation ratio $100 * Mg/[Mg + Fe^{total}]$) from floor to roof of the sills. This variable is used as a differentiation index because magnesium is more easily partitioned into early-fractionated minerals such as olivine and pyroxene than iron. I-shapes indicate uniform composition throughout the sill height and are usually explained by a uniform closed crystallizing system (Mangan and Marsh, 1992; Marsh, 1996). D-shapes are characterized by the least differentiated composition at the sill centre (i.e., highest $Mg\#$) and the most evolved composition at the sill margins (i.e., lowest $Mg\#$). Finally, S-shapes are hybrid shapes, with D-shapes in the lower part of the sill and C-shapes in the upper part (Gray and Crain, 1969; Fujii, 1974; Frenkel et al., 1988; Frenkel et al., 1989; Marsh, 1989). All intermediate types from these end-member types of shapes may be found.

I-shaped compositional profiles can be readily explained by uniform closed system crystallization or quenching (Mangan and Marsh, 1992; Marsh, 1996). In contrast, there is a wide range of processes that can explain the formation of D- and S-shaped profiles. Examples range from multiple or prolonged continuous magma influxes (S-shaped: Gorrying and Naslund, 1995), convective flux of refractory component within the crystal-liquid mush of the boundary layer during *in-situ* differentiation or compositional convection (S-shaped: Tait and Jaupart, 1996), and settling (S-shaped: Frenkel et al., 1989). Soret fractionation (Latypov, 2003a; Latypov, 2003b; Latypov et al., 2007) was recently proposed to explain the origin of the often observed marginal reversals in layered intrusions. This model was combined with the *in-situ* crystallization in thermal boundary layers of Tait and Jaupart (1996). Gravity-induced settling of crystals present in the magma at the time of the emplacement (Gray and Crain, 1969; Fujii, 1974; Marsh, 1989) and/or newly *in situ* grown minerals (Frenkel et al., 1988; Frenkel et al., 1989). An additional process is slow interdendritic flow, driven by shrinkage, geometry, solid deformation or gravity, summarizing the current understanding of macrosegregation (i.e., positive and negative) that causes differentiation within the liquid-solid zone in casting and ingots (Flemings, 2000).

A major problem with the D- and S-shaped profiles is that they fail to be explained by early stages of crystallization and mineral segregation through mechanisms such as convection and/or gravitational separation, resulting in fractional crystallization. Hence, D-

shaped profiles are inverse to what is expected of a cooling magma. Large layered mafic intrusions have typically mafic margins and felsic cores forming C-shaped geochemical profiles (e.g., Skaergaard intrusion, Wager and Brown, 1968; Naslund, 1984). Such C-shaped profiles can be called “normal zoning,” which is interpreted as the result of in situ processes of fractional crystallization involving convective fractionation (Rice, 1981). The lack of C-shaped profiles in relatively thin sills is significant, suggesting that processes occurring in large magmatic bodies are different from those in thin, i.e., 30 to 140 m thick, sills.

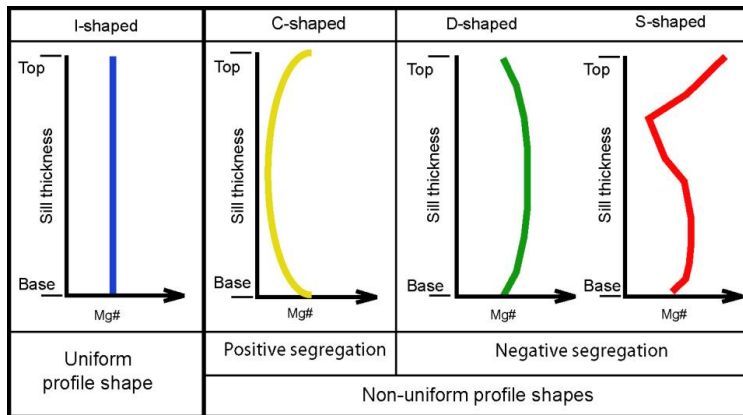


Figure 2: Characteristic shapes of compositional profiles defined on the basis of Mg# (differentiation index, $Mg\# = \text{molar } 100 \times \text{Mg}/[\text{Mg} + \text{Fe}_{\text{total}}]$) variations along vertical sections across igneous intrusives. The I-shaped profile is a uniform profile showing no chemical variation across the sill thickness. Non-uniform compositional profiles pattern in relatively thin sheet intrusions (100 m thick, e.g., Golden Valley Sill Complex) are characterized by D-and S-shaped compositional profiles also qualified as reversed or inverse segregation. C-shaped compositional profiles are characteristics of large magmatic plutons also qualified as positive (i.e., expected) segregation.

In order to tackle both emplacement mechanisms and magmatic differentiation in ~100 meter thick sills we carried out detailed field and geochemical investigations on a well exposed sill complex, the Golden Valley Sill Complex in the Karoo Basin, South Africa. The primary aim of my study was to characterize the geochemical architecture of a well exposed sill complex, in order to improve our understanding of sill complex emplacement. The exceptionally good exposure of the Golden Valley Sill Complex (Karoo Basin, South Africa) allowed us to produce a detailed geological map of the major sills and dykes, and to get an extensive and fairly uniform sample coverage. The chemical similarities and differences between the different units (sills and dykes) in the complex were compared by statistical analysis. Our results allowed us to construct a 3-D model of

the geochemical architecture of the Golden Valley Sill Complex and to draw conclusions with respect to the emplacement processes. This work is the object of the first paper listed in the thesis entitled “*Emplacement mechanisms of sill complexes: Information from the geochemical architecture of the Golden Valley Sill Complex, South Africa*” which is introduced throughout Chapters 2 and 3. Additional constraints and results from the first paper are discussed in a combined investigation with experimental modelling presented in *Paper II* entitled “*The shapes of the feeders control the 3D shapes of sills*”. Finally, the differentiation processes in ~100 meter thick sills is the object of *Paper III* which is introduced in chapter 4 and is entitled “*Magmatic Differentiation Processes in Saucer-Shaped Sills: Evidence from the Golden Valley Sill in the Karoo Basin, South Africa*”. In this paper we concentrate on compositional profiles from a single saucer-shaped sill: the Golden Valley Sill in the Golden Valley Sill Complex.

2. Geological setting

2.1. The Karoo Basin

The Karoo Basin covers 500,000 km² of southern Africa (Fig. 3a). It is the main sedimentary retroarc foreland basin to the Gondwanide (Cape) fold belt (Catuneanu et al., 1998; Catuneanu et al., 2005). The orogenic event responsible for the Cape Fold Belt was the Late Paleozoic-Early Mesozoic subduction of the paleo-Pacific plate underneath the Gondwana plate (Fig. 3b; e.g., Lock, 1980; Riley et al., 2006). In a regional context, the Cape Fold Belt was part of a more extensive Pan Gondwanian Mobile Belt generated through compression, collision and terrain accretion along the southern margin of Gondwana (Catuneanu et al., 1998). The associated foreland basin subsequently fragmented as a result of orogenic unloading and the Gondwana break-up is preserved today in South America (Parana Basin), southern Africa (Karoo Basin), Antarctica (Beacon Basin) and Australia (Bowen Basin). The flexural basin of Karoo formed between 246 and 180 Ma (Catuneanu et al., 1998). The continental sediments are locally accumulated to over a 5000 meter thickness prior to the volcanic event.

The Karoo Basin hosts a vast intrusive network of dykes and sills, which are now exposed by uplift and erosion. The whole magmatic episode has been dated to the period from 185 to 174 Ma (Jourdan et al., 2007). The authors concluded that the Karoo magmatism “represents an atypical province” with a relatively long-lasting and comparatively low-emission rate of the overall magmatic activity as compared to other LIPs. Finally, the re-evaluation of major Phanerozoic CFBs shows that for most of them, including the Karoo, the onset of oceanization shortly follows or is coeval with the latest CFB-related activity, indicating a closer relationship than previously thought (Jourdan et al., 2007).

Two main tectonic regimes prevailed during the magmatic emplacement of sills in the Karoo Basin. The earliest activity is the main Karoo magmatism pulse (185-177 Ma, Jourdan et al., 2007) and consists of the emplacement of basaltic intrusives and extrusives rocks (Marsh and Eales, 1984). This episode was essentially concentrated in the main Karoo basin. The stress regime during this episode appears to have been neutral. This

interpretation was motivated by the presence of large volumes of sill and sheets that appeared to be saucer-shaped sills that commonly have circular geometry. The basaltic rocks in the main Karoo Basin are strikingly uniform in composition and contrast with the further described bimodal suite of the Lebombo (e.g., Eales and Marsh, 1984).

The second tectonic regime is an episode of lithospheric thinning/rifting (Sweeney et al., 1994) that overlaps with the end of earliest activity (~179 Ma, Jourdan et al., 2007). It occurred along pre-existing lithospheric weakness and controlled the formations of radiating dyke swarms: the Lebombo dyke swarm, the Save Limpopo dyke swarm and the Okavango dyke swarm (Jourdan et al., 2006). This tectonic regime is associated with emplacement of diverse magmas, dominated by tholeiitic basalts and picrites of different compositions (Sweeney et al., 1991), but including minor nephelinites as well as large volumes of high-temperature anhydrous rhyolites and rhyodacites, in a bimodal suite. Along the Lebombo and Save monoclines the volcanic sequence dips eastward below younger sedimentary sequences underlying the coastal plain of Mozambique.

2.2. The volcanic basin of the Karoo

The Karoo igneous province in the main Karoo Basin is expressed through the emplacement of intrusive and extrusive rocks (Fig. 3a). The great network of sill complexes in the Karoo Basin appears to be dominantly constituted of sill intrusions over dykes (Fig. 4) that crop out through the entire Karoo sedimentary sequence (Figs. 3a-4a-b; e.g. Chevallier and Woodford, 1999; Svensen and Planke, 2003). Many sills form saucer-shaped sills (Fig. 4c). Some of the largest intrusive bodies which are more than 50 kilometres in diameter but are relatively thin (~50 meters) are emplaced in the lower part of the sedimentary sequence (Fig. 4a; Svensen and Planke, 2003). The most frequent exposures of saucer-shaped sills are observed in Beaufort Group where they form large sill complexes (e.g., Golden Valley Sill Complex). Although saucers in the shallow parts of the sedimentary sequence are smaller in size (i.e., 20 km in diameter for the Golden Valley Sill) than in deeper parts, they appear to be thicker (≥ 100 meters thick; Svensen and Planke, 2003). The saucer-shape disappears in the uppermost Clarens Formation underlying the Drakensberg Group mainly represented by the Lesotho remnant (Fig. 3a-4a). The dykes are relatively thin compared to the sills (2 to 15 m wide). The smallest

dykes are a tenth of a meter long, whereas a few of the widest dykes (15 meters) extend over 100 kilometres (Fig. 4d).

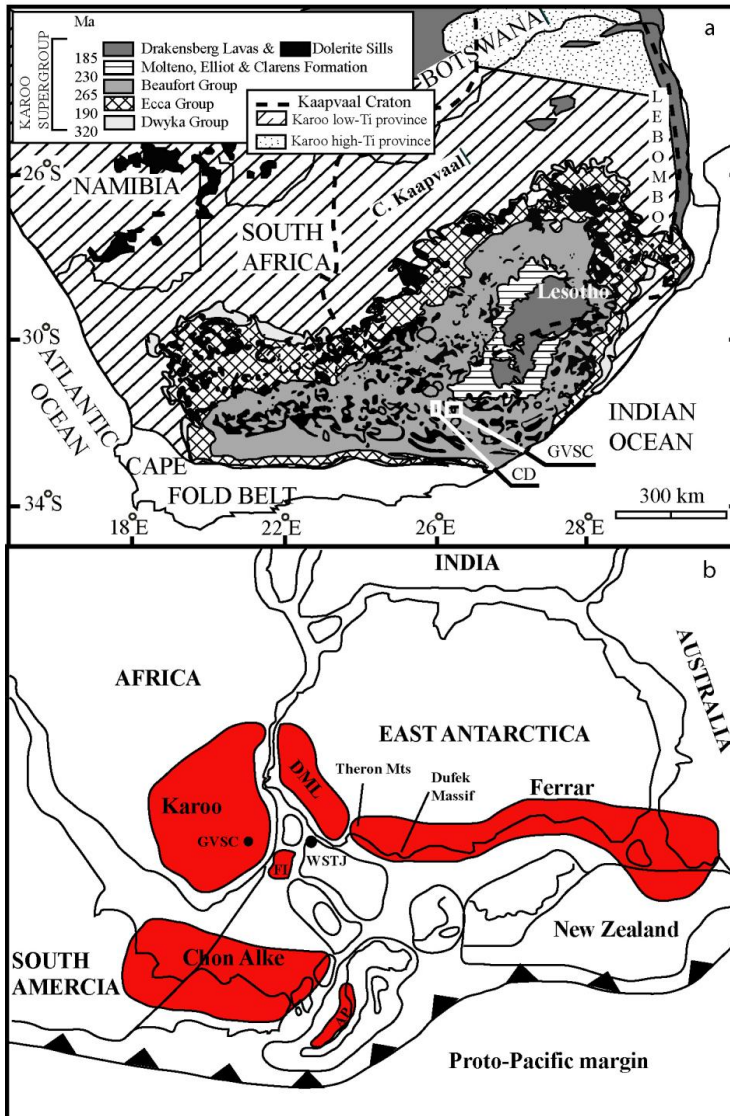


Figure 3: a. Map of the Jurassic Karoo flood basalt province in southern Africa showing the distribution of the dolerite sills (black), basaltic lavas (dark grey), and Karoo sediments (shades of grey) in the main Karoo Basin (modified after Ellam and Cox, 1991; Eglington and Armstrong, 2004; Jourdan et al., 2004). The flood basalts correspond to the uppermost stratigraphic sequences of the Karoo supergroup. The study areas, the Golden Valley Sill Complex (GVSC) and the Cradock Dyke (CD), south-west of Lesotho are indicated by white rectangles. The contour of the Kaapvaal Craton is marked by a thick dashed line. b. Pre-break-up Gondwana reconstruction (~180 Ma after, Riley et al., 2006) showing key igneous provinces of Karoo, Ferrar, and Chon Aike. FL, Falkland Islands; DML, Dronning Maud Land; WSTJ, Weddell Sea triple junction (Elliot and Fleming, 2004); AP, Antarctic Peninsula.

The Drakensberg Group represents the effusive counterpart of the Karoo intrusives. It is largely preserved in the Lesotho remnant (e.g., Marsh and Eales, 1984). Lavas of the Lesotho remnant cover 25,000 km² and are flows of mostly about ~100 meters thick (Cox and Hornung, 1966), forming a thick pile of >1.5 km flood basalts. Recent dating on the Golden Valley Sill Complex indicates a similar age, i.e., 182.7 ± 0.3 Ma (concordia age, Svensen et al., 2007) to the lavas of the Lesotho (e.g. Duncan et al., 1997). This result strongly suggests that the intrusives and the extrusives were emplaced simultaneously.

This main Karoo dolerites together with most of the lavas from the Drakensberg Group have been the focus of many studies, resulting in geochemical and petrological characterization of the Karoo igneous suite (e.g., Eales et al., 1984; Marsh and Eales, 1984; Marsh et al., 1997; Marsh and Mndaweni, 1998). Particularly in the special volume on the “Petrogenesis of the Volcanic Rock of the Karoo Province” (Erlank, 1984), it has been suggested, and later supported, that the mantle source rocks for the Central area must be chemically heterogeneous.

A typical chemical division into High-Ti and Low-Ti characterize the Karoo (Erlank, 1984). The High-Ti basalts dominantly occur north of line cutting NW across southern Africa from about Latitude 25°. The occurrence of both types in the Karoo igneous suite has lead several authors to consider a coeval occurrence of both types rising from two distinct sources (Sweeney et al., 1994). The Low-Ti, or “normal” basalts are tholeiitic and have low K, Ti, P, Ba Sr and Zr. The High-Ti type is referred to as “enriched” and has a relatively high concentration of Ti, K, P, and incompatible trace elements (Rb, Ba, Th, Nb, U, La, Ce, Zr, etc.). These differences could reflect different source materials, conditions of melting, or, alternatively, contamination by crustal components (Eales et al., 1984; Hawkesworth et al., 1984; Sweeney and Watkeys, 1990; Ellam and Cox, 1991; Sweeney et al., 1994; Jourdan, 2005; Riley et al., 2006).

Although both Low-Ti and High-Ti types are homogeneous, compositional differences exist. These allowed Marsh et al. (1997) to establish a comprehensive stratigraphic framework for the Drakensberg Group lavas based on differences in ratios between immobile highly-field-strength incompatible elements. Following Marsh et al. (1997), the Drakensberg Group has been geochemically subdivided into the older Barkley East Formation and the younger Lesotho Formation, each of which is subdivided into a series of units.

Karoo stratigraphy (Permian - Jurassic)

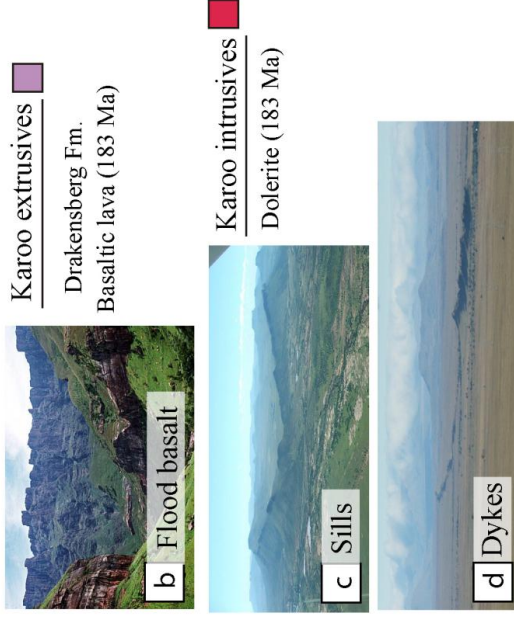
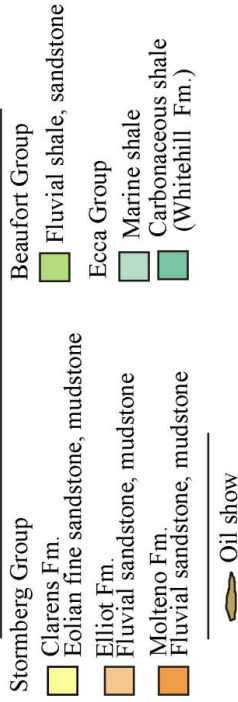


Figure 4: a. Schematic cross-section of the Karoo Basin showing the vertical and lateral distribution of the Karoo intrusives through the Karoo stratigraphy (Svensen and Planke, 2003). b. Photograph of the Karoo extrusives showing flood basalts sequences. c. Aerial photograph of the Golden Valley Sill showing typical saucer-shaped geometry. d. Photograph of ~100 kilometre long dykes.

Despite the voluminous literature currently available for the Karoo flood basalt lavas, surprisingly few geochemical studies have been done on the subvolcanic counterparts (Richardson, 1979; Marsh and Mndaweni, 1998). For instance, almost none of the existing literature presents the study of group of sills closely related into complex. This stands as a fundamental lack of knowledge as sill complexes such as dyke have the potential to be connected to the above flood basalts.

2.3. Sill Complex and saucer-shaped sills: example of the Golden Valley Sill Complex

Dykes are tabular, often vertical or steeply dipping sheets that cut across the structure (e.g., bedding) of the invaded rocks. Sills are tabular bodies concordant with the major structure (e.g., bedding or foliation) of the invaded rocks. A saucer-shaped sill consists of a near-horizontal tabular sill which continues outwards into transgressive sheets (average angle $<45^\circ$ with respect to the sedimentary layers). These cut through sedimentary layers, and finally ended in a flat outer sill following the original bedding of the invaded rocks. A group of sills and dykes which are closely associated in the field are termed a “sill complex.” Figure 5 presents a geological map of the main intrusives constituting the Golden Valley Sill Complex in South Africa and has all the characteristics of a sill complex.

The morphology of the Karoo sills varies with depth within the sedimentary sequence (Chevallier and Woodford, 1999). Large, flat sills are most common within the Dwyka and the Ecca groups in the lower part of the sedimentary sequence (Fig. 4a). Saucer-shaped sills (Fig. 5b) are most common and are thickest within the younger Beaufort Group (240-260 Ma, Svensen and Planke, 2003; Fig. 4a).

The Golden Valley Sill Complex, Karoo Basin, South Africa, consists of four major ~100 m thick elliptic saucer-shaped sills located SW of the Lesotho Plateau (Fig. 5a; Galerne et al., 2008; Aarnes et al., 2008; Galerne et al., in review). The saucers have been emplaced at two stratigraphic levels: the Morning Sun (MS) and Harmony Sill (HS) at the deeper level, and the Golden Valley Sill (GVS) and Glen Sill (GS) at a higher level (Galerne et al., 2008). The lower level saucers are larger than the higher level saucers (Fig. 5a). In addition, each sill at the higher level is located above a sill at the lower level, so that they appear to be stacked on top of each other (Fig. 5a). The saucers at the lower level have parallel long axes that trend NW-SE, whereas at the upper level the long axes trend roughly N-S. A minor saucer-shaped sill (MV Sill) is a direct continuation of the northwestern limb of GVS (Fig. 5a; Galerne et al.,

2008) and thus belongs to the upper level. In contrast to the major sills, the MV Sill is not elliptical. The Golden Valley Sill Complex area also includes the major Golden Valley Dyke (GVD) and four minor dykes (d1-d4 in Fig. 5a). The GVD is up to 15 m thick and 17 km long, d2 is ~5 m thick, and d1, d3, and d4 are only ~1 m thick. The dykes exhibit three main trends: NW-SE for GVD and d1, N-S for d4, and NE-SW for d2 and d3.

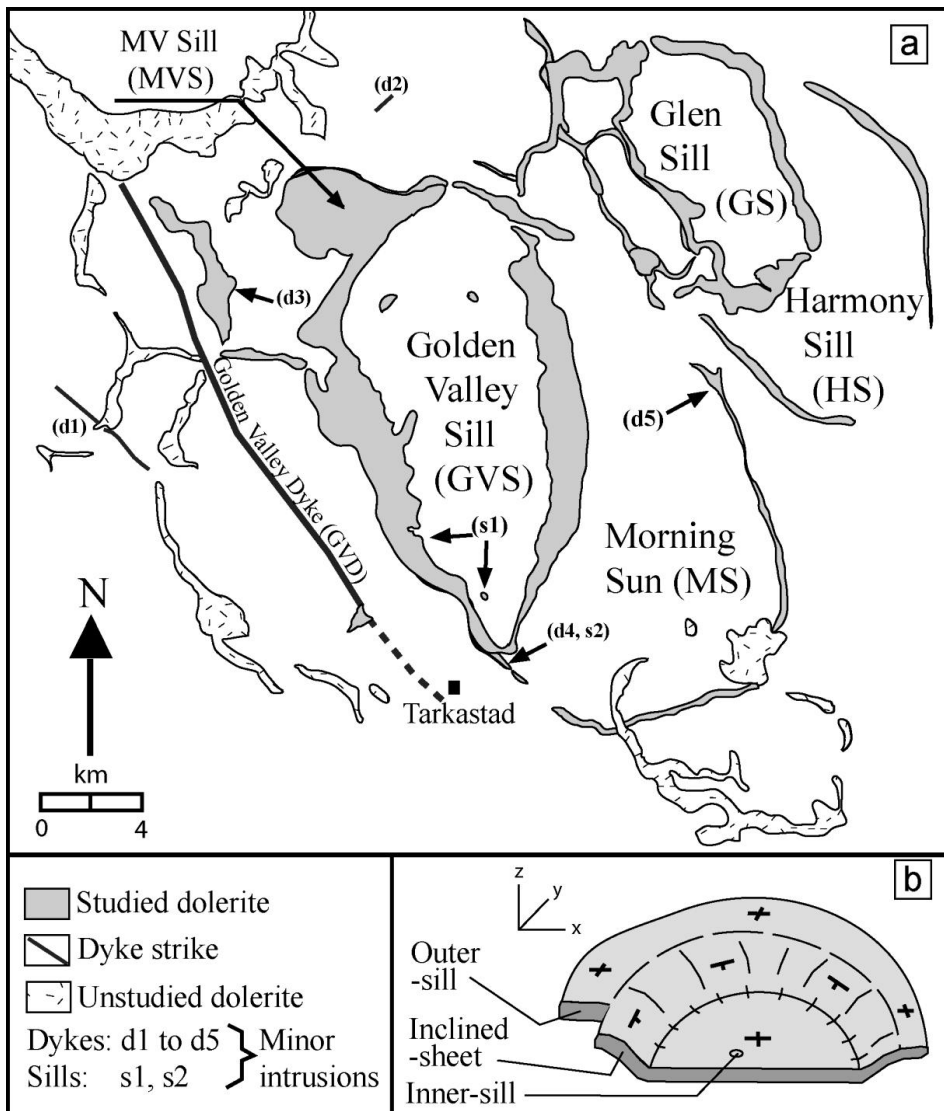


Figure 5: a. Simplified geological map of the Golden Valley Sill Complex (after Galerne et al., 2008). Five major saucer-shaped sills are included in this study (shown in grey): the Morning Sun (MS) and the Harmony Saucer (HS) at a lower stratigraphic level; the Golden Valley Sill (GVS) and the Glen Sill (GS), together with the small MV Sill (MVS) at a higher stratigraphic level. Also shown is a dyke,

the Golden Valley Dyke (GVD) within the Golden Valley Sill Complex area. The localities referred to as (s1, s2) and (d1 to d5) are minor sills and dykes, respectively. b. Morpho-structural diagram of typical saucer-shaped dolerite sill geometry, showing the inner sill, the inclined-sheet, and the outer sill.

In the Golden Valley Sill Complex we did not observe direct physical connections between the sills and the dykes. However, we noticed that the strikes of some of the dykes are parallel to the trends of the long axes of the large saucers (Galerie et al. in review): the GVD and d1 are parallel to the long axes of the sills at the deeper level (MS and HS), and d4 is parallel to the long axes of the higher sills (GVS and GS). Furthermore, the d4 dyke is exposed directly below the southern tip of the GVS (Galerie et al. in review).

3. Emplacement mechanisms

Several questions can be asked regarding the emplacement mechanism of sills, depending on the scale with which we are looking at them. Here we will review these questions and consider what geochemistry can bring into the discussion.

First, let us consider the sill complexes and their main structures, the saucer-shaped sills. Saucer-shaped sills on land, such as in the Karoo Basin, crop out forming single ridges or limb-like thick, inclined sheets. Their buried inner sills are rarely observed in these types of settings and are rarely even recognized (Du Toit, 1920), resulting in neglect of their full 3-D geometry as saucer-shapes (Fig. 5b). Recently, petroleum prospecting revealed that these structures were dominant and major structures of sill complexes. As evidence increased it was soon established that saucer-shaped sills are common in volcanic basins around the world (e.g., Symonds et al., 1998; Chevallier and Woodford, 1999; Svensen and Planke, 2003). This promoted interests in understanding the formation of sill complexes and saucer-shape sills. The Karoo Basin gives a unique access to very well exposed and preserved sill complexes, essentially formed by saucer-shaped sills. Thus, the Karoo Basin is an ideal field laboratory to study the mechanisms of formation and emplacement of sill complexes.

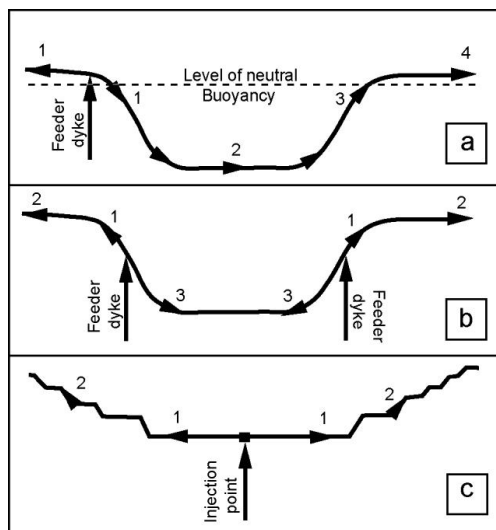


Figure 6: Sill emplacement models. a. Model after Francis (1982), explained in section 3.1.1. b. Model after Chevallier and Woodford (1999), explained in section 3.1.2. c. Model after Malthe-Sørenssen et al. (2004), explained in section 3.1.3. The numbers indicate the individual stages of development. Note that the magma flow geometries within the intrusion are different in the individual models.

Pollard and Johnson (1973) illustrated by laboratory experiment one of the earliest models of saucer-shaped sill emplacement, that the uplift of the overburden could lead to the formation of dykes climbing upwards from the sill tips. Bradley (1965) supported the idea that the sill follows the surface of neutral buoyancy, and that this surface is shaped as a saucer. The following models proposed by (Francis, 1982, Fig. 6a; Chevallier and Woodford, 1999; Fig. 6b) were essentially based on structural observations and supported laterally-fed sill models. More recently, Malthe-Sørenssen et al. (2004; Fig. 6c) made a quantitative model and their physical explanation was a centrally-fed sill model that opposed the previous models (Francis, 1982; Chevallier and Woodford, 1999).

3.1. The laterally-fed sills model

3.1.1. Model a: Francis (1982)

The model of Francis (1982) is based on the geometry of the Midland Valley Sill and the Whin Sill, northern Britain. The author proposed that the main emplacement mechanism of saucer-shaped sills is the buoyancy. The feeding is made through vertical dykes located on the flank of the future saucer-shaped sill. As the magma overshoots a layer of neutral buoyancy the vertical propagation of the magma stops for stress related reasons (discussed later) and tends to develop a horizontal sill. The author then proposed that the density difference between the invaded rock and the magma causes the magma to flow downward below the level of neutral buoyancy. At a certain point a flat step is achieved and the magma may follow horizontally following discontinuity formed by inter-bedding of sediments of different nature. This results in the accumulation of magma at the bottom part (Fig. 6a, stage 2). In order to achieve hydrostatic equilibrium, the magma then ascends up-dip that leads to the formation of the conjugate climbing sheet of the saucer-shaped sill (Fig. 6a, stage 3 and 4).

3.1.2. Model b: Chevallier and Woodford (1999)

The model of Chevallier and Woodford (1999) is based on the geometry of the Karoo intrusions. The authors proposed that the ring structure is fed by regional dykes that curve both along the strike and in vertical sections. The inclined sheet passes upwards into a flat-laying sill, uplifting the overlying sedimentary layers. The magma then propagates upwards,

forming the outer sill (Fig. 6b, stage 2). The uplifted sediment creates a dragging force upon the upper contact of the inclined sheet. The resulting uplift forces create an upwrapping of the sediment and results in the formation of an open crack at the lower level, adjacent to the sheet. The newly formed crack is then filled in with magma that spread by hydrofracturing, forming the inner sill (Fig. 6b, stage 3).

3.2. The centrally-fed sills model

3.2.1 Model c: Malthe-Sørenssen et al. (2004)

Malthe-Sørenssen et al. (2004) used a two-dimensional numerical model using a least-stress argument to explain the formation of saucer-shaped sills. The authors proposed that the formation of saucer-shaped sills in an initially homogeneous basin may be explained by the effect of an asymmetrical stress field generated by the sill intrusion itself. This model assumes a surrounding elastic matrix as equivalent to the sedimentary basin. In this 2-D model the sill initially extends linearly from an original vertical point source because of fluid overpressure; in 3-D this point source may represent either a feeder dyke or a pipe. When the sill reaches a length of approximately the thickness of the overburden, the localized stress field at the tip of the crack initiates an asymmetrical behaviour of the sill. This initiates a preferential vertical propagation of the sill, forming the roots of the inclined sheets. The ascent of the sheets is then controlled by the asymmetrical stress field generated by the uplifted overburdened, that determines a preferential angle of propagation away from its injection point. The lateral steps produce results from progressive reduction in pressure of the fluid inside the propagating crack. These steps, equivalent to the outer sills in nature, are shown to be larger when close to the inner horizontal crack, equivalent to the inner sill (Fig. 6c, between stage 1 and 2). This model has been further supported by analogue experiments (Galland et al., 2009), that successfully reproduced saucer-shaped intrusions as well as the associated doming effect of the overburdened.

3.2.2. The nested sill complex model

Recent studies using 3-D seismics brought a new insight in the formation of saucer-shaped sills and sill complexes. Thomson and Hutton (2004) produced results on the 3-D geometries of saucer-shaped sills and sill complexes from the North Rockall Trough Volcanic continental margin. Their results lead them to propose a model to explain the geometry and

growth of sill complexes. Their result generally supports the central feeder hypothesis of Malthe-Sørenssen et al. (2004). They suggest that each “radially symmetrical sill complex” is independently fed from a source located beneath the centre of the inner saucer (‘T’ junction, Fig. 7). In other words, this result suggests that sill complexes can be nested and could form in clusters of inter-feeding saucer-shaped sills.

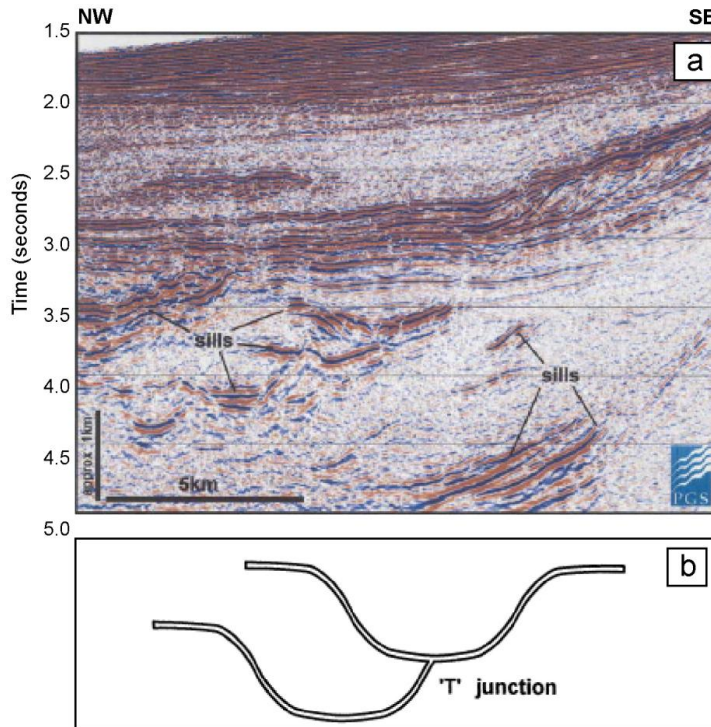


Figure 7: Figure after Thomson and Hutton (2004). a. Seismic section from the North Rockall Trough with high amplitude doleritic sills marked. b. Model proposed by Thompson and Hutton of ‘T’ junctions between saucer-shaped sills.

3.3. The geochemical test on emplacement mechanisms of sill complexes in sedimentary basins

The main questions with regard to the emplacement mechanism of saucer-shaped sills and sill complexes are: first, how are sills emplaced and what is the geometry of their feeders? Secondly, how do sill complexes form? Finally, why do sills turn into saucer-shaped sills? My interest in this thesis does not regard the last question, which is already addressed by several studies through different approaches: the study of the Golden Valley Sill Complex by Polteau

et al. (2007), analogue modelling by Galland et al. (2009), and numerical modelling by Malthe-Sørenssen et al. (2004).

Regarding the emplacement of sill complexes, the mechanisms are poorly understood. The reason is the limitations associated with the techniques used so far to infer the feeding mechanism. Firstly, seismic imaging fails to provide information on vertical or near-vertical structures such as dykes. This is linked to the resolution of the method that fails to provide information on high angle narrow structures such as dykes, and that offsets in sedimentary beddings are not usually associated with these intrusives (i.e., dykes and inclined sheets from saucer-shaped sills in volcanic basins). Secondly, the natural exposures of saucer-shaped sills and complexes of sills as in the Karoo Basin are patented by the lack of exposure of their feeders. Therefore, in this study we suggest the use of a new approach to tackle the problem of emplacement mechanisms of sill complexes.

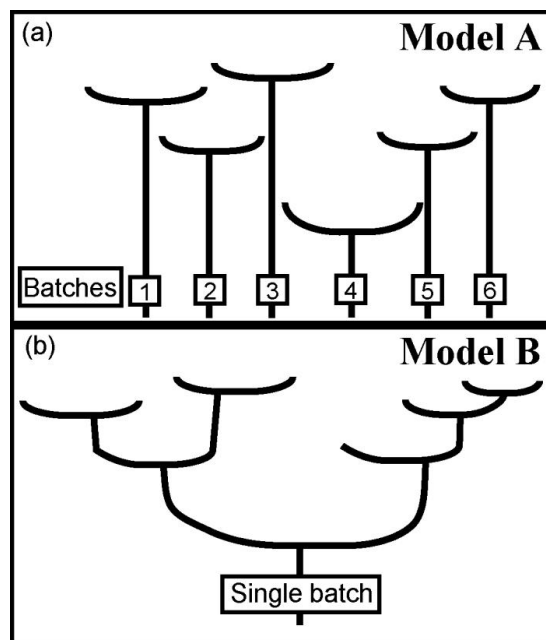


Figure 8: End member plumbing system models after Galerne et al., (2008). a) Model A: Each saucer-shaped sill represents a geochemically distinctive magma batch. b). Model B: A single batch of magma forms a physically connected, geochemically fairly uniform network of interconnected (nested) sills.

It is possible to simplify the above problem through two end-member models or emplacement scenarios that may be distinguished by geochemical fingerprinting. Model A (Fig. 8a) implies that the different sills in a sill complex are formed from different magma

batches emplaced at different times. These batches may have inherited different geochemical signatures from their mantle sources and/or have followed various fractionation processes en route to the surface. In this model we may expect uniform geochemical signatures of rocks formed from the same magma batch, and different geochemical signatures of rocks formed from separate magma batches. In model B (Fig. 8b), the sills are expected to have formed from a single magma batch and have similar geochemical characteristics. Small differences may result from in situ differentiation during the emplacement and/or contamination. However, it should be possible to identify the effects of local contamination, as it will affect the floor and roof of a sill more strongly than its central parts.

3.4. Case study: the Golden Valley Sill Complex

The main results from *Paper I* are that both single- and multi-batch feeding applies to the Golden Valley Sill Complex. Six distinct magma batches are involved in the formation of the major intrusive bodies that constitute this sill complex. We showed that some of the major intrusives carries a distinguishable chemical signature. Additionally, we showed that the saucer-shaped sills located at the uppermost stratigraphic level correspond to a single magma batch (*Paper I*). Because the minor MVS saucer-shaped sill is physically connected to the GVS we have suggested that the MVS was formed from a lateral overflow throughout the GVS West limb. Similarly, we proposed that an identical phenomenon had generated the GS saucer-shaped sill (Fig. 9a).

In the second paper we showed that the geometry of the feeder channel strongly controls the final shape of the resulting saucer-shaped sill. Evidence from field observations, geochemical signatures and analogue experiments lead us to propose that a feeder dyke resulted in the formation of strongly elliptical saucer-shaped sills (Fig. 9b). The hypothesis that the elliptical GS saucer-shaped sill had been fed from lateral overflow in fact contradicts the centrally fed model that we support in *Paper II*. Similarly to Francis (1986), it would mean that the magma first flows laterally, then downwards, then laterally again, forming the inner-sill before it climbs upward again forming the conjugated inclined sheet of the GS.

A schematic cross section could be drawn based on our results from *Paper II*, implying that all elliptical saucer-shaped sills hide a feeder dyke beneath their long axis (Fig. 9b). However, the similar, if not identical, geochemical signature of the GVS-MVS and GS suggests a common feeder to both major elliptical GVS and GS saucer-shaped sills. This

suggests that large saucer-shaped sills may be located deeper in the structure of the Golden Valley Sill Complex.

This hypothesis implies that a magma batch with a GVS-MVS-GS magma signature probably formed a saucer-shaped sill due to the stress heterogeneities created by the previously emplaced saucer-shaped sills. As the incline sheets formed, they encountered the overlying sills and the magma cut across in the manner of straight dykes. The position of the transition between vertical feeder channels at this point can only be speculated, but similar conditions should apply to the formation of both GVS and GS saucer-shaped sills, resulting in fairly similar characteristics: size, elasticity, long axis trend, and geochemical signature (Fig. 9c). This would reconcile the end-member models in *Paper I*. It suggests that the first order feeding mechanism of saucer-shaped sills would be central feeding, with 1) dyke feeding, and 2) saucer-shaped feeding. A second order mechanism would be the lateral overflow mechanism demonstrated by the GVS feeding the smaller MVS saucer-shaped sill (*Paper I*).

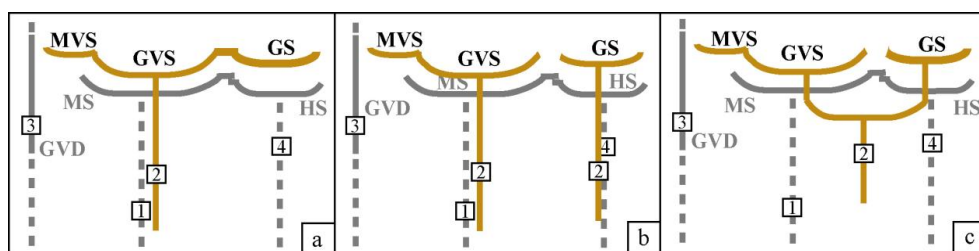


Figure 9: Schematic cross section of the Golden Valley Sill Complex. The vertical feeding channels for each magma batch (dashed lined) are arbitrarily placed beneath the centres of the inner sills. a. Model after (Galerie et al., 2008); the GVS, the MVS and the GS formed from a single magma batch [2] through overflow from one saucer-shaped sill to another. The MS, HS and the GVD are formed from separate magma batches (respectively, [1], [3], [4]). b. Model discussed in *Paper II* (Galerie et al., in review); the major GVS and GS elliptic saucer-shaped sill are centrally fed by independent feeder dykes of identical geochemical signature. c. Integrated model of the Golden Valley Sill Complex plumbing system after (Galerie et al., 2008; Galerie et al., in review). Due to their identical geochemical signature GVS and GS are suggested to be fed from a common saucer-shaped sill located deeper in the stratigraphy of the Golden Valley Sill Complex.

4. Differentiation of tholeiitic magma

4.1. Physics of magmatic differentiation in tholeiitic magma

Magmatic differentiation refers to any process that causes magma to evolve. One of the most efficient processes is fractional crystallization. Fractional crystallization is any process that prevents a solid and a melt, originally at equilibrium, to continuously re-equilibrate during physico-chemical changes (e.g., cooling). This leads to chemical changes. In detail, fractionation (i.e., segregation) processes may differ. During the early stages of crystallization in a magma, crystals may be segregated by processes such as convective fractionation (e.g., Sparks et al., 1984), or crystal settling. Thus, early formed minerals may collect in the calm part of a convecting magma body or at the cooling margins (Fig. 10a). During late stages of crystallization the magma body consists of a continuous crystal mush and convection has stopped. In this regime melt/solid separation can only occur through a flow of the remaining melt fraction through the porous crystal framework (Fig. 10b, e.g., Aarnes et al., 2008). Thus, fractional crystallization embraces a wide range of processes that occur in a cooling mass from the earliest to the latest stages of crystallization.

Igneous sill complexes emplaced in sedimentary basins such as the Golden Valley Sill Complex, South Africa, Karoo Basin, may carry chemical signatures related to both early (i.e., mineral separation from the ambient melt) and late stage segregation (melt porous flow through crystalline mush) processes leading to fractional crystallization. In this thesis I studied the magmatic processes related to the shallow magma emplacement into sedimentary basins. This topic is treated in *Paper III* and investigates the process of fractional crystallization at both the emplacement stage and post-emplacement stage to explain the various types of compositional profiles found in a single saucer-shaped sill. The question of the deep origin of the melt is not being addressed in this thesis. One of the main reasons for this is that such a question is related to a much larger scale than the main themes of my thesis. A manuscript in this direction is in preparation.

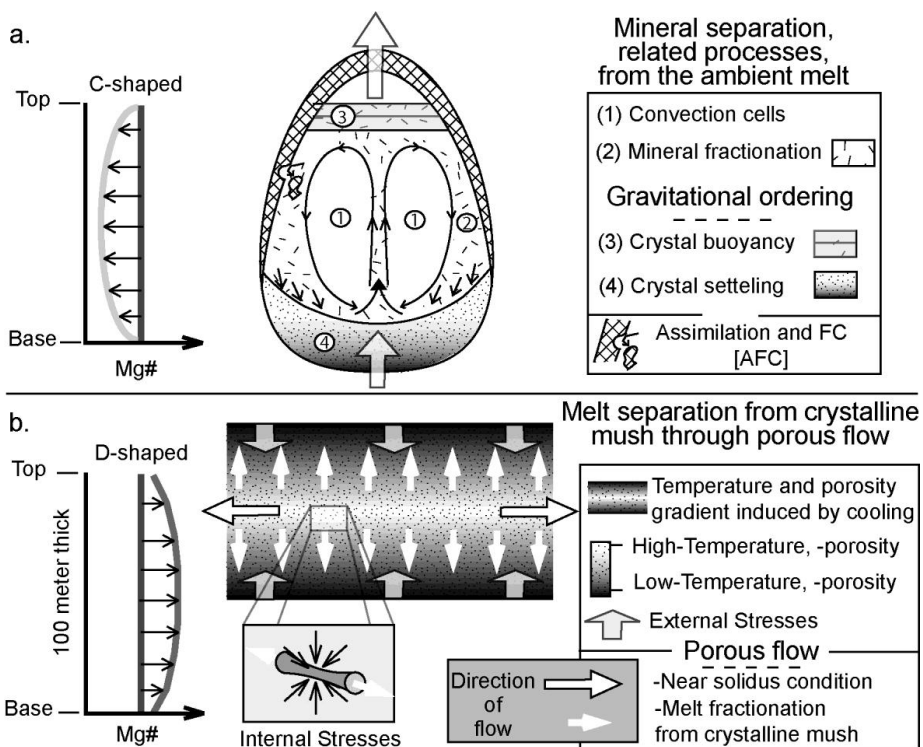


Figure 10: a. Conventional schematic figure of large magma chamber (kilometre scale, after Maury, 1993) where the magma differentiates by early segregation process of mineral separation inducing fractional crystallization. The shape of the magma chamber is arbitrary. Under the inherent effect of gravity a convective current is organized (1). As mineral phases crystallize (2), gravitational ordering can occur according to the various densities of the different minerals phases, i.e., crystal buoyancy (3) and crystal settling (4). In large layered intrusions the convective removal of high temperature mineral fractionated at the cold margins is usually invoked to explain the C-shaped compositional zoning pattern in a Mg# nomenclature (Rice, 1981). We attribute this zoning pattern to a normal profile shape. b. Schematic figure of melt fractionation inducing magma differentiation in 100 meter thick sills. Cooled from the outside, solidification fronts produce a porosity gradient, with higher porosity in the mid-plane of the sill. External stresses (i.e., thermal stress) induce marginal melt flow in the sill (Aarnes et al., 2008). Internal stresses acting on the porous skeleton provoke general compaction of the porous mush zone that induces melt to be expelled preferentially along the high mid-plane porosity (model presented in *Paper III*). This process of melt fractionation induces D-shaped profiles.

4.2. The concept of melt fractionation inducing magma differentiation in tholeiitic sills

4.2.1. Thermal stresses related to melt fractionation

The mechanism of melt fractionation has been recently tested and proposed to produce D-shaped compositional profiles in strictly horizontal intrusions (Aarnes et al., 2008). Based on geochemical studies and numerical modelling the authors proposed that differentiation is caused by a separation of melt and crystals by a porous flow through rigid crystal networks.

This will induce a bulk differentiation in the sill through melt segregation. Aarnes et al. (2008) showed numerically that such flow may be induced by thermal stresses associated with cooling and crystallization in a horizontal intrusion. The thermal stresses induce a large under-pressure developed at the cooling margins, where melt will be sucked in by a porous flow. As a result the margins will be enriched in the incompatible elements, while the centre will be depleted.

4.2.2. Buoyancy related melt fractionation

Paper III shows that all types of compositional profiles can be found in a single saucer-shaped sill, the Golden Valley Sill. Furthermore, we show that the various profile types are systematically distributed around the sill. I-shaped profiles are located at the limb-tips of the elliptic GVS and the differentiated D- and S-shaped profiles are located in the central regions of the conjugated limbs. Similarly to Aarnes et al. (2008) we found a negative correlation between compatible and incompatible elements.

The mechanism that we suggest in *Paper III* is similar to that of Aarnes et al (2008); that the melt segregation and flow through crystalline mush produces bulk-rock differentiation. However, in order to explain the systematic space distribution in saucer-shaped sills we suggest the contribution of buoyancy to the previous model. A saucer-shaped sill produces large density differences between the horizontal inner-sill and horizontal outer-sill, connected through inclined sheets. We suggest that the relatively buoyant porous mush will tend to move upward relative to the surrounding material. This motion will create a dynamic over-pressure at the front of the moving mass (outer-sills). On the other hand, an under-pressure will be generated beneath, probably near the transition between the inclined-sheet and inner-sill. The pressure gradient is followed by a preferential flow and the saturated melt fraction will percolate against the gravity field through the mid-plane porosity of the saucer-shaped sill. Based on further arguments developed in *Paper III* we suggest that differentiated D-, and S-shaped profiles preferentially occur at high points of inclined and outer-sills. We propose that profiles at the transition between inclined and inner-sill could carry a C-shaped signature.

5. On the quantification and validity of post-emplacement melt flow differentiation

Magmatic differentiation in saucer-shaped sills emplaced at shallow levels in sedimentary basins is undeniably a complex process. Phase equilibria (i.e., mass balance) are strongly coupled with thermo-mechanical work during porous reactive flow. Modelling of multi-component multi-phase systems is best suited to constrain magmatic differentiation processes and the modelling results are also of fundamental interest to petrologists. Recent progress in the development of continuum engineering models and the increase in computational power brings numerical testing and quantification of processes such as fractional crystallization and porous reactive flow within reach (Bergantz, 1995).

Crystallization and melting are both basic processes that induce differentiation of the Earth and are therefore two of the most fundamental processes to be studied in magmatic petrology. In both cases, the porosity of the system changes drastically and the evolution of porosity is a first order process determining the behaviour of the system. However, it is difficult to quantitatively model the evolution of porosity in time and space in a manner that is consistent with geological observations. The time evolution of porosity in magmatic systems can be reduced to the problems of precipitation and dissolution of crystals. The quantification of this mass exchange rate is essential in the evaluation of dynamic crystallizing systems. Slow kinetics of reactions associated with diffusion appear to be non-trivial to estimate. However, as a first approach we can assume local thermodynamic equilibrium at the computed pressure, temperature and composition for each time step. This can be done using thermodynamic databases (Holland and Powell, 1998) and the principle of minimization of Gibbs free energy, in combination with the physical balance laws and the second law of thermodynamics. The retardation factor can then be evaluated for the system of interest.

Existing continuum models, however, are usually only capable of solving simplified end-member problems approaching complex magmatic systems. Over-simplification of the problem results in models that are at odds with the data provided by the observations. Thus, these models remain a first order approach and are too simplified to solve real petrological and geological problems in a truly quantitative way. Before any realistic quantification of magmatic processes, we face the urgent need of a truly complete continuum description of a system of equations that is thermodynamically consistent. Several attempts in this direction

have been realized, but suffer from the complexity of the derivations and often result, again, in simplified models designed to solve a specific part of a given problem in detail (e.g., influence of mechanical work on mass exchange, Nauman and He, 2001; Šrámek et al., 2007), but neglecting others. Thus, the identification of the controlling parameters remains problematic as it can result in the underestimation of certain parameters involved in specific petrological processes.

During my PhD I have been involved in a project of deriving a closed system of equations aimed at numerical testing and quantification of the specific magmatic differentiation processes that occur during the formation of saucer-shaped sills. The results of this work are presented in Tantserev's PhD thesis (2008) and in Tantserev et al. (in review).

In Tantserev et al. (in review) we present a general system of equations derived from the fundamental balance laws of mass, momentum, energy, and entropy that is capable of capturing the behaviour of multi-phase multi-component systems. Based on the assumption of local equilibrium and the second law of thermodynamics we derive the admissible fluxes and sources of the considered system. We present the derived closed system of equations in a general form. A comparison to existing continuum descriptions is then provided in order to validate our model. Additionally, we derive a relation between our continuum model to fit the exact solution of Gassman's relation for poroelasticity. Even though our study was aimed at the particular problem of melt segregation at near-solidus conditions, the general theoretical outcome of our work may be applicable to a wide variety of geological processes.

6. Authorship statement

This thesis is presented as a collection of three scientific papers dealing with the emplacement mechanisms and magmatic differentiation in tholeiitic sill complexes.

During this PhD work I was responsible for the sample collection and Electron Micro-Probe-analysis, except for the bulk rock chemical analysis which was performed at Royal Holloway, University of London, and at the University of Bergen (Norway). The sample responsibility in the field was partly shared in early stage of the fieldwork with Ingrid Aarnes and Kirsten Haarberg. The general structural relationships of the Golden Valley Sill Complex were established in collaboration with Stephan Polteau during two excursions on the field (more than a month and-a-half on site).

I initiated and wrote the first paper. In this work I carried out a statistical treatment of the whole-rock geochemical data set using a type of principal component analysis called Forward-Step Discriminant Function Analysis. All co-authors contributed to the paper through discussions. Else-Ragnhild Neumann in particular assisted me in writing the paper.

The second article was initiated by a discussion with Olivier Galland confronting both results from my study and his results from experimental modelling. The hypothesis of a possible linear feeder dyke to the Golden Valley Sill based on my results lead us to an original experiment that was designed and realized by Olivier Galland. I wrote first drafts of the manuscript and corrected it in collaboration with Olivier Galland. All co-authors contributed through the paper by discussions and suggestions.

In the third paper I lead the overview study of the profile chemistry on the Golden Valley Sill. This study presents 18 compositional profiles of the Golden Valley Sill that included four profiles on the responsibility of Ingrid Aarnes and Kirsten Haaberg. The specific detailed microprobe analyses that I realized was carried out after I discovered the textural pattern observed in differentiated profiles. The mechanism of post-emplacement melt fractionation was suggested after collegial discussion that involved Yuri Podladshikov, Ingrid Aarnes and Kirsten Haarberg, Else-Ragnhild Neumann, and myself. I initiated and wrote the paper. Else-Ragnhild Neumann Ingrid Aarnes and Sverre Planke contributed to the paper through discussions and reviews of the manuscript.

The papers are arranged in a logical sequence which ties together the observations and results obtained though the duration of my Ph.D. These three papers aim to answer the major

questions addressed by my PhD project originally entitled “Emplacement Mechanisms and Magma Flow in Sheet Intrusion in Sedimentary Basins” granted by the Norwegian Research Council (NFR). The first two papers address the question of emplacement mechanisms of sill complexes in sedimentary basins inferred from field observations, geochemistry, which were combined and integrated with the results of experimental modelling in the second paper. The last paper deals with the magmatic differentiation process within saucer-shaped sills that relates to a post-emplacement melt flow. Ongoing work on larger scale processes related to the source of the magmas and the link to the Karoo-Ferrar Large Igneous Events appears to be out of the scope of this thesis that focused on shallow related magmatic processes. The originally planned numerical modelling and quantification of the process has been withdrawn from the present thesis. This is due to the fact that no consistent continuum description of the required system of equations was available. This led me instead to collaborate with Evgeniy Tantserev on the development of a general continuum description based on fundamental balance laws of physics and thermodynamics. This project is aimed at producing the correct governing equations to implement a Finite Element Method-code.

7. References

- Aarnes, I., Podladchikov, Y.Y. and Neumann, E.-R., 2008. Post-emplacement melt flow induced by thermal stresses: Implications for differentiation in sills. *Earth and Planetary Science Letters*, 276(1-2): 152-166.
- Anderson, D.L., 1995. Lithosphere, Asthenosphere, and Perisphere. *Reviews of Geophysics*, 33(1): 125-149.
- Bergantz, G.W., 1995. Changing Techniques and Paradigms for the Evaluation of Magmatic Processes. *Journal of Geophysical Research-Solid Earth*, 100(B9): 17603-17613.
- Bowen, N.L., 1928. *The evolution of igneous rocks*. Princeton University Press, Princeton, 332 pp.
- Bradley, J., 1965. Intrusion of Major Dolerite Sills. *Transactions of the Royal Society of New Zealand*, 3: 2755.
- Bryan, S.E. and Ernst, R.E., 2008. Revised definition of large igneous provinces (LIPs). *Earth-Science Reviews*, 86(1-4): 175-202.
- Catuneanu, O., Hancox, P.J. and Rubidge, B.S., 1998. Reciprocal flexural behaviour and contrasting stratigraphies: a new basin development model for the Karoo retroarc foreland system, South Africa. *Basin Research*, 10(4): 417-439.
- Catuneanu, O., Wopfner, H., Eriksson, P.G., Cairncross, B., Rubidge, B.S., Smith, R.M.H. and Hancox, P.J., 2005. The Karoo basins of south-central Africa. *Journal of African Earth Sciences*, 43(1-3): 211-253.
- Chevallier, L. and Woodford, A., 1999. Morpho-tectonics and mechanism of emplacement of the dolerite rings and sills of the western Karoo, South Africa. *South African Journal of Geology*, 102(1): 43-54.
- Coffin, M.F. and Eldholm, O., 1994. Large igneous provinces: Crustal structure, dimensions, and external consequences. *Reviews of Geophysics*, 32(1): 1-36.
- Cox, K.G. and Hornung, G., 1966. The Petrology of the Karoo Basalts of Basutoland. *American Mineralogist*, 51: 1414-1432.
- Du Toit, A.I., 1920. The Karoo dolerites. *Transactions of the Geological Society South Africa*, 33: 1-42.
- Duncan, R.A., Hooper, P.R., Rehacek, J., Marsh, J.S. and Duncan, A.R., 1997. The timing and duration of the Karoo igneous event, southern Gondwana. *Journal of Geophysical Research-Solid Earth*, 102(B8): 18127-18138.

- Eales, H.V., Marsh, J.S. and Cox, K.G., 1984. The Karoo Igneous Province: an introduction. Special Publication of the Geological Society of South Africa, in Erlank A.J. (Editor), Petrogenesis of the Volcanic Rocks of the Karoo Province(13): 1-26.
- Eglington, B.M. and Armstrong, R.A., 2004. The Kaapvaal Craton and adjacent orogens, southern Africa: a geochronological database and overview of the geological development of the craton. *South African Journal of Geology*, 107(1-2): 13-32.
- Ellam, R.M. and Cox, K.G., 1991. An Interpretation of Karoo Picrite Basalts in Terms of Interaction between Asthenospheric Magmas and the Mantle Lithosphere. *Earth and Planetary Science Letters*, 105(1-3): 330-342.
- Elliot, D.H. and Fleming, T.H., 2004. Occurrence and Dispersal of Magmas in the Jurassic Ferrar Large Igneous Province, Antarctica. *Gondwana Research*, 7(1): 223-237.
- Erlank, A.J.E., 1984. Petrogenesis of the Volcanic Rocks of the Karoo Province. Special Publication of the Geological Society of South Africa, 13: 395 p.
- Flemings, M.C., 2000. Our understanding of macrosegregation: Past and present. *Isij International*, 40(9): 833-841.
- Francis, E.H., 1982. Magma and sediment - I. Emplacement mechanism of late Carboniferous tholeiite sills in northern Britain. *Journal of the Geological Society, London*, 139(1): 1-20.
- Frenkel, M.Y., Yaroshevsky, A.A., Ariskin, A.A., Barmina, G.S., Koptev-Dvornikov, E.V. and Kireev, B.S., 1988. Dynamics of in situ differentiation of Mafic Magmas, Moscow.
- Frenkel, M.Y., Yaroshevsky, A.A., Ariskin, A.A., Barmina, G.S., Koptev-Dvornikov, E.V. and Kireev, B.S., 1989. Convective cumulate model simulating the formation process of stratified intrusions. In: B. Bonin et al. (Editors), *Magma-Crust Interactions and Evolution*. Theophrastus, Athens, pp. 3-88.
- Fujii, T., 1974. Crystal settling in a sill. *Lithos*, 7(3): 133-137.
- Galerne, C.Y., Galland, O., Neumann, E.R. and Planke, S., in review. The shapes of the feeders control the 3D shapes of sills. *Geology*.
- Galerne, C.Y., Neumann, E.-R. and Planke, S., 2008. Emplacement mechanisms of sill complexes: Information from the geochemical architecture of the Golden Valley Sill Complex, South Africa. *Journal of Volcanology and Geothermal Research*, 177(2): 425-440.

- Galland, O., Planke, S., Neumann, E.R. and Malthe-Sørenssen, A., 2009. Experimental modelling of shallow magma emplacement: application to saucer-shaped intrusions. *Earth and Planetary Science Letters*.
- Gibb, F.G.F. and Henderson, C.M.B., 1992. Convection and Crystal Settling in Sills. *Contributions to Mineralogy and Petrology*, 109(4): 538-545.
- Gorring, M.L. and Naslund, H.R., 1995. Geochemical Reversals within the Lower 100 M of the Palisades Sill, New-Jersey. *Contributions to Mineralogy and Petrology*, 119(2-3): 263-276.
- Gray, N.H. and Crain, I.K., 1969. Crystal settling in sills: A model for suspension settling. *Can. J. Earth Sci.*, 6(5): 1211-1216.
- Hansen, D.M. and Cartwright, J.A., 2006. Saucer-shaped sill with lobate morphology revealed by 3D seismic data: implications for resolving a shallow-level sill emplacement mechanism. *Journal of the Geological Society, London*, 163: 509-523.
- Hansen, D.M., Cartwright, J.A. and Thomas, D., 2004a. 3D seismic analysis of the geometry of igneous sills and sill junction relationships. *3D seismic technology: application to the exploration of sedimentary basins*, 29. *Geol Soc London Mem*, pp. 199-208
- Hansen, D.M., Cartwright, J.A. and Thomas, D., 2004b. 3D seismic analysis of the geometry of igneous sills and sill junctions relationships. In: R.J. Davies, J.A. Cartwright, S.A. Stewart, M. Lappin and J.R. Underhill (Editors), *3D Seismic Technology: Application to the Exploration of Sedimentary Basins*. Geological Society, London, Memoir, pp. 199-208.
- Hawkesworth, C.J., Marsh, J.S., duncan, A.R., Erlank, A.J. and Norry, M.J., 1984. The role of continental lithosphere in the generation of the Karoo volcanic rocks: evidence from combined Nd- and Sr-isotope studies. *Special Publication of the Geological Society of South Africa*, 13: 341-354.
- Holland, T.J.B. and Powell, R., 1998. An internally consistent thermodynamic data set for phases of petrological interest. *Journal of Metamorphic Geology*, 16(3): 309-343.
- Hyndman, D.W. and Alt, D., 1987. Radial dikes, lacoliths, and gelatin models. *Journal of Geology*, 95: 763-774.
- Jourdan, F., 2005. La province magmatic du Karoo: géochronologie géochimie et implications géodynamiques. PhD Thesis, Université de Nice-Sophia Antipolis, Nice-Sophia Antipolis, 394 p.
- Jourdan, F., Feraud, G., Bertrand, H., Kampunzu, A.B., Watkeys, M.K., Le Gall, B. and Tshoso, G., 2004. New age constraints on the Karoo Large Igneous Province: Triple

- junction and brevity questioned. *Geochimica Et Cosmochimica Acta*, 68(11): A575-A575.
- Jourdan, F., Feraud, G., Bertrand, H. and Watkeys, M.K., 2007. From flood basalts to the inception of oceanization: Example from the Ar-40/Ar-39 high-resolution picture of the Karoo large igneous province. *Geochem. Geophys. Geosyst.*, 8, Q02002, doi:10.1029/2006GC001392.
- Jourdan, F., Feraud, G., Bertrand, H., Watkeys, M.K., Kampunzu, A.B. and Le Gall, B., 2006. Basement control on dyke distribution in Large Igneous Provinces: Case study of the Karoo triple junction. *Earth and Planetary Science Letters*, 241(1-2): 307-322.
- Latypov, R.M., 2003a. The origin of basic-ultrabasic sills with S-, D-, and I-shaped compositional profiles by *in situ* crystallization of a single input of phenocryst-poor parental magma. *Journal of Petrology*, 44(9): 1619-1656.
- Latypov, R.M., 2003b. The origin of marginal compositional reversals in basic-ultrabasic sills and layered intrusions by Soret fractionation. *Journal of Petrology*, 44(9): 1579-1618.
- Latypov, R.M., Chistyakova, S. and Alapieti, T., 2007. Revisiting problem of chilled margins associated with marginal reversals in mafic-ultramafic intrusive bodies. *Lithos*.
- Lock, B.E., 1980. Flat-plate subduction and the Cape Fold Belts of South Africa. *Geology*, 8: 35-39.
- Malthe-Sørenssen, A., Planke, S., Svensen, H. and Jamtveit, B., 2004. Formation of saucer-shaped sills. In: C. Breitkreuz and N. Petford (Editors), *Physical geology of high-level magmatic systems*. Geological Society, London, Special Publication, pp. 215-227.
- Mangan, M.T. and Marsh, B.D., 1992. Solidification Front Fractionation in Phenocryst-Free Sheet-Like Magma Bodies. *Journal of Geology*, 100(5): 605-620.
- Marsh, B.D., 1989. On Convective Style and Vigor in Sheet-Like Magma Chambers. *Journal of Petrology*, 30(3): 479-530.
- Marsh, B.D., 1996. Solidification fronts and magmatic evolution. *Mineralogical Magazine*, 60(398): 5-40.
- Marsh, J.S. and Eales, H.V., 1984. The chemistry and petrogenesis of igneous rocks of the Karoo Central area, southern Africa. Special Publication of the Geological Society of South Africa, in Erlank A.J. (Editor), *Petrogenesis of the Volcanic Rocks of the Karoo Province*(13): 27-67.
- Marsh, J.S., Hooper, P.R., Rehacek, J., Duncan, R.A. and Duncan, A.R., 1997. Stratigraphy in age of Karoo Basalts of Lesotho and implications for correlations within the Karoo Igneous Province. *Geophysical Monographs*, 100: 247-272.

- Marsh, J.S. and Mndaweni, M.J., 1998. Geochemical variations in a long Karoo dyke, Eastern Cape. *South African Journal of Geology*, 101(2): 119-122.
- Maurly, R.C., 1993. Les séries volcaniques. In: M.d.I.S.G.d. France (Editor), *Pleins feux sur les volcans*, pp. 39-55.
- Naslund, H.R., 1984. Petrology of the Upper Border Series of the Skaergaard Intrusion. *Journal of Petrology*, 25(1): 185-212.
- Nauman, E.B. and He, D.Q., 2001. Nonlinear diffusion and phase separation. *Chemical Engineering Science*, 56(6): 1999-2018.
- Planke, S., Rasmussen, T., Rey, S.S. and Myklebust, R., 2005. Seismic characteristics and distribution of volcanic intrusions and hydrothermal vent complexes in the Vøring and Møre basins. In: A.G. Doré and B.A. Vining (Editors), *Petroleum geology: Northwestern Europe and global perspectives - Proceedings of the 6th Petroleum Geology Conference*. Geological Society, London.
- Pollard, D.D. and Johnson, A.M., 1973. Mechanics of growth of some laccolithic intrusions in the Henry Mountains, Utah, II. Bending and failure of overburden layers and sill formation. *Tectonophysics*, 18: 311-354.
- Polteau, S., Mazzini, A., Galland, O., Planke, S. and Malthe-Sørenssen, A., 2008. Saucer-shaped intrusions: occurrences, emplacement and implications. *Earth and Planetary Science Letters*, 266(1-2): 195-204.
- Polteau, S., Planke, S., Ferré, E.C., Svensen, H., Malthe-Sørenssen, A., Neumann, E.R. and Podladchikov, Y.Y., submitted. Emplacement mechanisms of saucer-shaped sill intrusion as inferred from detailed fieldwork and AMS analyses of the Golden Valley Sill Complex, South Africa. *Journal of Geophysical Research*.
- Puffer, J.H., 2001. Contrasting high field strength element contents of continental flood basalts from plume versus reactivated-arc sources. *Geology*, 29(8): 675-678.
- Rice, A., 1981. Convective Fractionation - a Mechanism to Provide Cryptic Zoning (Macrosegregation), Layering, Crescumulates, Banded Tuffs and Explosive Volcanism in Igneous Processes. *Journal of Geophysical Research*, 86(Nb1): 405-417.
- Richardson, S.H., 1979. Chemical variation induced by flow differentiation in an extensive Karoo dolerite sheet, southern Namibia. *Geochimica et Cosmochimica Acta*, 43(9): 1433-1441.
- Riley, T.R., Curtis, M.L., Leat, P.T., Watkeys, M.K., Duncan, R.A., Millar, I.L. and Owens, W.H., 2006. Overlap of Karoo and Ferrar magma types in KwaZulu-Natal, South Africa. *Journal of Petrology*, 47(3): 541-566.

- Sheth, H.C., 2007. `Large Igneous Provinces (LIPs)': Definition, recommended terminology, and a hierarchical classification. *Earth-Science Reviews*, 85(3-4): 117-124.
- Sparks, R.S.J., Huppert, H.E. and Turner, J.S., 1984. The Fluid-Dynamics of Evolving Magma Chambers. *Philosophical Transactions of the Royal Society of London Series a-Mathematical Physical and Engineering Sciences*, 310(1514): 511-&.
- Šrámek, O., Ricard, Y. and Bercovici, D., 2007. Simultaneous melting and compaction in deformable two-phase media. *Geophysical Journal International*, 168(3): 964-982.
- Svensen, H., and Planke, S., 2003 (Eds). Appendix B: Karoo Field Report. VBPR/TGS-NOPEC. "Petroleum Implications of Sill Intrusion" report, Oslo, Norway. 178pp.
- Svensen, H., Planke, S., Chevallier, L., Malthé-Sorensen, A., Corfu, F. and Jamtveit, B., 2007. Hydrothermal venting of greenhouse gases triggering Early Jurassic global warming. *Earth and Planetary Science Letters*, 256(3-4): 554-566.
- Sweeney, R.J., Duncan, A.R. and Erlank, A.J., 1994. Geochemistry and Petrogenesis of Central Lebombo Basalts of the Karoo Igneous Province. *Journal of Petrology*, 35(1): 95-125.
- Sweeney, R.J., Falloon, T.J., Green, D.H. and Tatsumi, Y., 1991. The mantle origins of Karoo picrites. *Earth and Planetary Science Letters*, 107(2): 256-271.
- Sweeney, R.J. and Watkeys, M.K., 1990. A Possible Link between Mesozoic Lithospheric Architecture and Gondwana Flood Basalts. *Journal of African Earth Sciences*, 10(4): 707-716.
- Symonds, P.A., Planke, S., Frey, Ø. and Skogseid, J., 1998. Volcanic development of the Western Australian continental margin and its implications for basin development. In: P.G.a.R.R. Purcell (Editor), *The Sed. Basins of W Australia 2: Proc. of Expl. Soc. of Australia Symp.*, Perth, pp. 33-54.
- Tait, S.R. and Jaupart, C., 1996. The production of chemically stratified and accumulate plutonic igneous rocks. *Mineralogical Magazine*, 60(398): 99-114.
- Tantserev, E., 2008. Time Reverse Methods in Modeling of Diffusive, Convective and Ractive Transport. Dissertation for the degree of Doctor Scientiarum Thesis, Faculty of Mathematics and Natural Sciences, Oslo.
- Tantserev, E., Galerne, C.Y. and Podladchikov, Y.Y., in review. Reactive flow in multi-component visco-elastic media: closed system of equations. The Fourth Biot Conference on Poromechanics.
- Thomson, K. and Hutton, D., 2004. Geometry and growth of sill complexes: insights using 3D seismic from the North Rockall Trough. *Bulletin of Volcanology*, 66(4): 364-375.

Wager, L.R. and Brown, G.M., 1968. Layered igneous rocks. WH Freeman, San Francisco.

8. Papers

***Paper I: Emplacement mechanisms of sill complexes: Information
from the geochemical architecture of the Golden Valley Sill
Complex, South Africa***

Christophe Y. Galerne^{a,*}, Else-Ragnhild Neumann^a, Sverre Planke^{a,b}

^a PGP – Physics of Geological Processes, University of Oslo, PO BOX 1048 Blindern, 0316 Oslo, Norway

^b VBPR – Volcanic Basin Research, Forskningsparken, Oslo Norway

Published in Journal of Volcanology and Geothermal Research 177 (2008) 425-440

Paper II: The shapes of feeders control the 3D shapes of sills

**Christophe Galerne^{a,b,*}, Olivier Galland^a, Else-Ragnhild Neumann^a,
Sverre Planke^{a,c}**

^aPGP – Physics of Geological Processes, University of Oslo, PO BOX 1048 Blindern, 0316 Oslo, Norway

^bGeodynamik/Geophysik, Universität Bonn, Steinmann-Institut, Germany

^cVBPR – Volcanic Basin Research, Forskningsparken, Oslo Norway

Submitted to Terra Nova

***Paper III: Magmatic Differentiation Processes in Saucer-Shaped
Sills: Evidence from the Golden Valley Sill in the Karoo Basin,
South Africa***

**Christophe Galerne^{a,b}, Else-Ragnhild Neumann^a, Ingrid Aarnes^a,
Sverre Planke^{a,c}**

^aPGP – Physics of Geological Processes, University of Oslo, PO BOX 1048 Blindern, 0316 Oslo, Norway

^bGeodynamik/Geophysik, Universität Bonn, Steinmann-Institut, Germany

^cVBPR – Volcanic Basin Research, Forskningsparken, Oslo Norway

Submitted to Geosphere

Appendix

Appendix A: Sampling locations

This appendix gives the detail of the samples locations through three maps. The following table are complementary data from the *paper I*, published in *Journal of Volcanology and Geothermal Research*.

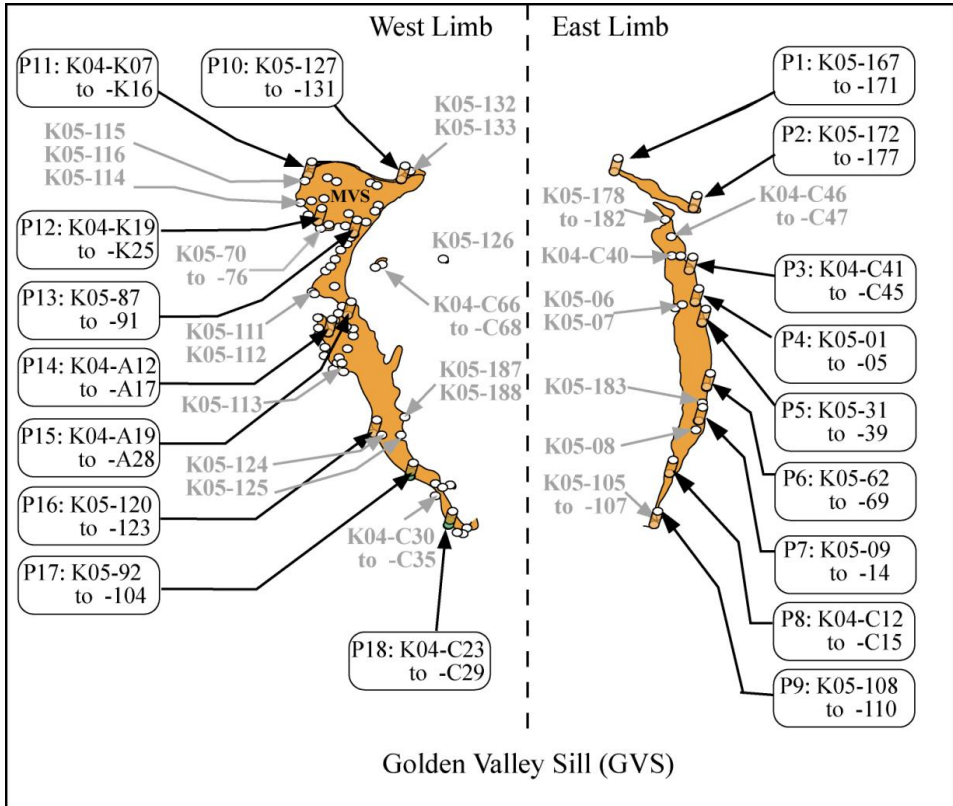


Figure A.1: Sampling locations of the Golden Valley Sill.

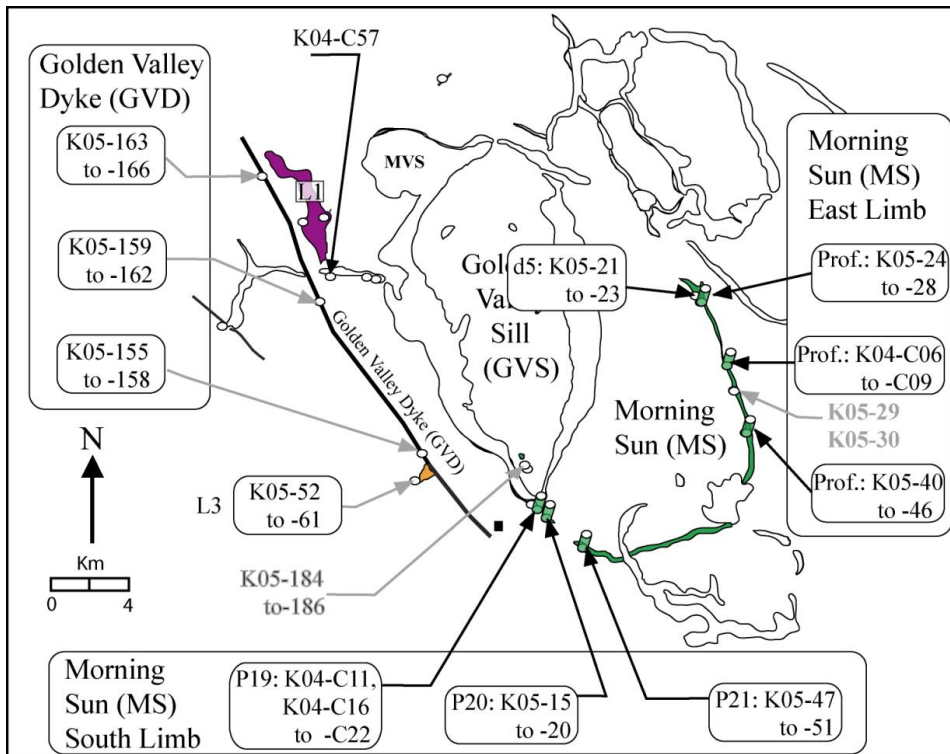


Figure A.2: Sampling locations of the Morning Sun saucer-shaped sill, Golden Valley Dyke and the sills from localities L1 and L3.

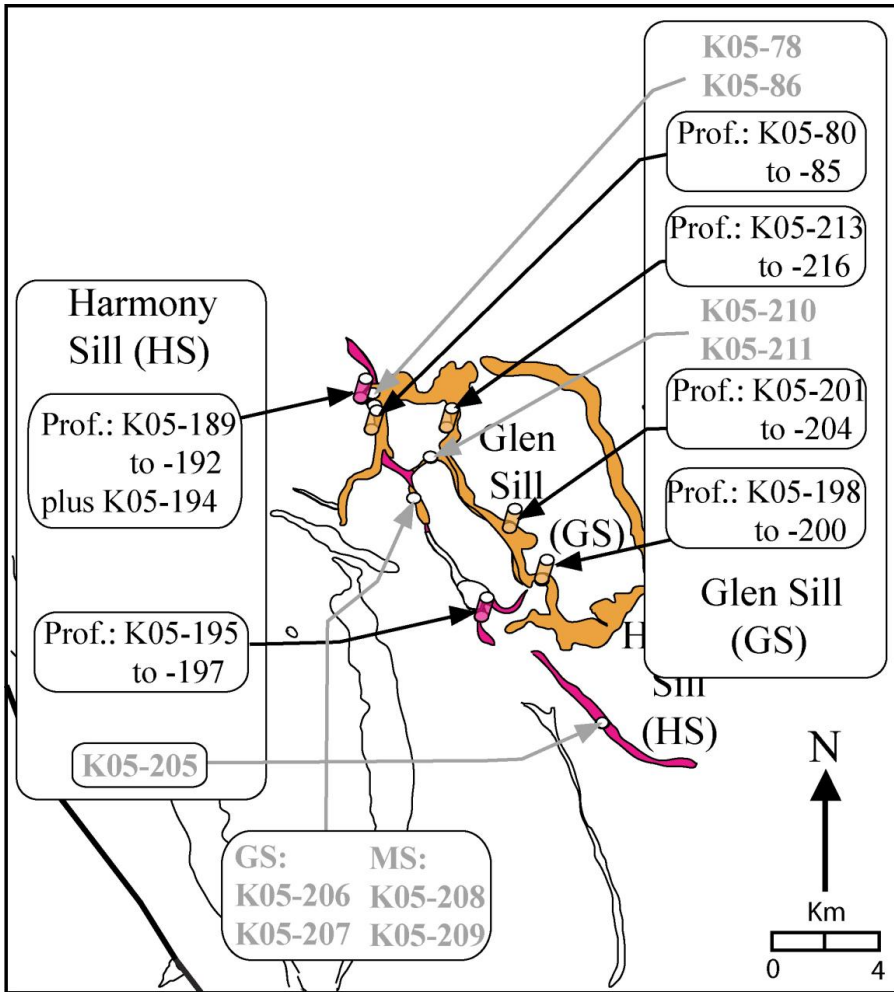


Figure A.3: Sampling locations of the saucer-shaped sills: Harmony Sill and Glen Sill.

**Appendix B. Complementary data Table 2; Galerne et al.
(2008).**

Sample:	K04-C11	K04-C17	K04-C18	K04-C19	K04-C20	K04-C21	K04-C22
Magma b./Loc.:	MS	MS	MS	MS	MS	MS	MS
Latitude (N):	-32,0011	-31,9986	-31,9989	-31,9989	-31,9989	-31,9988	-31,9988
Longitude (E):	26,2847	26,2793	26,2790	26,2790	26,2791	26,2791	26,2792
Altitude (m):	1377	1505	1488	1490	1496	1500	1505
SiO2 (wt %)	50,76	50,21	50,29	50,87	50,47	50,47	50,68
TiO2 (wt %)	0,91	0,91	0,93	0,93	0,88	0,93	0,92
Al2O3 (wt %)	15,47	15,25	15,41	15,60	15,33	15,44	15,18
Fe2O3(T) (wt %)	10,74	10,69	10,82	10,83	11,02	10,92	11,15
MnO (wt %)	0,17	0,17	0,17	0,17	0,17	0,17	0,17
MgO (wt %)	7,02	6,72	6,99	7,07	7,51	7,15	7,23
CaO (wt %)	11,03	10,81	10,95	10,98	10,69	10,84	10,75
Na2O (wt %)	2,32	2,40	2,20	2,39	2,33	2,39	2,30
K2O (wt %)	0,37	0,43	0,41	0,41	0,40	0,46	0,44
P2O5 (wt %)	0,12	0,13	0,12	0,12	0,11	0,12	0,13
SUM	98,9	97,7	98,3	99,4	98,9	98,9	98,9
Cs (ppm)	0,8	0,5	1,1	1,0	0,5	0,5	0,6
Tl (ppm)	b.d.	b.d.	b.d.	b.d.	b.d.	b.d.	b.d.
Rb (ppm)	7	9	8	8	8	9	7
Ba (ppm)	143	147	146	147	142	151	149
Th (ppm)	b.d.	b.d.	b.d.	b.d.	b.d.	b.d.	b.d.
U (ppm)	0,16	0,17	0,21	0,18	0,17	0,19	0,15
Nb (ppm)	5,1	5,0	5,4	5,8	7,0	5,7	5,1
Ta (ppm)	0,26	0,28	0,27	0,30	0,29	0,30	0,28
La (ppm)	7,78	7,28	7,36	7,98	7,87	7,28	6,68
Ce (ppm)	16,97	16,25	16,71	17,95	16,22	16,66	15,72
Pb (ppm)	5	2	2	6	7	4	7
Pr (ppm)	2,13	2,11	2,14	2,34	2,08	2,09	2,01
Mo (ppm)	0,7	1,1	0,9	1,0	0,9	0,8	0,7
Sr (ppm)	188	183	190	193	189	193	183
Nd (ppm)	10,8	11,2	10,4	12,5	11,5	10,9	10,4
Zr (ppm)	80	81	81	81	79	79	77
Hf (ppm)	2,05	1,83	1,90	2,06	2,11	1,94	1,76
Sm (ppm)	2,85	2,90	2,83	3,04	2,76	3,25	2,51
Eu (ppm)	0,97	0,91	0,94	1,10	0,98	1,00	0,96
Sn (ppm)	b.d.	b.d.	b.d.	b.d.	b.d.	b.d.	b.d.
Gd (ppm)	3,00	3,07	2,90	3,18	3,15	2,98	2,85
Dy (ppm)	3,79	3,79	3,81	3,98	3,75	3,81	3,76
Li (ppm)	8	b.d.	8	2	b.d.	b.d.	13
Y (ppm)	25	24	25	25	23	24	24
Ho (ppm)	b.d.	b.d.	b.d.	b.d.	b.d.	b.d.	b.d.
Er (ppm)	1,97	2,08	1,99	2,15	1,94	2,04	1,90
Yb (ppm)	2,06	1,99	2,05	2,17	2,08	2,08	2,00
Lu (ppm)	0,33	0,31	0,34	0,32	0,28	0,31	0,30
Co (ppm)	34	35	34	35	36	35	36
Cr (ppm)	352	393	363	378	420	404	368
Cu (ppm)	100	98	101	100	97	98	97
Ni (ppm)	96	95	99	108	121	108	104
Sc (ppm)	35	33	35	34	33	34	33
V (ppm)	256	245	247	252	234	247	241
Zn (ppm)	86	87	86	87	88	86	87
Tb (ppm)	0,6	0,5	0,5	0,6	0,5	0,6	0,5
Tm (ppm)	0,3	0,3	0,3	0,3	0,3	0,3	0,3
S I	1,16	0,11	0,87	2,06	2,68	1,93	-0,01
S II	8,17	7,76	8,73	8,86	7,71	8,37	7,81
S III	-2,16	-1,53	-2,65	-0,04	-0,14	-0,52	-1,72

Sample:	K05-15	K05-16	K05-17	K05-18	K05-19	K05-20	K05-47
Magma b./Loc.:	MS	MS	MS	MS	MS	MS	MS
Latitude (N):	-32,0070	-32,0069	-32,0067	-32,0067	-32,0068	-32,0067	-32,0215
Longitude (E):	26,2898	26,2899	26,2899	26,2901	26,2904	26,2906	26,3100
Altitude (m):	1320	1342	1357	1358	1357	1354	1407
SiO2 (wt %)	50,21	49,95	50,36	50,73	50,17	50,64	48,92
TiO2 (wt %)	0,92	0,88	0,98	1,03	0,87	1,00	0,91
Al2O3 (wt %)	15,24	15,11	15,38	15,69	15,89	15,46	14,82
Fe2O3(T) (wt %)	11,01	11,01	11,60	11,54	11,16	11,60	11,42
MnO (wt %)	0,17	0,17	0,18	0,18	0,18	0,19	0,17
MgO (wt %)	7,03	7,81	7,67	7,67	7,84	7,26	7,75
CaO (wt %)	10,85	10,87	10,91	10,85	11,07	11,12	10,93
Na2O (wt %)	2,31	2,36	2,42	2,48	2,34	2,32	2,39
K2O (wt %)	0,36	0,36	0,40	0,41	0,37	0,36	0,41
P2O5 (wt %)	0,12	0,12	0,13	0,14	0,11	0,13	0,12
SUM	98,2	98,6	100,0	100,7	100,0	100,1	97,8
Cs (ppm)	0,9	0,7	0,5	0,6	1,2	0,9	0,5
Tl (ppm)	b.d.	b.d.	b.d.	b.d.	0,2	0,2	b.d.
Rb (ppm)	8	8	8	9	14	8	8
Ba (ppm)	140	139	149	155	133	201	143
Th (ppm)	b.d.	b.d.	b.d.	1,3	b.d.	1,9	b.d.
U (ppm)	0,17	0,17	0,15	0,21	0,31	0,17	0,19
Nb (ppm)	5,3	5,2	5,1	5,9	5,1	5,3	6,1
Ta (ppm)	0,27	0,26	0,28	0,29	0,30	0,27	0,30
La (ppm)	6,99	6,72	6,85	7,51	6,68	7,18	6,88
Ce (ppm)	15,98	15,17	15,88	17,06	14,66	16,89	15,90
Pb (ppm)	4	2	3	5	4	2	3
Pr (ppm)	1,93	1,87	2,01	2,15	1,80	2,07	2,01
Mo (ppm)	1,7	1,4	1,5	1,1	1,2	1,4	1,3
Sr (ppm)	182	185	198	201	198	205	193
Nd (ppm)	10,1	9,7	10,2	10,4	9,3	10,8	10,7
Zr (ppm)	72	69	71	75	65	74	70
Hf (ppm)	1,79	1,82	1,91	2,02	1,64	2,00	1,78
Sm (ppm)	2,81	2,76	2,94	3,07	2,57	3,03	2,98
Eu (ppm)	0,96	0,88	1,00	1,00	0,91	1,00	1,06
Sn (ppm)	b.d.	b.d.	b.d.	0,6	0,6	b.d.	b.d.
Gd (ppm)	2,88	2,87	2,91	3,18	2,60	3,02	2,85
Dy (ppm)	3,54	3,38	3,50	3,82	3,21	3,68	3,21
Li (ppm)	9	5	6	5	6	12	5
Y (ppm)	23	23	23	24	21	24	24
Ho (ppm)	b.d.	b.d.	b.d.	b.d.	b.d.	b.d.	b.d.
Er (ppm)	1,98	2,03	2,16	2,20	1,81	2,12	2,14
Yb (ppm)	2,17	2,01	2,03	2,08	1,83	2,28	2,13
Lu (ppm)	0,31	0,30	0,31	0,31	0,28	0,30	0,29
Co (ppm)	36	39	37	38	38	37	35
Cr (ppm)	366	417	384	358	390	340	370
Cu (ppm)	97	91	94	94	93	98	100
Ni (ppm)	101	126	105	108	121	101	116
Sc (ppm)	34	33	34	34	33	35	35
V (ppm)	247	239	251	253	234	250	255
Zn (ppm)	85	86	86	87	84	87	87
Tb (ppm)	0,6	0,6	0,5	0,6	0,5	0,6	0,6
Tm (ppm)	0,3	0,3	0,3	0,3	0,3	0,3	0,3
S I	1,19	0,86	-0,42	-0,59	1,07	1,33	2,54
S II	8,16	9,85	8,09	9,42	7,91	8,21	8,16
S III	-0,81	-0,57	-0,64	-1,02	-1,47	-1,27	-1,35

Sample:	K05-48	K05-49	K05-50	K05-51	K05-24	K05-25	K05-26
Magma b./Loc.:	MS	MS	MS	MS	MS	MS	MS
Latitude (N):	-32,0216	-32,0218	-32,0217	-32,0212	-31,8977	-31,9011	-31,9012
Longitude (E):	26,3102	26,3105	26,3106	26,3097	26,3724	26,3748	26,3745
Altitude (m):	1413	1425	1431	1412	1390	1351	1361
SiO2 (wt %)	50,41	49,80	49,74	50,39	50,63	50,46	50,57
TiO2 (wt %)	1,00	0,85	0,73	0,90	0,93	0,93	0,93
Al2O3 (wt %)	15,26	14,94	15,26	15,33	15,73	15,42	15,43
Fe2O3(T) (wt %)	11,97	11,13	10,55	10,81	11,42	11,12	11,06
MnO (wt %)	0,18	0,17	0,17	0,17	0,18	0,17	0,17
MgO (wt %)	7,76	8,74	8,56	6,94	7,68	7,15	7,34
CaO (wt %)	11,16	10,59	11,48	11,02	11,17	11,08	11,05
Na2O (wt %)	2,42	2,36	2,30	2,25	2,42	2,42	2,56
K2O (wt %)	0,42	0,37	0,28	0,33	0,42	0,41	0,39
P2O5 (wt %)	0,13	0,12	0,08	0,12	0,12	0,12	0,12
SUM	100,7	99,1	99,1	98,3	100,7	99,3	99,6
Cs (ppm)	0,4	0,2	0,2	1,9	0,4	0,9	0,2
Tl (ppm)	b.d.	b.d.	b.d.	0,3	b.d.	b.d.	b.d.
Rb (ppm)	8	8	6	8	8	8	7
Ba (ppm)	153	134	113	133	146	152	147
Th (ppm)	b.d.	b.d.	b.d.	b.d.	b.d.	1,1	b.d.
U (ppm)	0,19	0,15	b.d.	0,17	0,14	0,14	0,17
Nb (ppm)	5,7	6,1	4,7	5,5	5,1	5,3	5,2
Ta (ppm)	0,29	0,29	0,24	0,28	0,26	0,28	0,27
La (ppm)	7,73	7,28	5,22	7,17	6,82	6,86	6,86
Ce (ppm)	16,56	15,62	12,02	16,07	15,33	15,61	15,75
Pb (ppm)	3	4	5	5	5	6	6
Pr (ppm)	2,01	1,93	1,53	2,01	1,93	1,97	1,95
Mo (ppm)	1,4	1,2	1,1	1,1	1,3	1,2	1,1
Sr (ppm)	198	176	182	180	208	196	191
Nd (ppm)	11,2	10,0	7,7	10,3	9,9	9,9	10,2
Zr (ppm)	75	80	56	72	69	74	70
Hf (ppm)	1,82	1,89	1,38	1,85	1,72	1,86	1,69
Sm (ppm)	2,90	2,85	2,23	2,83	2,73	2,85	2,89
Eu (ppm)	1,05	1,00	0,87	1,01	0,96	1,05	1,04
Sn (ppm)	0,5	b.d.	b.d.	b.d.	b.d.	b.d.	b.d.
Gd (ppm)	2,92	2,77	2,33	2,83	2,72	2,73	2,77
Dy (ppm)	3,43	3,32	2,71	3,44	3,29	3,47	3,46
Li (ppm)	5	5	4	11	5	11	4
Y (ppm)	24	22	18	23	21	23	22
Ho (ppm)	b.d.	b.d.	b.d.	b.d.	b.d.	b.d.	b.d.
Er (ppm)	2,15	1,97	1,70	2,25	1,94	2,14	1,94
Yb (ppm)	2,18	2,13	1,69	2,18	1,99	2,06	2,09
Lu (ppm)	0,33	0,29	0,26	0,30	0,31	0,27	0,30
Co (ppm)	35	37	34	34	37	36	36
Cr (ppm)	375	444	571	341	374	358	358
Cu (ppm)	107	91	78	96	100	102	98
Ni (ppm)	108	153	136	101	110	99	99
Sc (ppm)	36	32	35	34	34	36	34
V (ppm)	266	231	233	246	244	263	247
Zn (ppm)	91	86	79	86	87	87	86
Tb (ppm)	0,6	0,6	0,5	0,6	0,5	0,6	0,6
Tm (ppm)	0,3	0,3	0,2	0,3	0,3	0,3	0,3
S I	1,05	1,81	2,95	1,02	1,44	2,63	1,29
S II	7,38	9,23	8,95	8,79	6,87	7,37	6,28
S III	-2,49	0,40	2,42	0,23	-1,00	-0,13	-1,24

Sample:	K05-27	K05-29	K05-30	K05-40	K05-41	K05-42	K05-44
Magma b./Loc.:	MS	MS	MS	MS	MS	MS	MS
Latitude (N):	-31,9013	-31,9443	-31,9445	-31,9637	-31,9635	-31,9634	-31,9638
Longitude (E):	26,3742	26,3921	26,3923	26,3989	26,3983	26,3981	26,3973
Altitude (m):	1368	1365	1359	1353	1363	1367	1359
SiO2 (wt %)	50,90	50,75	50,27	49,95	50,78	50,27	50,76
TiO2 (wt %)	1,01	0,90	0,97	0,93	0,90	0,70	0,82
Al2O3 (wt %)	15,21	15,84	15,53	15,46	15,95	16,40	16,12
Fe2O3(T) (wt %)	12,04	11,44	11,51	11,17	11,06	11,21	10,50
MnO (wt %)	0,19	0,18	0,18	0,17	0,17	0,17	0,16
MgO (wt %)	7,27	7,44	7,36	7,49	7,62	7,85	7,55
CaO (wt %)	10,95	10,87	10,73	10,72	10,68	10,94	11,11
Na2O (wt %)	2,44	2,39	2,41	2,25	2,29	2,13	2,22
K2O (wt %)	0,38	0,37	0,41	0,42	0,43	0,28	0,36
P2O5 (wt %)	0,12	0,11	0,12	0,12	0,12	0,08	0,11
SUM	100,5	100,3	99,5	98,7	100,0	100,0	99,7
Cs (ppm)	0,4	0,1	0,2	0,8	0,3	0,3	0,2
Tl (ppm)	b.d.	b.d.	b.d.	b.d.	b.d.	b.d.	b.d.
Rb (ppm)	7	9	9	10	11	5	7
Ba (ppm)	147	142	149	156	150	116	135
Th (ppm)	b.d.	b.d.	b.d.	b.d.	b.d.	b.d.	b.d.
U (ppm)	0,14	0,15	0,17	0,20	0,18	0,14	0,17
Nb (ppm)	5,5	5,1	5,6	5,8	5,7	3,7	5,0
Ta (ppm)	0,28	0,25	0,27	0,29	0,28	0,20	0,22
La (ppm)	6,70	6,96	7,82	7,79	7,63	5,30	6,83
Ce (ppm)	15,63	15,22	17,25	16,52	16,40	11,32	14,69
Pb (ppm)	4	3	6	6	6	7	6
Pr (ppm)	1,94	1,83	2,14	2,03	2,02	1,39	1,88
Mo (ppm)	1,7	1,1	1,1	1,1	1,0	0,9	1,0
Sr (ppm)	197	197	199	191	188	194	189
Nd (ppm)	10,1	9,9	11,7	9,9	10,2	7,0	9,3
Zr (ppm)	71	69	74	75	75	50	67
Hf (ppm)	1,92	1,83	1,86	1,98	1,92	1,39	1,69
Sm (ppm)	2,77	2,71	3,13	2,95	2,86	2,03	2,64
Eu (ppm)	1,00	1,09	1,10	0,90	0,91	0,79	0,84
Sn (ppm)	b.d.	b.d.	b.d.	0,7	0,6	b.d.	0,6
Gd (ppm)	2,85	2,69	2,92	2,97	2,90	2,10	2,59
Dy (ppm)	3,59	3,21	3,63	3,45	3,53	2,60	3,17
Li (ppm)	5	4	4	8	6	5	5
Y (ppm)	22	23	24	24	24	17	21
Ho (ppm)	b.d.	b.d.	b.d.	b.d.	b.d.	b.d.	b.d.
Er (ppm)	2,21	1,94	2,22	2,09	2,13	1,53	1,90
Yb (ppm)	2,09	2,02	2,14	2,01	2,07	1,51	1,90
Lu (ppm)	0,31	0,31	0,31	0,30	0,31	0,23	0,30
Co (ppm)	36	37	36	41	41	44	39
Cr (ppm)	346	349	339	405	403	445	472
Cu (ppm)	98	97	97	97	97	103	85
Ni (ppm)	92	105	101	110	115	124	101
Sc (ppm)	36	32	34	35	34	33	35
V (ppm)	265	231	244	245	242	215	239
Zn (ppm)	89	86	86	86	84	82	79
Tb (ppm)	0,6	0,6	0,6				
Tm (ppm)	0,3	0,3	0,3				
S I	1,19	0,75	1,19	0,31	1,42	3,66	0,13
S II	6,14	6,55	6,86	8,40	7,89	5,25	8,17
S III	-0,68	-2,91	-2,05	-1,25	-1,51	-2,59	-1,03

Sample:	K05-46	K05-208	K05-209	K05-93	K05-94	K05-95	K05-96
Magma b./Loc.:	MS	MS/L7	MS/L7	MS/L4b	MS/L4b	MS/L4b	MS/L4b
Latitude (N):	-31,9638	-31,8177	-31,8175	-31,9730	-31,9713	-31,9713	-31,9713
Longitude (E):	26,3973	26,3198	26,3200	26,2544	26,2518	26,2518	26,2517
Altitude (m):	1366	1933	1917	1539	1673	1673	1670
SiO2 (wt %)	49,99	50,26	50,44	50,75	50,87	51,36	50,46
TiO2 (wt %)	0,70	0,95	0,97	0,94	0,95	0,95	0,91
Al2O3 (wt %)	15,74	15,29	15,40	15,58	15,67	15,67	15,84
Fe2O3(T) (wt %)	9,93	11,25	11,99	11,17	11,19	11,40	10,91
MnO (wt %)	0,16	0,17	0,18	0,17	0,17	0,17	0,17
MgO (wt %)	8,05	7,00	7,53	7,22	7,05	7,06	7,50
CaO (wt %)	11,61	10,81	10,69	10,66	10,71	10,70	10,66
Na2O (wt %)	2,14	2,42	2,46	2,24	2,25	2,33	2,20
K2O (wt %)	0,32	0,43	0,44	0,42	0,34	0,40	0,41
P2O5 (wt %)	0,09	0,12	0,12	0,12	0,13	0,13	0,12
SUM	98,7	98,7	100,2	99,3	99,3	100,2	99,2
Cs (ppm)	0,2	1,5	0,6	1,1	2,1	0,6	1,2
Tl (ppm)	b.d.	b.d.	b.d.	b.d.	0,2	0,2	0,2
Rb (ppm)	7	9	8	10	8	8	9
Ba (ppm)	117	150	161	155	132	153	146
Th (ppm)	b.d.	b.d.	b.d.	b.d.	1,0	b.d.	b.d.
U (ppm)	0,16	0,19	0,16	0,21	0,20	0,22	0,22
Nb (ppm)	4,6	5,5	5,4	5,5	5,3	7,2	5,3
Ta (ppm)	0,21	0,29	0,27	0,29	0,30	0,31	0,25
La (ppm)	6,26	7,87	6,93	7,80	7,87	8,02	7,82
Ce (ppm)	13,29	17,78	16,18	16,79	17,29	17,35	16,86
Pb (ppm)	6	2	4	5	7	6	8
Pr (ppm)	1,71	2,22	2,01	2,13	2,13	2,20	2,07
Mo (ppm)	1,0	1,2	1,0	0,8	0,8	1,4	1,0
Sr (ppm)	182	187	200	190	192	189	187
Nd (ppm)	8,0	12,0	10,7	10,6	10,9	10,4	10,4
Zr (ppm)	58	80	78	78	81	80	78
Hf (ppm)	1,56	1,89	1,71	2,08	2,04	2,10	2,13
Sm (ppm)	2,45	2,90	2,63	3,21	3,06	3,11	2,89
Eu (ppm)	0,75	1,12	0,95	0,89	0,89	0,88	0,89
Sn (ppm)	0,5	b.d.	b.d.	0,5	0,5	0,7	0,6
Gd (ppm)	2,40	3,34	2,68	3,06	3,18	3,07	3,01
Dy (ppm)	2,77	3,90	3,73	3,72	3,67	3,62	3,58
Li (ppm)	6	2	b.d.	9	11	9	7
Y (ppm)	20	26	23	25	24	25	24
Ho (ppm)	b.d.	b.d.	b.d.	b.d.	b.d.	b.d.	b.d.
Er (ppm)	1,74	2,01	2,03	2,15	2,21	2,29	2,13
Yb (ppm)	1,64	2,15	2,10	2,22	2,32	2,26	2,07
Lu (ppm)	0,28	0,30	0,33	0,34	0,35	0,33	0,34
Co (ppm)	38	35	35	40	41	41	40
Cr (ppm)	600	372	392	322	322	421	332
Cu (ppm)	73	100	95	99	101	102	94
Ni (ppm)	108	99	101	102	99	101	109
Sc (ppm)	37	34	34	35	36	35	35
V (ppm)	241	246	240	251	261	252	245
Zn (ppm)	72	87	85	84	85	86	83
Tb (ppm)		0,6	0,5				
Tm (ppm)		0,3	0,3				
S I	1,09	-0,59	-1,20	0,81	1,05	2,12	0,46
S II	9,75	9,23	8,31	8,87	9,39	7,99	8,94
S III	0,56	-0,83	-0,71	-1,91	0,23	-0,34	-1,87

Sample:	K05-97	K05-98	K05-100	K05-189	K05-190	K05-191A	K05-191B
Magma b./Loc.:	MS/L4b	MS/L4b	MS/L4b	HS/L8	HS/L8	HS/L8	HS/L8
Latitude (N):	-31,9713	-31,9714	-31,9713	-31,7827	-31,7827	-31,7811	-31,7811
Longitude (E):	26,2518	26,2518	26,2518	26,2994	26,2994	26,2992	26,2992
Altitude (m):	1673	1672	1669	1813	1823	1851	1851
SiO2 (wt %)	51,47	50,93	50,91	52,42	52,64	53,04	53,60
TiO2 (wt %)	0,94	0,89	0,89	1,20	1,14	1,37	1,87
Al2O3 (wt %)	15,85	16,47	15,80	15,06	15,58	14,33	12,95
Fe2O3(T) (wt %)	11,15	10,39	11,12	10,62	10,27	11,48	13,04
MnO (wt %)	0,17	0,16	0,17	0,16	0,15	0,17	0,18
MgO (wt %)	7,27	7,33	7,53	6,16	5,98	5,23	3,78
CaO (wt %)	10,60	10,77	10,61	9,14	9,32	8,90	7,23
Na2O (wt %)	2,23	2,23	2,18	2,48	2,50	2,51	2,92
K2O (wt %)	0,41	0,43	0,42	0,91	0,86	1,12	1,71
P2O5 (wt %)	0,13	0,13	0,12	0,20	0,19	0,23	0,32
SUM	100,2	99,7	99,7	98,3	98,6	98,4	97,6
Cs (ppm)	0,7	0,6	1,2	0,4	0,8	0,4	0,9
Tl (ppm)	b.d.	b.d.	0,2	b.d.	b.d.	b.d.	0,2
Rb (ppm)	9	10	11	16	17	23	43
Ba (ppm)	166	156	144	335	260	307	468
Th (ppm)	b.d.	b.d.	1,1	2,1	2,0	2,4	3,4
U (ppm)	0,21	0,22	0,19	0,39	0,36	0,42	0,70
Nb (ppm)	6,4	5,8	5,7	5,0	5,5	6,7	8,7
Ta (ppm)	0,32	0,32	0,30	0,31	0,26	0,34	0,50
La (ppm)	8,26	7,98	8,18	12,02	13,03	15,96	21,27
Ce (ppm)	18,10	17,46	17,96	27,03	28,94	36,42	48,39
Pb (ppm)	6	7	7	7	6	2	7
Pr (ppm)	2,35	2,21	2,25	3,28	3,51	4,30	5,61
Mo (ppm)	1,0	0,9	0,9	1,5	2,0	1,9	1,8
Sr (ppm)	191	191	183	203	204	200	226
Nd (ppm)	11,7	10,7	10,7	16,7	16,5	20,9	27,4
Zr (ppm)	84	81	83	111	104	124	162
Hf (ppm)	2,24	2,10	2,16	3,01	2,79	3,52	4,59
Sm (ppm)	3,16	3,12	2,87	4,10	3,79	5,13	6,41
Eu (ppm)	0,91	0,90	0,91	1,31	1,28	1,50	1,67
Sn (ppm)	0,5	b.d.	b.d.	b.d.	0,6	0,7	0,9
Gd (ppm)	3,08	3,15	3,02	3,80	3,85	4,76	5,98
Dy (ppm)	3,73	3,54	3,73	4,44	4,21	5,30	6,97
Li (ppm)	7	6	10	2	5	2	8
Y (ppm)	28	25	25	26	28	36	45
Ho (ppm)	b.d.	b.d.	b.d.	b.d.	b.d.	1	1
Er (ppm)	2,21	2,12	2,26	2,45	2,26	2,85	3,38
Yb (ppm)	2,25	2,21	2,28	2,40	2,47	2,82	3,53
Lu (ppm)	0,35	0,34	0,36	0,36	0,35	0,42	0,53
Co (ppm)	40	39	42	32	31	33	37
Cr (ppm)	339	306	393	336	349	227	100
Cu (ppm)	99	89	100	33	32	31	27
Ni (ppm)	101	112	117	13	13	9	6
Sc (ppm)	35	33	34	29	27	31	32
V (ppm)	249	239	244	220	210	239	256
Zn (ppm)	84	80	85	93	103	99	120
Tb (ppm)				0,7	0,7	0,8	1,1
Tm (ppm)				0,3	0,4	0,5	0,6
S I	0,71	1,68	1,36	-27,81	-30,02	-24,92	-29,57
S II	9,53	10,05	7,94	1,17	-0,62	1,07	-1,16
S III	-2,85	-1,46	-0,30	1,64	0,74	1,33	4,05

Sample:	K05-192	K05-194	K05-195	K05-196	K05-197	K05-205	K05-167
Magma b./Loc.:	HS/L8	HS/L8	HS/L6	HS/L6	HS/L6	HS/L5	GVS
Latitude (N):	-31,7810	-31,7740	-31,8586	-31,8586	-31,8586	-31,8586	-31,8237
Longitude (E):	26,2994	26,3006	26,3466	26,3466	26,3466	26,3466	26,2672
Altitude (m):	1905	1951	1590	1651	1603	1329	1481
SiO2 (wt %)	54,68	53,73	51,73	51,51	53,07	52,96	51,01
TiO2 (wt %)	1,76	1,96	1,15	0,88	1,26	1,14	0,99
Al2O3 (wt %)	13,33	12,84	15,28	15,80	15,19	15,64	15,47
Fe2O3(T) (wt %)	13,00	13,77	10,51	9,33	10,83	10,09	12,02
MnO (wt %)	0,17	0,18	0,15	0,14	0,18	0,15	0,18
MgO (wt %)	4,20	3,60	6,39	7,20	5,99	6,12	6,16
CaO (wt %)	8,06	7,69	9,24	9,02	9,10	9,18	10,51
Na2O (wt %)	2,61	2,78	2,49	2,41	2,37	2,49	2,58
K2O (wt %)	1,49	1,50	0,88	0,79	0,82	0,91	0,69
P2O5 (wt %)	0,31	0,35	0,19	0,14	0,21	0,20	0,15
SUM	99,6	98,4	98,0	97,2	99,0	98,9	99,8
Cs (ppm)	0,6	0,6	0,3	0,6	0,3	0,7	0,2
Tl (ppm)	0,3	b.d.	b.d.	b.d.	0,2	b.d.	b.d.
Rb (ppm)	30	30	16	18	16	20	12
Ba (ppm)	401	456	271	226	271	262	203
Th (ppm)	3,5	3,4	1,8	1,5	1,9	2,0	1,6
U (ppm)	b.d.	b.d.	b.d.	b.d.	b.d.	b.d.	0,32
Nb (ppm)	7,8	8,4	5,0	4,0	5,4	6,2	8,1
Ta (ppm)	0,40	0,50	0,28	0,23	0,30	0,31	0,42
La (ppm)	18,43	20,78	11,40	8,89	12,30	13,89	10,86
Ce (ppm)	42,19	47,45	26,17	20,84	28,11	31,16	22,60
Pb (ppm)	11	4	b.d.	4	5	7	b.d.
Pr (ppm)	4,98	5,48	3,17	2,43	3,37	3,60	2,58
Mo (ppm)	1,8	2,0	2,0	1,0	1,7	1,3	0,4
Sr (ppm)	197	186	210	218	193	216	206
Nd (ppm)	25,5	27,9	16,0	12,4	17,0	18,9	13,4
Zr (ppm)	161	176	103	85	110	106	91
Hf (ppm)	4,14	5,02	2,71	2,11	2,82	3,09	2,35
Sm (ppm)	5,78	6,99	3,47	2,76	4,14	4,46	3,23
Eu (ppm)	1,52	1,72	1,20	1,01	1,34	1,34	1,13
Sn (ppm)	0,9	0,8	0,5	b.d.	b.d.	b.d.	0,8
Gd (ppm)	5,33	6,40	3,42	2,89	3,80	4,18	3,19
Dy (ppm)	5,96	7,39	4,26	3,21	4,54	4,66	3,88
Li (ppm)	12	2	b.d.	3	9	3	b.d.
Y (ppm)	39	45	25	20	28	31	26
Ho (ppm)	1	1	b.d.	b.d.	b.d.	b.d.	b.d.
Er (ppm)	3,68	3,79	2,23	1,66	2,58	2,62	2,17
Yb (ppm)	3,48	3,86	2,36	1,77	2,56	2,57	2,43
Lu (ppm)	0,51	0,56	0,35	0,26	0,37	0,37	0,35
Co (ppm)	35	39	31	29	31	32	32
Cr (ppm)	117	57	379	486	305	375	277
Cu (ppm)	30	28	34	32	33	36	103
Ni (ppm)	7	5	15	14	11	15	64
Sc (ppm)	35	33	28	25	30	27	37
V (ppm)	270	263	211	184	227	214	262
Zn (ppm)	117	124	89	78	93	90	91
Tb (ppm)	1,1	1,2	0,6	0,5	0,8	0,7	0,6
Tm (ppm)	0,5	0,6	0,3	0,3	0,4	0,4	0,3
S I	-27,56	-30,01	-27,83	-30,14	-25,17	-27,24	3,19
S II	0,27	1,45	1,91	-0,01	1,18	1,86	0,21
S III	-0,10	1,64	2,07	2,96	0,57	2,36	-0,48

Sample:	K05-168	K05-169	K05-170	K05-171	K05-172	K05-173	K05-174
Magma b./Loc.:	GVS	GVS	GVS	GVS	GVS	GVS	GVS
Latitude (N):	-31,8239	-31,8240	-31,8241	-31,8242	-31,8419	-31,8412	-31,8413
Longitude (E):	26,2674	26,2675	26,2674	26,2674	26,3086	26,3099	26,3099
Altitude (m):	1537	1538	1547	1552	1819	1766	1780
SiO2 (wt %)	51,14	51,11	50,87	50,79	51,42	51,05	49,89
TiO2 (wt %)	1,05	1,06	0,97	1,05	1,09	1,11	1,03
Al2O3 (wt %)	14,93	14,91	15,49	15,22	15,10	15,00	14,30
Fe2O3(T) (wt %)	11,86	11,86	11,50	11,60	12,38	12,48	11,86
MnO (wt %)	0,18	0,18	0,18	0,18	0,19	0,19	0,18
MgO (wt %)	6,09	6,02	6,30	6,27	6,12	6,15	6,29
CaO (wt %)	10,32	10,35	10,37	10,56	10,35	10,38	10,41
Na2O (wt %)	2,71	2,55	2,61	2,52	2,74	2,64	2,47
K2O (wt %)	0,76	0,71	0,66	0,70	0,75	0,75	0,68
P2O5 (wt %)	0,16	0,16	0,16	0,17	0,16	0,17	0,16
SUM	99,2	98,9	99,1	99,1	100,3	99,9	97,3
Cs (ppm)	0,5	0,2	0,2	0,2	0,2	0,5	0,3
Tl (ppm)	b.d.	b.d.	b.d.	b.d.	b.d.	b.d.	b.d.
Rb (ppm)	17	13	15	13	14	15	12
Ba (ppm)	216	211	198	207	222	223	206
Th (ppm)	1,5	1,5	1,3	1,3	1,4	1,4	1,4
U (ppm)	0,30	0,29	0,29	0,28	0,28	0,28	0,26
Nb (ppm)	8,2	8,1	8,7	8,1	8,4	8,4	7,8
Ta (ppm)	0,48	0,50	0,43	0,45	0,50	0,48	0,46
La (ppm)	11,16	11,82	11,38	11,91	11,45	11,96	10,88
Ce (ppm)	24,46	25,28	25,52	24,82	25,42	25,76	23,35
Pb (ppm)	4	4	6	4	b.d.	7	5
Pr (ppm)	3,04	2,90	2,97	2,87	3,02	3,04	2,71
Mo (ppm)	0,4	0,2	b.d.	0,2	0,4	0,7	0,5
Sr (ppm)	197	197	203	198	207	209	189
Nd (ppm)	14,7	14,8	15,6	15,2	15,4	14,5	13,4
Zr (ppm)	103	105	95	100	107	107	104
Hf (ppm)	2,51	2,47	2,50	2,52	2,54	2,56	2,38
Sm (ppm)	3,70	3,97	3,66	3,61	3,65	3,64	3,32
Eu (ppm)	1,05	1,13	1,16	1,11	1,06	1,14	1,03
Sn (ppm)	0,6	2,9	b.d.	0,5	0,7	0,8	0,7
Gd (ppm)	3,47	3,30	3,53	3,40	3,30	3,65	3,22
Dy (ppm)	4,00	4,16	4,15	4,25	4,31	3,97	3,96
Li (ppm)	3	b.d.	5	b.d.	2	b.d.	22
Y (ppm)	27	27	28	27	27	28	25
Ho (ppm)	b.d.	b.d.	b.d.	b.d.	b.d.	b.d.	b.d.
Er (ppm)	2,34	2,27	2,49	2,16	2,34	2,13	2,04
Yb (ppm)	2,25	2,37	2,50	2,27	2,31	2,28	2,25
Lu (ppm)	0,34	0,36	0,39	0,35	0,37	0,35	0,34
Co (ppm)	34	34	32	34	34	34	35
Cr (ppm)	272	269	251	274	284	268	301
Cu (ppm)	106	109	99	105	109	109	106
Ni (ppm)	62	63	64	65	64	64	66
Sc (ppm)	37	37	37	38	38	38	38
V (ppm)	267	264	245	265	267	265	274
Zn (ppm)	94	94	89	92	95	94	97
Tb (ppm)	0,7	0,6	0,7	0,6	0,6	0,7	0,6
Tm (ppm)	0,4	0,4	0,3	0,3	0,4	0,4	0,4
S I	2,21	2,69	3,10	2,73	4,14	3,29	1,76
S II	-1,75	-1,83	-1,21	-1,20	-2,47	-1,54	-2,23
S III	1,87	1,15	0,06	0,92	2,43	2,01	1,46

Sample:	K05-175	K05-176	K05-177	K05-178	K05-179	K05-180	K05-181
Magma b./Loc.:	GVS	GVS	GVS	GVS	GVS	GVS	GVS
Latitude (N):	-31,8414	-31,8415	-31,8415	-31,8469	-31,8467	-31,8465	-31,8473
Longitude (E):	26,3096	26,3097	26,3096	26,2953	26,2947	26,2941	26,2947
Altitude (m):	1804	1818	1831	1522	1527	1527	1552
SiO2 (wt %)	51,33	48,03	51,10	51,18	51,25	50,12	49,94
TiO2 (wt %)	1,02	1,05	1,05	1,06	1,00	1,06	0,95
Al2O3 (wt %)	15,16	14,01	14,72	15,05	15,23	14,55	14,99
Fe2O3(T) (wt %)	11,88	12,04	12,00	11,85	11,77	12,12	11,07
MnO (wt %)	0,19	0,19	0,19	0,19	0,19	0,19	0,17
MgO (wt %)	6,24	6,25	6,38	6,24	6,09	6,26	6,60
CaO (wt %)	10,43	10,39	10,42	10,52	10,20	10,52	10,73
Na2O (wt %)	2,45	2,43	2,63	2,67	2,55	2,60	2,50
K2O (wt %)	0,62	0,66	0,68	0,71	0,68	0,75	0,64
P2O5 (wt %)	0,15	0,16	0,15	0,16	0,15	0,17	0,15
SUM	99,5	95,2	99,3	99,6	99,1	98,3	97,7
Cs (ppm)	0,4	0,4	0,4	0,2	0,2	0,3	0,3
Tl (ppm)	b.d.	b.d.	b.d.	b.d.	b.d.	b.d.	b.d.
Rb (ppm)	14	14	13	13	14	13	12
Ba (ppm)	194	199	208	224	210	223	200
Th (ppm)	1,4	1,2	1,4	1,6	1,4	1,3	1,3
U (ppm)	0,22	0,23	0,29	0,29	0,26	0,28	0,26
Nb (ppm)	9,0	8,3	7,8	10,5	8,7	7,8	7,3
Ta (ppm)	0,45	0,42	0,44	0,51	0,47	0,47	0,42
La (ppm)	11,06	11,31	11,27	10,76	10,75	10,49	10,39
Ce (ppm)	25,36	25,17	24,33	24,05	24,44	23,25	22,62
Pb (ppm)	6	6	3	2	6	6	4
Pr (ppm)	2,96	2,90	2,93	2,88	2,88	2,80	2,67
Mo (ppm)	b.d.	b.d.	0,3	0,3	b.d.	0,5	b.d.
Sr (ppm)	199	198	200	202	195	211	201
Nd (ppm)	15,2	14,7	15,0	14,7	15,3	13,8	13,1
Zr (ppm)	97	95	96	107	102	105	96
Hf (ppm)	2,50	2,36	2,49	2,77	2,61	2,43	2,14
Sm (ppm)	3,61	3,58	3,58	3,44	3,44	3,16	3,08
Eu (ppm)	1,25	1,19	1,15	1,13	1,15	1,13	1,07
Sn (ppm)	0,7	0,5	0,7	1,9	b.d.	0,8	0,6
Gd (ppm)	3,19	3,32	3,24	3,24	3,27	3,13	2,82
Dy (ppm)	3,96	3,84	4,10	4,11	3,72	3,90	3,63
Li (ppm)	5	6	4	4	7	4	b.d.
Y (ppm)	27	27	27	26	26	25	23
Ho (ppm)	b.d.	b.d.	b.d.	b.d.	b.d.	b.d.	b.d.
Er (ppm)	2,47	2,32	2,12	2,18	2,30	2,11	1,96
Yb (ppm)	2,42	2,35	2,19	2,26	2,40	2,17	2,04
Lu (ppm)	0,34	0,36	0,34	0,35	0,36	0,34	0,32
Co (ppm)	33	34	35	34	34	34	33
Cr (ppm)	257	256	287	273	277	288	304
Cu (ppm)	102	104	111	103	104	108	98
Ni (ppm)	64	63	66	63	68	63	68
Sc (ppm)	38	38	40	39	36	38	38
V (ppm)	262	271	279	276	244	269	267
Zn (ppm)	92	94	95	95	93	97	90
Tb (ppm)	0,7	0,7	0,6	0,6	0,7	0,6	0,6
Tm (ppm)	0,3	0,3	0,3	0,3	0,4	0,3	0,3
S I	4,35	2,60	3,45	5,59	4,07	2,07	2,19
S II	-2,41	-1,95	-1,72	-2,23	-2,94	-2,46	-1,44
S III	2,17	1,33	0,81	3,37	1,50	1,40	2,10

Sample:	K05-182	K05-183	K05-32	K05-33	K05-34	K05-31	K05-35
Magma b./Loc.:	GVS	GVS	GVS	GVS	GVS	GVS	GVS
Latitude (N):	-31,8477	-31,9557	-31,8984	-31,8984	-31,8983	-31,8983	-31,8886
Longitude (E):	26,2947	26,2986	26,3144	26,3146	26,3147	26,3148	26,3115
Altitude (m):	1570	1467	1579	1567	1557	1542	1675
SiO2 (wt %)	51,09	49,88	52,11	51,96	52,29	52,33	51,30
TiO2 (wt %)	0,99	1,06	0,72	0,92	1,30	1,19	1,07
Al2O3 (wt %)	15,13	14,60	15,86	15,19	14,17	15,24	15,45
Fe2O3(T) (wt %)	12,03	12,12	10,75	12,37	13,63	13,01	11,81
MnO (wt %)	0,19	0,19	0,18	0,20	0,21	0,19	0,17
MgO (wt %)	6,65	6,28	7,09	6,28	5,35	5,71	5,91
CaO (wt %)	10,75	10,40	10,99	10,43	9,36	10,06	10,21
Na2O (wt %)	2,68	2,51	2,27	2,32	2,54	2,55	2,40
K2O (wt %)	0,70	0,74	0,51	0,59	0,86	0,82	0,72
P2O5 (wt %)	0,14	0,17	0,11	0,11	0,20	0,19	0,17
SUM	100,3	97,9	100,6	100,4	99,9	101,3	99,2
Cs (ppm)	0,2	0,2	0,3	0,3	0,3	0,4	0,3
Tl (ppm)	b.d.	b.d.	b.d.	b.d.	b.d.	0,2	b.d.
Rb (ppm)	12	13	12	13	17	19	14
Ba (ppm)	212	220	161	193	264	255	220
Th (ppm)	1,3	1,6	1,3	1,4	2,2	1,9	1,8
U (ppm)	0,24	0,27	0,24	0,27	0,40	0,37	0,34
Nb (ppm)	7,3	7,6	7,0	7,5	10,8	10,3	8,7
Ta (ppm)	0,40	0,45	0,38	0,39	0,60	0,55	0,48
La (ppm)	9,94	10,60	9,35	10,20	14,71	14,44	12,32
Ce (ppm)	21,71	23,71	19,49	21,31	30,80	30,07	26,03
Pb (ppm)	3	5	5	7	7	7	8
Pr (ppm)	2,53	2,89	2,40	2,66	4,01	3,76	3,21
Mo (ppm)	0,4	0,3	b.d.	1,3	1,3	1,4	1,3
Sr (ppm)	212	205	199	198	195	203	198
Nd (ppm)	12,8	13,8	11,1	12,6	18,3	17,4	15,1
Zr (ppm)	98	103	79	88	133	117	111
Hf (ppm)	2,20	2,35	2,18	2,24	3,64	3,19	2,91
Sm (ppm)	2,79	3,43	2,78	3,12	4,36	4,42	4,16
Eu (ppm)	1,07	1,16	0,90	1,00	1,24	1,20	1,09
Sn (ppm)	0,7	0,7	0,5	0,5	0,8	0,8	0,6
Gd (ppm)	2,81	3,19	2,84	3,26	4,42	4,27	3,82
Dy (ppm)	3,62	3,92	3,17	3,72	5,22	4,71	4,39
Li (ppm)	b.d.	b.d.	6	8	7	8	10
Y (ppm)	24	25	23	26	35	36	28
Ho (ppm)	b.d.	b.d.	b.d.	b.d.	1	1	b.d.
Er (ppm)	1,94	2,20	1,91	2,29	3,07	2,88	2,58
Yb (ppm)	2,04	2,16	1,94	2,30	3,27	3,06	2,76
Lu (ppm)	0,34	0,37	0,29	0,32	0,49	0,46	0,41
Co (ppm)	34	35	35	38	39	40	38
Cr (ppm)	298	259	261	262	110	176	241
Cu (ppm)	98	111	70	98	130	130	109
Ni (ppm)	68	64	65	55	40	52	61
Sc (ppm)	39	39	39	41	43	40	38
V (ppm)	272	273	240	271	303	282	260
Zn (ppm)	92	96	79	96	108	103	94
Tb (ppm)	0,6	0,6					
Tm (ppm)	0,3	0,3					
S I	3,44	3,09	3,76	3,39	3,80	3,13	2,45
S II	-0,95	-2,89	-0,79	-3,61	-5,81	-2,87	-1,93
S III	1,78	0,71	-0,27	-2,10	-2,34	-3,51	-0,29

Sample:	K05-36	K05-37	K05-38	K05-39	K05-1	K05-2	K05-3
Magma b./Loc.:	GVS	GVS	GVS	GVS	GVS	GVS	GVS
Latitude (N):	-31,8984	-31,8983	-31,8883	-31,8982	-31,8882	-31,8881	-31,8882
Longitude (E):	26,3149	26,3153	26,3118	26,3153	26,3117	26,3115	26,3114
Altitude (m):	1541	1564	1652	1616	1649	1664	1673
SiO2 (wt %)	51,47	51,38	51,71	51,99	51,35	51,27	51,01
TiO2 (wt %)	1,01	0,96	1,07	1,07	1,08	1,04	1,04
Al2O3 (wt %)	15,40	15,21	15,32	15,29	15,02	15,59	15,12
Fe2O3(T) (wt %)	11,81	11,96	11,79	12,03	12,62	12,55	12,99
MnO (wt %)	0,18	0,18	0,18	0,18	0,19	0,19	0,20
MgO (wt %)	6,19	6,24	6,08	6,06	6,37	6,68	6,67
CaO (wt %)	10,35	10,25	10,19	10,15	10,95	11,17	10,74
Na2O (wt %)	2,30	2,31	2,33	2,35	2,66	2,36	2,40
K2O (wt %)	0,65	0,65	0,70	0,70	0,69	0,65	0,64
P2O5 (wt %)	0,15	0,16	0,17	0,17	0,18	0,15	0,14
SUM	99,5	99,3	99,5	100,0	101,1	101,7	101,0
Cs (ppm)	0,4	0,4	0,4	0,4	0,4	0,3	0,3
Tl (ppm)	b.d.	0,2	b.d.	b.d.	b.d.	b.d.	b.d.
Rb (ppm)	14	14	17	18	15	14	13
Ba (ppm)	203	206	214	214	206	198	200
Th (ppm)	1,8	1,6	1,7	1,6	1,4	1,3	1,2
U (ppm)	0,31	0,35	0,32	0,30	0,29	0,23	0,23
Nb (ppm)	8,7	8,2	10,2	9,8	9,5	8,0	7,6
Ta (ppm)	0,47	0,46	0,51	0,45	0,49	0,44	0,42
La (ppm)	11,71	11,67	13,00	12,74	10,85	10,34	9,97
Ce (ppm)	24,65	24,68	27,46	26,79	24,89	23,17	22,44
Pb (ppm)	8	7	7	7	6	6	4
Pr (ppm)	2,99	3,08	3,31	3,29	2,89	2,78	2,60
Mo (ppm)	1,2	1,3	1,1	1,3	2,9	2,0	2,2
Sr (ppm)	193	193	192	192	198	210	208
Nd (ppm)	14,6	14,3	15,3	15,6	14,4	13,2	12,4
Zr (ppm)	103	104	111	110	96	92	90
Hf (ppm)	2,82	2,71	2,79	2,92	2,70	2,37	2,27
Sm (ppm)	3,72	3,62	4,10	3,71	3,80	3,29	3,15
Eu (ppm)	1,01	1,09	1,10	1,07	1,05	1,08	1,04
Sn (ppm)	0,9	0,7	0,7	0,6	0,6	0,7	0,6
Gd (ppm)	3,52	3,65	3,75	3,82	3,38	3,06	3,11
Dy (ppm)	4,07	4,10	4,24	4,20	4,01	3,71	3,57
Li (ppm)	7	8	6	6	5	5	4
Y (ppm)	27	27	32	31	27	25	24
Ho (ppm)	b.d.	b.d.	b.d.	b.d.	b.d.	b.d.	b.d.
Er (ppm)	2,48	2,52	2,48	2,60	2,41	2,28	2,28
Yb (ppm)	2,57	2,58	2,57	2,66	2,46	2,30	2,25
Lu (ppm)	0,38	0,38	0,37	0,40	0,37	0,32	0,34
Co (ppm)	39	39	38	38	38	37	39
Cr (ppm)	271	285	246	262	325	297	290
Cu (ppm)	102	102	107	108	111	104	105
Ni (ppm)	64	67	62	62	66	70	68
Sc (ppm)	38	38	38	38	39	38	40
V (ppm)	261	252	268	269	284	269	287
Zn (ppm)	92	92	93	94	99	94	97
Tb (ppm)					0,7	0,6	0,6
Tm (ppm)					0,4	0,3	0,3
S I	2,56	2,66	2,73	2,76	4,52	3,48	3,70
S II	-1,47	-1,92	-0,55	-1,42	-2,90	-1,84	-3,27
S III	0,29	-0,86	-0,13	-0,18	2,41	0,93	1,62

Sample:	K05-4	K05-5	K05-6	K05-7	K05-8	K05-9	K05-10
Magma b./Loc.:	GVS	GVS	GVS	GVS	GVS	GVS	GVS
Latitude (N):	-31,8882	-31,8887	-31,8895	-31,8907	-31,9731	-31,9697	-31,9697
Longitude (E):	26,3113	26,3115	26,3043	26,3004	26,2955	26,2989	26,2987
Altitude (m):	1670	1679	1564	1494	1503	1481	1507
SiO2 (wt %)	51,70	51,57	51,62	51,68	51,08	51,40	51,11
TiO2 (wt %)	0,98	0,89	0,99	1,02	0,95	1,04	1,03
Al2O3 (wt %)	15,60	15,69	14,85	15,05	15,20	15,10	14,96
Fe2O3(T) (wt %)	11,53	11,48	12,23	11,58	11,45	11,73	11,64
MnO (wt %)	0,18	0,18	0,19	0,18	0,18	0,18	0,18
MgO (wt %)	5,93	6,06	6,37	5,99	6,44	5,96	6,05
CaO (wt %)	10,30	10,15	10,22	9,92	10,19	10,06	10,05
Na2O (wt %)	2,50	2,42	2,29	2,37	2,36	2,36	2,44
K2O (wt %)	0,71	0,63	0,55	0,65	0,62	0,66	0,63
P2O5 (wt %)	0,15	0,15	0,13	0,16	0,15	0,16	0,17
SUM	99,6	99,2	99,4	98,6	98,6	98,6	98,3
Cs (ppm)	0,3	0,4	0,3	0,3	0,3	0,3	0,3
Tl (ppm)	b.d.	b.d.	b.d.	0,2	b.d.	b.d.	b.d.
Rb (ppm)	16	16	13	15	16	14	14
Ba (ppm)	210	196	179	203	194	202	199
Th (ppm)	1,4	1,6	1,1	2,7	2,4	1,2	1,3
U (ppm)	0,24	0,30	0,25	0,30	0,25	0,29	0,26
Nb (ppm)	8,7	8,1	7,8	8,6	7,9	9,8	8,7
Ta (ppm)	0,46	0,44	0,41	0,48	0,40	0,46	0,46
La (ppm)	11,32	10,54	9,60	11,14	10,43	11,14	11,24
Ce (ppm)	25,85	23,64	21,67	25,89	23,80	24,79	24,87
Pb (ppm)	6	5	7	5	8	8	8
Pr (ppm)	3,10	2,76	2,56	3,09	2,76	2,88	2,91
Mo (ppm)	1,7	1,5	1,8	1,8	1,6	1,7	1,7
Sr (ppm)	199	201	189	185	193	193	188
Nd (ppm)	14,4	13,4	12,5	14,8	13,5	14,4	14,7
Zr (ppm)	103	93	83	102	93	97	96
Hf (ppm)	2,82	2,50	2,27	2,66	2,36	2,49	2,55
Sm (ppm)	3,60	3,45	3,31	3,63	3,53	3,76	3,60
Eu (ppm)	1,13	1,18	1,05	1,18	1,00	1,12	1,12
Sn (ppm)	b.d.	1,8	0,6	0,8	0,5	0,5	0,6
Gd (ppm)	3,48	3,19	3,26	3,60	3,25	3,35	3,50
Dy (ppm)	3,89	3,74	3,75	4,03	3,78	4,07	4,03
Li (ppm)	5	5	6	4	5	4	4
Y (ppm)	27	25	24	26	26	27	27
Ho (ppm)	b.d.	b.d.	b.d.	b.d.	b.d.	b.d.	b.d.
Er (ppm)	2,37	2,33	2,15	2,70	2,31	2,37	2,45
Yb (ppm)	2,45	2,30	2,27	2,59	2,25	2,37	2,43
Lu (ppm)	0,38	0,35	0,37	0,37	0,32	0,37	0,35
Co (ppm)	33	33	36	35	34	34	34
Cr (ppm)	221	249	292	261	300	268	286
Cu (ppm)	93	91	106	106	96	103	105
Ni (ppm)	58	60	64	63	68	62	64
Sc (ppm)	36	35	39	37	36	37	37
V (ppm)	251	227	277	253	250	262	262
Zn (ppm)	89	87	92	92	87	91	93
Tb (ppm)	0,7	0,7	0,6	0,7	0,6	0,7	0,7
Tm (ppm)	0,4	0,3	0,3	0,4	0,3	0,3	0,3
S I	3,28	2,35	3,63	2,47	1,68	3,46	2,24
S II	-2,57	-2,93	-2,49	-3,58	-1,33	-1,55	-1,97
S III	2,69	0,53	0,84	1,62	1,27	2,16	1,76

Sample:	K05-11	K05-12	K05-13	K05-14	K05-62	K05-63	K05-64
Magma b./Loc.:	GVS	GVS	GVS	GVS	GVS	GVS	GVS
Latitude (N):	-31,9693	-31,9690	-31,9690	-31,9686	-31,9447	-31,9448	-31,9448
Longitude (E):	26,2989	26,2991	26,2986	26,2987	26,3135	26,3135	26,3133
Altitude (m):	1518	1541	1564	1580	1729	1745	1766
SiO2 (wt %)	51,19	51,25	51,34	51,17	50,50	51,26	50,03
TiO2 (wt %)	1,05	1,09	0,91	0,80	1,07	1,07	1,08
Al2O3 (wt %)	14,94	15,02	15,50	16,14	14,78	15,15	14,70
Fe2O3(T) (wt %)	12,14	12,40	11,77	10,99	12,17	11,99	11,97
MnO (wt %)	0,18	0,19	0,18	0,17	0,19	0,19	0,19
MgO (wt %)	6,22	6,12	6,48	5,87	6,27	6,37	6,29
CaO (wt %)	10,33	10,24	10,59	10,82	10,53	10,51	10,48
Na2O (wt %)	2,47	2,56	2,51	2,56	2,39	2,48	2,41
K2O (wt %)	0,69	0,69	0,65	0,54	0,67	0,70	0,70
P2O5 (wt %)	0,15	0,20	0,14	0,14	0,16	0,16	0,17
SUM	99,4	99,8	100,1	99,2	98,7	99,9	98,0
Cs (ppm)	0,2	0,2	0,3	0,2	0,8	0,4	0,4
Tl (ppm)	b.d.	b.d.	b.d.	b.d.	b.d.	b.d.	b.d.
Rb (ppm)	15	15	14	11	15	14	13
Ba (ppm)	206	208	192	184	206	207	206
Th (ppm)	1,4	1,5	2,5	1,3	1,5	1,6	1,7
U (ppm)	0,30	0,31	0,28	0,22	0,25	0,29	0,24
Nb (ppm)	8,6	8,8	7,6	7,3	8,1	8,5	7,8
Ta (ppm)	0,47	0,46	0,40	0,40	0,47	0,46	0,42
La (ppm)	10,99	11,45	10,19	9,46	10,83	11,03	11,37
Ce (ppm)	24,38	25,64	22,75	21,20	24,31	25,63	26,02
Pb (ppm)	4	5	3	7	4	3	4
Pr (ppm)	2,88	3,08	2,63	2,57	3,01	3,08	3,05
Mo (ppm)	1,7	1,7	1,5	1,7	1,7	1,6	1,5
Sr (ppm)	194	193	200	200	199	202	210
Nd (ppm)	14,0	15,3	12,8	12,3	14,4	15,4	15,3
Zr (ppm)	97	99	92	78	96	97	92
Hf (ppm)	2,59	2,57	2,52	2,11	2,46	2,50	2,44
Sm (ppm)	3,66	3,92	3,42	3,03	3,63	3,49	3,59
Eu (ppm)	1,05	1,16	0,98	1,12	1,17	1,13	1,13
Sn (ppm)	0,6	0,8	b.d.	0,6	0,7	0,7	0,7
Gd (ppm)	3,31	3,75	3,09	2,88	3,49	3,65	3,36
Dy (ppm)	3,95	4,22	3,62	3,53	3,76	3,91	3,91
Li (ppm)	5	6	5	5	6	6	6
Y (ppm)	26	28	24	23	26	26	26
Ho (ppm)	b.d.	b.d.	b.d.	b.d.	b.d.	b.d.	b.d.
Er (ppm)	2,42	2,59	2,32	2,10	2,45	2,47	2,39
Yb (ppm)	2,50	2,68	2,26	2,09	2,35	2,40	2,21
Lu (ppm)	0,34	0,38	0,33	0,34	0,33	0,36	0,33
Co (ppm)	36	36	34	34	34	34	34
Cr (ppm)	251	246	268	241	222	224	215
Cu (ppm)	106	110	95	88	108	106	109
Ni (ppm)	62	61	67	65	67	67	64
Sc (ppm)	38	37	35	35	38	39	39
V (ppm)	268	265	236	220	269	270	270
Zn (ppm)	94	95	88	88	95	95	95
Tb (ppm)	0,7	0,7	0,6	0,6	0,7	0,7	0,7
Tm (ppm)	0,4	0,4	0,3	0,3	0,4	0,4	0,3
S I	2,82	2,41	2,23	5,34	3,44	3,94	3,72
S II	-2,79	-2,56	-2,51	-2,65	-1,95	-3,18	-4,17
S III	0,70	0,14	0,51	0,76	1,10	1,33	1,46

Sample:	K05-65	K05-66	K05-67	K05-68	K05-69	S66	K05-105
Magma b./Loc.:	GVS	GVS	GVS	GVS	GVS	GVS	GVS
Latitude (N):	-31,9448	-31,9449	-31,9451	-31,9456	-31,9459	-31,9464	-31,9963
Longitude (E):	26,3133	26,3133	26,3134	26,3131	26,3133	26,3133	26,2828
Altitude (m):	1753	1757	1764	1780	1795	1812	1550
SiO2 (wt %)	50,97	51,34	51,12	51,17	51,38	50,92	50,93
TiO2 (wt %)	0,99	1,07	1,07	0,98	0,99	0,91	0,94
Al2O3 (wt %)	15,02	15,12	15,33	14,04	13,00	15,87	15,89
Fe2O3(T) (wt %)	11,70	12,31	12,23	12,32	12,69	11,21	11,20
MnO (wt %)	0,18	0,20	0,19	0,20	0,21	0,17	0,17
MgO (wt %)	6,55	6,52	6,19	7,51	8,08	6,56	5,99
CaO (wt %)	10,78	10,65	10,49	10,90	10,69	10,97	10,61
Na2O (wt %)	2,41	2,48	2,56	2,31	2,11	2,58	2,48
K2O (wt %)	0,60	0,61	0,70	0,58	0,60	0,68	0,61
P2O5 (wt %)	0,13	0,17	0,16	0,14	0,14	0,13	0,14
SUM	99,3	100,5	100,0	100,1	99,9	100,0	99,0
Cs (ppm)	0,3	0,4	0,2	0,3	0,2	0,3	0,4
Tl (ppm)	b.d.	b.d.	b.d.	b.d.	b.d.	b.d.	b.d.
Rb (ppm)	12	13	15	13	14	13	13
Ba (ppm)	188	201	205	177	179	193	182
Th (ppm)	1,3	1,5	1,3	1,1	1,4	1,2	1,2
U (ppm)	0,23	0,26	0,25	0,24	0,30	0,26	0,24
Nb (ppm)	7,4	8,9	8,9	7,5	8,3	7,1	7,5
Ta (ppm)	0,40	0,46	0,48	0,41	0,43	0,42	0,39
La (ppm)	9,12	11,34	11,62	9,97	10,23	9,24	9,63
Ce (ppm)	21,57	26,15	26,13	22,69	23,76	21,61	21,47
Pb (ppm)	5	4	4	5	4	5	4
Pr (ppm)	2,53	3,07	3,11	2,70	2,75	2,62	2,52
Mo (ppm)	1,4	1,8	1,7	1,2	1,7	0,8	1,1
Sr (ppm)	193	206	203	178	169	209	204
Nd (ppm)	12,3	15,0	14,9	13,4	13,4	12,9	12,5
Zr (ppm)	88	96	100	88	94	93	86
Hf (ppm)	2,14	2,40	2,48	2,37	2,45	2,09	2,20
Sm (ppm)	3,17	3,41	3,73	3,39	3,56	3,30	3,66
Eu (ppm)	1,07	1,12	1,11	0,99	1,02	0,93	1,07
Sn (ppm)	0,5	0,7	b.d.	0,6	0,5	b.d.	0,5
Gd (ppm)	3,03	3,55	3,62	3,22	3,39	2,87	2,92
Dy (ppm)	3,58	3,98	4,10	3,73	4,03	3,50	3,41
Li (ppm)	4	5	6	6	4	b.d.	7
Y (ppm)	23	27	28	26	27	23	24
Ho (ppm)	b.d.	b.d.	b.d.	b.d.	b.d.	b.d.	b.d.
Er (ppm)	2,24	2,46	2,60	2,48	2,62	1,89	2,20
Yb (ppm)	2,19	2,37	2,39	2,26	2,44	1,96	2,00
Lu (ppm)	0,32	0,36	0,36	0,34	0,36	0,31	0,32
Co (ppm)	34	34	33	35	38	32	32
Cr (ppm)	289	279	261	390	442	321	253
Cu (ppm)	101	107	104	102	99	84	98
Ni (ppm)	73	69	66	82	90	73	66
Sc (ppm)	39	39	37	42	44	36	35
V (ppm)	261	268	259	286	290	236	244
Zn (ppm)	93	94	94	94	96	86	89
Tb (ppm)	0,6	0,7	0,7	0,7	0,7	0,5	0,6
Tm (ppm)	0,3	0,3	0,4	0,3	0,3	0,3	0,3
S I	4,13	4,46	3,62	2,79	1,92	2,19	3,46
S II	-2,04	-2,29	-2,27	-1,38	-2,17	0,48	-0,64
S III	0,69	1,65	1,97	0,07	-0,82	2,27	0,95

Sample:	K05-106	K05-107	K05-108	K05-109	K05-110	K05-87	K05-88
Magma b./Loc.:	GVS	GVS	GVS	GVS	GVS	GVS	GVS
Latitude (N):	-31,9962	-31,9964	-31,9959	-31,9958	-31,9955	-31,8517	-31,8517
Longitude (E):	26,2829	26,2826	26,2845	26,2846	26,2847	26,2208	26,2207
Altitude (m):	1555	1558	1534	1538	1551	1643	1633
SiO2 (wt %)	50,99	51,40	51,97	50,90	51,75	51,09	50,83
TiO2 (wt %)	0,99	1,10	1,08	1,05	1,03	1,11	1,03
Al2O3 (wt %)	15,27	15,02	15,29	14,86	15,31	15,07	15,62
Fe2O3(T) (wt %)	11,66	12,18	12,19	12,03	12,00	12,01	11,63
MnO (wt %)	0,18	0,19	0,19	0,18	0,19	0,19	0,18
MgO (wt %)	6,11	6,28	6,16	6,33	6,51	6,13	6,23
CaO (wt %)	10,46	10,35	10,45	10,36	10,45	10,26	10,55
Na2O (wt %)	2,49	2,55	2,54	2,59	2,50	2,55	2,45
K2O (wt %)	0,61	0,65	0,69	0,68	0,67	0,69	0,65
P2O5 (wt %)	0,15	0,19	0,16	0,16	0,15	0,15	0,16
SUM	98,9	99,9	100,7	99,1	100,6	99,2	99,3
Cs (ppm)	0,3	0,3	0,6	0,3	0,3	0,2	0,2
Tl (ppm)	b.d.	b.d.	b.d.	b.d.	0,2	b.d.	b.d.
Rb (ppm)	12	14	14	14	15	15	13
Ba (ppm)	192	206	208	205	197	200	197
Th (ppm)	1,4	1,5	1,5	1,6	1,5	1,5	1,7
U (ppm)	0,23	0,24	0,28	0,26	0,32	0,29	0,25
Nb (ppm)	7,4	8,6	8,4	8,2	8,1	8,3	7,7
Ta (ppm)	0,43	0,43	0,46	0,44	0,45	0,46	0,43
La (ppm)	9,94	11,22	11,18	11,21	10,69	10,66	10,53
Ce (ppm)	22,81	25,52	25,85	25,41	23,98	23,96	24,31
Pb (ppm)	4	7	5	6	3	4	5
Pr (ppm)	2,67	3,11	3,10	3,12	2,75	2,88	3,05
Mo (ppm)	1,0	1,4	1,2	1,5	1,1	1,4	1,2
Sr (ppm)	199	200	206	194	201	200	210
Nd (ppm)	13,3	15,1	14,8	15,0	13,8	13,7	13,8
Zr (ppm)	87	93	101	96	93	96	89
Hf (ppm)	2,20	2,38	2,75	2,41	2,39	2,46	2,24
Sm (ppm)	3,43	3,95	3,91	3,68	3,59	3,50	3,69
Eu (ppm)	1,11	1,21	1,21	1,19	1,15	1,07	1,07
Sn (ppm)	0,5	1,4	b.d.	b.d.	b.d.	0,6	b.d.
Gd (ppm)	3,18	3,54	3,34	3,26	3,10	3,31	3,11
Dy (ppm)	3,62	4,02	4,10	3,83	3,76	4,15	3,82
Li (ppm)	4	5	5	4	3	5	4
Y (ppm)	25	27	28	26	26	26	24
Ho (ppm)	b.d.	b.d.	b.d.	b.d.	b.d.	b.d.	b.d.
Er (ppm)	2,13	2,41	2,48	2,33	2,41	2,46	2,20
Yb (ppm)	2,16	2,42	2,41	2,38	2,39	2,43	2,15
Lu (ppm)	0,35	0,36	0,38	0,38	0,35	0,35	0,33
Co (ppm)	34	35	34	34	34	33	32
Cr (ppm)	259	264	261	256	293	269	288
Cu (ppm)	103	115	108	111	104	103	102
Ni (ppm)	67	65	64	65	68	64	68
Sc (ppm)	37	39	38	39	38	37	36
V (ppm)	258	277	267	275	267	266	251
Zn (ppm)	93	97	95	96	92	92	89
Tb (ppm)	0,6	0,7	0,7	0,7	0,7	0,7	0,6
Tm (ppm)	0,3	0,3	0,3	0,3	0,3	0,3	0,3
S I	3,53	3,75	2,99	3,56	2,46	2,95	3,13
S II	-2,16	-3,25	-1,65	-3,74	-1,55	-1,18	-2,08
S III	1,45	1,39	1,28	1,42	0,83	1,89	2,83

Sample:	K05-89	K05-90	K05-91	K05-111	K05-112	K05-113	K05-119
Magma b./Loc.:	GVS	GVS	GVS	GVS	GVS	GVS	GVS
Latitude (N):	-31,8517	-31,8516	-31,8515	-31,8817	-31,8782	-31,9151	-31,9496
Longitude (E):	26,2206	26,2206	26,2208	26,1993	26,1987	26,2142	26,2307
Altitude (m):	1665	1626	1617	1770	1755	1954	1818
SiO ₂ (wt %)	51,56	51,10	51,31	51,46	50,36	50,60	50,05
TiO ₂ (wt %)	0,98	0,97	1,02	0,96	1,08	0,83	1,04
Al ₂ O ₃ (wt %)	15,38	14,59	15,00	15,36	14,78	15,80	12,51
Fe ₂ O ₃ (T) (wt %)	11,49	12,10	11,75	11,31	11,57	11,11	13,41
MnO (wt %)	0,18	0,19	0,18	0,18	0,18	0,17	0,21
MgO (wt %)	6,38	6,80	6,31	6,05	6,19	6,52	8,15
CaO (wt %)	10,34	10,51	10,36	10,33	10,42	10,87	10,84
Na ₂ O (wt %)	2,56	2,48	2,58	2,64	2,55	2,53	2,09
K ₂ O (wt %)	0,63	0,57	0,70	0,66	0,61	0,51	0,40
P ₂ O ₅ (wt %)	0,15	0,15	0,16	0,16	0,16	0,13	0,12
SUM	99,6	99,5	99,4	99,1	97,9	99,1	98,8
Cs (ppm)	0,2	0,2	0,2	0,2	0,2	0,2	0,2
Tl (ppm)	b.d.	b.d.	b.d.	b.d.	b.d.	b.d.	b.d.
Rb (ppm)	13	12	15	14	12	11	9
Ba (ppm)	195	188	201	205	214	175	146
Th (ppm)	1,4	1,2	1,7	1,6	1,3	1,1	0,9
U (ppm)	0,28	0,25	0,26	0,28	0,24	0,18	0,18
Nb (ppm)	8,1	7,1	8,3	8,4	8,3	6,5	6,7
Ta (ppm)	0,43	0,37	0,45	0,47	0,47	0,34	0,32
La (ppm)	10,56	9,63	11,39	10,74	10,33	8,55	7,75
Ce (ppm)	24,21	21,97	25,97	24,72	23,65	19,07	17,79
Pb (ppm)	5	6	4	6	6	3	6
Pr (ppm)	2,75	2,69	3,03	2,97	2,78	2,34	2,13
Mo (ppm)	1,2	1,1	1,3	1,4	1,3	1,0	1,2
Sr (ppm)	197	191	192	193	208	206	162
Nd (ppm)	13,9	12,6	14,9	13,5	13,0	11,1	10,4
Zr (ppm)	94	87	98	98	93	76	70
Hf (ppm)	2,44	2,09	2,53	2,57	2,38	1,80	1,76
Sm (ppm)	3,76	3,17	3,78	3,41	3,68	3,00	2,91
Eu (ppm)	1,15	1,05	1,21	1,13	1,20	1,09	0,91
Sn (ppm)	0,5	2,0	b.d.	0,8	0,6	b.d.	b.d.
Gd (ppm)	3,24	3,11	3,40	3,28	3,17	2,58	2,89
Dy (ppm)	3,78	3,67	3,78	3,88	3,92	3,27	3,57
Li (ppm)	5	5	5	5	7	4	5
Y (ppm)	25	24	27	26	25	21	22
Ho (ppm)	b.d.	b.d.	b.d.	b.d.	b.d.	b.d.	b.d.
Er (ppm)	2,29	2,24	2,45	2,37	2,34	1,88	2,13
Yb (ppm)	2,41	2,22	2,26	2,28	2,33	2,10	2,12
Lu (ppm)	0,35	0,33	0,39	0,33	0,33	0,29	0,34
Co (ppm)	33	35	34	32	34	32	41
Cr (ppm)	280	325	283	249	260	272	450
Cu (ppm)	103	105	104	103	113	90	123
Ni (ppm)	68	76	70	61	60	66	91
Sc (ppm)	37	39	37	37	39	38	47
V (ppm)	260	271	257	255	294	247	349
Zn (ppm)	91	97	93	93	95	87	104
Tb (ppm)	0,7	0,6	0,7	0,7	0,7	0,6	0,5
Tm (ppm)	0,3	0,3	0,4	0,4	0,3	0,3	0,3
S I	2,90	2,38	3,17	3,56	3,66	4,42	3,89
S II	-2,04	-2,88	-2,86	-3,64	-2,11	-1,83	-2,74
S III	1,55	0,25	2,10	1,44	2,70	0,80	-0,68

Sample:	K05-120	K05-121	K05-122	K05-123	K05-124	K05-125	K05-127
Magma b./Loc.:	GVS	GVS	GVS	GVS	GVS	GVS	GVS
Latitude (N):	-31,9504	-31,9504	-31,9506	-31,9505	-31,9499	-31,9504	-31,8249
Longitude (E):	26,2319	26,2318	26,2319	26,2319	26,2358	26,2468	26,2481
Altitude (m):	1769	1766	1779	1778	1679	1478	1701
SiO2 (wt %)	51,16	50,49	51,17	50,84	51,31	50,86	51,65
TiO2 (wt %)	1,00	0,95	1,04	1,05	1,03	1,07	0,98
Al2O3 (wt %)	15,34	14,49	15,09	15,01	15,13	14,89	16,09
Fe2O3(T) (wt %)	11,61	12,07	11,77	12,00	11,95	12,21	10,95
MnO (wt %)	0,18	0,19	0,18	0,18	0,18	0,19	0,16
MgO (wt %)	6,45	6,72	5,95	6,00	6,35	6,17	6,43
CaO (wt %)	10,53	10,67	10,23	10,26	10,46	10,39	10,45
Na2O (wt %)	2,48	2,41	2,47	2,46	2,46	2,46	2,35
K2O (wt %)	0,61	0,53	0,67	0,64	0,61	0,67	0,69
P2O5 (wt %)	0,16	0,13	0,16	0,16	0,16	0,16	0,15
SUM	99,5	98,6	98,7	98,6	99,6	99,1	99,9
Cs (ppm)	0,3	0,3	0,3	0,3	0,3	0,7	0,2
Tl (ppm)	0,1	b.d.	b.d.	b.d.	b.d.	b.d.	b.d.
Rb (ppm)	14	10	14	11	12	14	16
Ba (ppm)	199	176	209	187	199	214	206
Th (ppm)	1,3	1,0	1,5	1,2	1,3	1,4	1,7
U (ppm)	0,24	0,21	0,31	0,22	0,28	0,25	0,33
Nb (ppm)	7,8	7,8	8,5	7,0	8,2	8,6	9,6
Ta (ppm)	0,41	0,38	0,42	0,34	0,43	0,44	0,50
La (ppm)	10,48	8,74	10,75	8,82	10,42	11,49	12,40
Ce (ppm)	23,55	19,95	24,88	20,26	23,56	25,21	26,30
Pb (ppm)	7	4	7	4	6	3	7
Pr (ppm)	2,71	2,39	2,90	2,44	2,76	2,89	3,30
Mo (ppm)	1,0	1,3	1,3	1,0	1,1	0,9	0,8
Sr (ppm)	204	195	199	198	202	204	202
Nd (ppm)	13,6	11,6	14,4	11,7	13,1	14,9	15,0
Zr (ppm)	92	77	101	80	93	98	107
Hf (ppm)	2,47	2,00	2,77	1,99	2,45	2,53	2,72
Sm (ppm)	3,07	2,89	3,45	2,83	3,64	3,52	3,72
Eu (ppm)	1,14	1,04	1,10	0,93	1,15	1,10	1,07
Sn (ppm)	b.d.	0,7	0,5	b.d.	b.d.	b.d.	0,6
Gd (ppm)	3,36	2,91	3,36	2,72	3,41	3,45	3,46
Dy (ppm)	3,74	3,36	4,13	3,40	3,79	3,99	4,04
Li (ppm)	4	4	4	5	4	8	6
Y (ppm)	25	23	27	22	25	27	28
Ho (ppm)	b.d.	b.d.	1	1	1	1	1
Er (ppm)	2,34	2,17	2,42	2,05	2,52	2,41	2,39
Yb (ppm)	2,25	1,99	2,45	2,11	2,35	2,33	2,48
Lu (ppm)	0,31	0,28	0,35	0,28	0,36	0,34	0,37
Co (ppm)	34	35	33	34	34	34	36
Cr (ppm)	299	362	272	244	279	280	294
Cu (ppm)	105	97	103	105	105	142	94
Ni (ppm)	69	75	63	63	65	64	71
Sc (ppm)	37	38	36	37	38	37	36
V (ppm)	265	263	256	261	274	262	248
Zn (ppm)	92	95	93	94	94	96	86
Tb (ppm)	0,7	0,6	0,6	0,5	0,7	0,7	
Tm (ppm)	0,3	0,3	0,4	0,3	0,4	0,3	
S I	2,76	2,46	1,80	2,54	2,61	5,02	2,08
S II	-2,14	-1,24	-1,33	-1,85	-1,75	-4,64	0,26
S III	2,02	1,66	0,68	0,76	1,40	-0,54	1,95

Sample:	K05-128	K05-129	K05-130	K05-131	K05-132	K05-133	K05-92
Magma b./Loc.:	GVS	GVS	GVS	GVS	GVS	GVS	GVS
Latitude (N):	-31,8250	-31,8250	-31,8252	-31,8254	-31,8213	-31,8206	-31,9720
Longitude (E):	26,2482	26,2483	26,2479	26,2474	26,2505	26,2515	26,2539
Altitude (m):	1704	1723	1730	1742	1581	1541	1651
SiO2 (wt %)	51,47	51,41	51,53	51,67	51,92	51,12	51,31
TiO2 (wt %)	0,91	1,05	1,00	0,99	1,00	0,95	0,98
Al2O3 (wt %)	15,94	15,75	16,41	16,53	15,58	15,24	14,88
Fe2O3(T) (wt %)	11,32	11,78	11,26	11,31	11,52	11,84	12,21
MnO (wt %)	0,17	0,18	0,17	0,17	0,17	0,18	0,19
MgO (wt %)	6,46	6,35	5,80	5,41	5,85	6,81	6,70
CaO (wt %)	10,56	10,47	10,32	10,25	9,93	10,52	10,47
Na2O (wt %)	2,34	2,34	2,48	2,49	2,38	2,23	2,26
K2O (wt %)	0,64	0,65	0,69	0,70	0,69	0,57	0,63
P2O5 (wt %)	0,15	0,15	0,16	0,16	0,16	0,14	0,16
SUM	100,0	100,1	99,8	99,7	99,2	99,6	99,8
Cs (ppm)	0,3	0,2	0,3	0,2	0,2	0,2	0,3
Tl (ppm)	b.d.	b.d.	b.d.	b.d.	b.d.	b.d.	b.d.
Rb (ppm)	14	14	15	14	16	13	15
Ba (ppm)	197	198	208	220	211	186	198
Th (ppm)	1,7	1,5	1,9	1,7	1,7	1,3	1,6
U (ppm)	0,31	0,29	0,32	0,32	0,33	0,25	0,29
Nb (ppm)	8,5	8,5	8,9	8,7	9,3	7,9	9,0
Ta (ppm)	0,45	0,45	0,47	0,47	0,46	0,41	0,46
La (ppm)	11,29	10,87	11,59	11,70	12,28	10,45	11,34
Ce (ppm)	23,86	23,88	24,71	24,93	26,18	21,53	24,45
Pb (ppm)	6	7	7	7	10	7	9
Pr (ppm)	2,89	2,90	3,00	2,99	3,27	2,69	3,04
Mo (ppm)	0,8	0,9	0,8	0,8	0,9	0,8	1,1
Sr (ppm)	197	198	205	213	196	194	188
Nd (ppm)	13,7	13,5	14,1	14,3	14,7	12,4	14,5
Zr (ppm)	100	104	112	108	113	92	100
Hf (ppm)	2,57	2,54	2,69	2,68	2,89	2,32	2,59
Sm (ppm)	3,40	3,60	3,66	3,79	3,81	3,37	3,96
Eu (ppm)	1,00	0,99	1,06	1,07	1,12	0,96	1,00
Sn (ppm)	0,6	b.d.	0,5	0,9	0,7	b.d.	0,6
Gd (ppm)	3,35	3,18	3,32	3,29	3,77	2,99	3,48
Dy (ppm)	3,75	3,84	3,83	4,04	4,13	3,53	3,90
Li (ppm)	6	6	7	6	8	7	7
Y (ppm)	26	26	26	26	29	25	28
Ho (ppm)	1	1	1	1	1	1	1
Er (ppm)	2,24	2,27	2,43	2,49	2,51	2,09	2,43
Yb (ppm)	2,39	2,43	2,51	2,56	2,59	2,11	2,55
Lu (ppm)	0,37	0,33	0,36	0,37	0,40	0,37	0,38
Co (ppm)	38	38	36	34	37	40	41
Cr (ppm)	293	260	229	209	242	331	292
Cu (ppm)	93	102	98	100	101	99	104
Ni (ppm)	70	67	59	53	58	75	72
Sc (ppm)	37	38	35	35	36	38	40
V (ppm)	246	275	245	239	252	263	267
Zn (ppm)	87	90	88	91	90	90	92
Tb (ppm)							
Tm (ppm)							
S I	3,11	3,13	2,65	2,81	2,14	2,09	4,45
S II	-0,93	-0,46	-1,10	-2,28	-1,66	-0,26	-2,13
S III	0,77	1,40	1,40	0,74	0,30	0,24	-0,33

Sample:	K05-99	K05-101	K05-102	K05-103	K05-104	K05-186	K05-126
Magma b./Loc.:	GVS	GVS	GVS	GVS	GVS	GVS	GVS
Latitude (N):	-31,971763	-31,971638	-31,971646	-31,971511	-31,984306	-31,864722	
Longitude (E):	26,252645	26,25266	26,25261	26,252764	26,272787	26,270747	
Altitude (m):	1680	1682	1724	1714	1405	1419	
SiO2 (wt %)	51,83	51,36	51,99	51,35	51,46	51,18	50,93
TiO2 (wt %)	1,07	1,00	1,03	1,06	1,03	1,06	1,05
Al2O3 (wt %)	15,10	14,99	15,40	15,33	15,57	15,11	15,02
Fe2O3(T) (wt %)	12,19	12,00	11,84	12,10	11,67	11,98	11,86
MnO (wt %)	0,18	0,18	0,18	0,18	0,18	0,18	0,19
MgO (wt %)	6,35	6,71	6,10	6,24	6,33	6,25	6,04
CaO (wt %)	10,24	10,31	10,16	10,25	10,19	10,36	10,49
Na2O (wt %)	2,49	2,28	2,33	2,40	2,35	2,70	2,53
K2O (wt %)	0,74	0,66	0,69	0,64	0,66	0,74	0,33
P2O5 (wt %)	0,17	0,15	0,15	0,16	0,16	0,16	0,16
SUM	100,4	99,6	99,9	99,7	99,6	99,7	98,6
Cs (ppm)	0,3	0,3	0,6	0,5	0,5	0,3	0,4
Tl (ppm)	0,2	b.d.	0,2	b.d.	b.d.	b.d.	b.d.
Rb (ppm)	17	14	16	15	15	14	6
Ba (ppm)	218	202	213	205	212	220	199
Th (ppm)	1,7	1,6	1,6	1,6	1,7	1,4	1,3
U (ppm)	0,36	0,30	0,34	0,33	0,31	0,28	0,29
Nb (ppm)	9,4	8,6	9,3	9,4	9,6	8,2	7,8
Ta (ppm)	0,50	0,48	0,48	0,47	0,46	0,41	0,43
La (ppm)	12,81	11,00	11,83	11,93	12,40	11,83	10,56
Ce (ppm)	26,91	24,36	25,36	25,05	26,69	25,49	23,96
Pb (ppm)	8	8	9	9	5	3	4
Pr (ppm)	3,32	3,03	3,07	3,08	3,20	3,12	2,85
Mo (ppm)	1,0	0,7	0,8	1,1	1,0	1,9	0,8
Sr (ppm)	195	185	188	192	192	205	203
Nd (ppm)	15,7	13,9	14,7	14,8	14,9	14,6	14,4
Zr (ppm)	113	106	116	108	108	102	96
Hf (ppm)	2,81	2,65	2,71	2,73	2,75	2,37	2,49
Sm (ppm)	3,85	3,71	3,79	3,82	3,82	3,54	3,32
Eu (ppm)	1,03	0,97	1,02	1,03	1,10	1,27	1,11
Sn (ppm)	0,7	b.d.	0,6	0,6	0,5	b.d.	b.d.
Gd (ppm)	3,72	3,53	3,73	3,62	3,69	3,53	3,45
Dy (ppm)	4,18	3,91	4,14	3,90	4,03	4,11	3,82
Li (ppm)	9	6	7	7	7	3	12
Y (ppm)	30	27	27	27	29	27	26
Ho (ppm)	1	1	1	1	1	1	b.d.
Er (ppm)	2,54	2,34	2,51	2,51	2,40	2,29	2,39
Yb (ppm)	2,61	2,41	2,65	2,62	2,59	2,39	2,34
Lu (ppm)	0,40	0,38	0,39	0,39	0,39	0,33	0,35
Co (ppm)	40	40	38	39	38	34	34
Cr (ppm)	239	314	262	285	289	245	246
Cu (ppm)	111	103	106	107	105	108	106
Ni (ppm)	64	73	63	68	67	63	63
Sc (ppm)	40	39	38	38	38	38	37
V (ppm)	275	269	262	265	264	271	263
Zn (ppm)	95	92	93	94	91	94	95
Tb (ppm)						0,6	0,7
Tm (ppm)						0,3	0,3
S I	3,33	2,54	2,63	2,81	2,35	2,64	2,65
S II	-2,06	-1,48	-2,16	-1,20	-0,56	-1,63	0,17
S III	-0,87	0,67	0,42	0,78	0,77	0,90	-0,22

Sample:	K04-C16	K05-70	K05-71	K05-72	K05-73	K05-74	K05-75
Magma b./Loc.:	GVS	MVS	MVS	MVS	MVS	MVS	MVS
Latitude (N):	-31,998349	-31,847305	-31,847368	-31,847349	-31,847381	-31,847365	-31,847039
Longitude (E):	26,279713	26,200067	26,200026	26,200094	26,200063	26,200083	26,200174
Altitude (m):	1505	1688	1690	1714	1720	1723	1724
SiO2 (wt %)	50,97	50,88	51,09	51,40	50,90	50,86	50,20
TiO2 (wt %)	1,01	0,93	0,94	0,85	0,95	0,96	0,90
Al2O3 (wt %)	15,15	15,66	15,67	15,23	15,13	15,54	15,34
Fe2O3(T) (wt %)	11,35	11,10	11,35	11,52	12,11	11,43	11,17
MnO (wt %)	0,18	0,17	0,18	0,18	0,19	0,18	0,18
MgO (wt %)	5,93	6,64	6,48	7,00	7,34	6,56	6,69
CaO (wt %)	10,59	11,01	10,81	10,87	10,93	10,81	10,88
Na2O (wt %)	2,42	2,49	2,45	2,40	2,30	2,39	2,48
K2O (wt %)	0,45	0,57	0,62	0,57	0,57	0,62	0,57
P2O5 (wt %)	0,16	0,15	0,15	0,13	0,14	0,14	0,15
SUM	98,2	99,6	99,7	100,2	100,6	99,5	98,6
Cs (ppm)	0,6	0,2	0,2	0,2	0,2	0,2	0,2
Tl (ppm)	b.d.	b.d.	b.d.	b.d.	b.d.	b.d.	b.d.
Rb (ppm)	8	13	14	12	10	12	12
Ba (ppm)	190	182	192	181	178	183	177
Th (ppm)	1,4	1,4	1,3	1,3	1,2	1,3	1,3
U (ppm)	0,27	0,25	0,26	0,23	0,21	0,23	0,23
Nb (ppm)	7,7	7,5	7,1	7,4	6,7	7,1	7,3
Ta (ppm)	0,47	0,40	0,42	0,42	0,36	0,37	0,35
La (ppm)	10,59	9,57	10,23	9,40	8,78	9,03	9,27
Ce (ppm)	24,49	21,93	23,06	21,55	20,77	21,42	21,19
Pb (ppm)	5	4	5	b.d.	5	6	8
Pr (ppm)	2,91	2,63	2,71	2,62	2,36	2,47	2,53
Mo (ppm)	0,9	1,2	1,2	0,9	1,2	1,1	1,1
Sr (ppm)	197	194	204	194	203	204	196
Nd (ppm)	16,0	12,8	13,4	13,2	11,5	11,7	11,9
Zr (ppm)	103	88	89	85	80	82	83
Hf (ppm)	2,59	2,31	2,39	2,29	2,13	1,99	2,10
Sm (ppm)	3,60	3,04	3,31	3,31	3,14	3,04	3,16
Eu (ppm)	1,15	0,97	1,02	1,01	0,98	0,96	0,97
Sn (ppm)	0,6	b.d.	0,6	b.d.	b.d.	0,5	b.d.
Gd (ppm)	3,56	3,41	3,24	3,02	3,01	2,87	2,80
Dy (ppm)	4,00	3,57	3,70	3,60	3,36	3,34	3,49
Li (ppm)	2	5	4	4	5	5	5
Y (ppm)	27	24	25	23	22	23	22
Ho (ppm)	b.d.	b.d.	b.d.	b.d.	b.d.	b.d.	b.d.
Er (ppm)	2,26	2,19	2,40	2,17	2,12	2,00	2,08
Yb (ppm)	2,28	2,21	2,20	2,21	2,01	2,11	2,11
Lu (ppm)	0,35	0,33	0,34	0,33	0,30	0,32	0,31
Co (ppm)	33	33	33	34	35	33	33
Cr (ppm)	250	291	276	341	336	295	283
Cu (ppm)	108	95	94	97	99	98	96
Ni (ppm)	64	74	72	81	81	74	75
Sc (ppm)	37	36	36	39	37	36	36
V (ppm)	265	250	248	245	252	247	247
Zn (ppm)	94	88	88	88	89	88	88
Tb (ppm)	0,6	0,6	0,7	0,6	0,6	0,6	0,6
Tm (ppm)	0,4	0,3	0,3	0,3	0,3	0,3	0,3
S I	2,82	2,85	3,16	5,73	2,24	3,38	3,59
S II	-0,21	-0,01	-0,92	-2,85	-1,87	-1,02	-1,28
S III	0,66	0,45	0,65	1,11	0,70	1,01	0,61

Sample:	K05-76	S71	K05-114	K05-115	K05-116	K04K-03	K05-78
Magma b./Loc.:	MVS	MVS	MVS	MVS	MVS	MVS	GS
Latitude (N):	-31,846733	-31,847753	-31,836163	-31,821451	-31,821843	-31,823025	-31,781047
Longitude (E):	26,200017	26,201153	26,194101	26,195134	26,195395	26,20672	26,301448
Altitude (m):	1701	1746	1519	1528	1584	1521	2148
SiO2 (wt %)	50,71	50,49	51,72	51,15	51,04	51,29	51,27
TiO2 (wt %)	0,96	0,89	1,01	1,08	1,19	1,09	1,03
Al2O3 (wt %)	15,45	15,56	15,28	15,20	14,92	14,61	15,14
Fe2O3(T) (wt %)	11,49	11,12	11,52	11,90	12,18	12,15	11,87
MnO (wt %)	0,18	0,17	0,18	0,18	0,19	0,19	0,18
MgO (wt %)	6,61	6,70	5,92	6,16	6,54	5,99	6,08
CaO (wt %)	10,75	11,08	10,28	10,42	10,50	10,46	10,37
Na2O (wt %)	2,45	2,44	2,62	2,48	2,50	2,43	2,52
K2O (wt %)	0,60	0,64	0,66	0,63	0,60	0,68	0,66
P2O5 (wt %)	0,16	0,14	0,17	0,16	0,15	0,16	0,16
SUM	99,4	99,2	99,4	99,4	99,8	99,0	99,3
Cs (ppm)	0,2	0,2	0,2	0,2	0,2	0,3	0,5
Tl (ppm)	b.d.	b.d.	b.d.	b.d.	b.d.	b.d.	b.d.
Rb (ppm)	13	12	15	13	13	15	14
Ba (ppm)	187	181	213	199	198	213	199
Th (ppm)	1,3	1,2	1,3	1,4	1,3	2,0	1,5
U (ppm)	0,25	0,24	0,29	0,26	0,25	0,25	0,25
Nb (ppm)	7,7	7,4	8,3	8,4	8,3	8,3	8,9
Ta (ppm)	0,40	0,42	0,41	0,42	0,43	0,45	0,46
La (ppm)	10,04	9,56	10,94	10,71	10,24	10,78	12,02
Ce (ppm)	23,53	22,16	24,85	24,21	23,21	24,76	27,14
Pb (ppm)	5	5	7	4	4	8	7
Pr (ppm)	2,68	2,74	2,90	2,85	2,85	2,92	3,10
Mo (ppm)	1,6	0,8	1,2	1,1	1,1	1,4	1,6
Sr (ppm)	201	198	204	205	204	195	192
Nd (ppm)	13,4	13,4	14,3	13,9	13,5	14,5	15,1
Zr (ppm)	87	92	94	95	93	98	103
Hf (ppm)	2,23	2,09	2,53	2,46	2,46	2,47	2,43
Sm (ppm)	3,08	3,12	3,49	3,34	3,17	3,82	3,91
Eu (ppm)	1,04	1,04	1,24	1,16	1,20	1,15	1,21
Sn (ppm)	0,6	b.d.	0,5	0,6	0,6	0,6	0,6
Gd (ppm)	3,17	2,97	3,56	3,17	3,28	3,34	3,39
Dy (ppm)	3,55	3,58	4,06	3,85	3,71	3,91	3,86
Li (ppm)	5	3	5	5	5	5	5
Y (ppm)	24	24	27	26	25	26	27
Ho (ppm)	b.d.	b.d.	b.d.	b.d.	b.d.	b.d.	b.d.
Er (ppm)	2,32	2,06	2,47	2,34	2,22	2,35	2,46
Yb (ppm)	2,04	1,98	2,30	2,19	2,39	2,40	5,06
Lu (ppm)	0,34	0,29	0,32	0,33	0,34	0,37	0,38
Co (ppm)	34	33	33	34	36	34	33
Cr (ppm)	307	343	228	285	284	278	239
Cu (ppm)	98	97	104	107	114	123	106
Ni (ppm)	73	73	57	64	66	60	62
Sc (ppm)	36	37	37	38	40	38	37
V (ppm)	246	246	257	275	312	269	266
Zn (ppm)	89	88	94	94	99	96	94
Tb (ppm)	0,7	0,6	0,7	0,7	0,6	0,7	0,7
Tm (ppm)	0,3	0,3	0,4	0,3	0,3	0,3	0,3
S I	2,79	2,91	2,52	2,77	1,52	4,43	3,63
S II	-1,90	-0,72	-2,74	-1,34	-0,66	-4,10	-4,12
S III	1,54	0,71	0,07	1,69	2,13	0,24	2,96

Sample:	K05-80	K05-81	K05-82	K05-83	K05-84	S76	K05-85
Magma b./Loc.:	GS	GS	GS	GS	GS	GS	GS
Latitude (N):	-31,793876	-31,793829	-31,793753	-31,793633	-31,793609	-31,79295	-31,792983
Longitude (E):	26,303327	26,303277	26,303378	26,30346	26,303351	26,302633	26,302783
Altitude (m):	2011	2010	2008	2000	1986	1967	1972
SiO2 (wt %)	50,81	51,24	50,45	50,57	51,38	50,67	50,60
TiO2 (wt %)	1,01	0,98	0,90	0,97	1,06	1,02	1,06
Al2O3 (wt %)	14,91	15,09	15,42	15,17	15,00	14,99	14,87
Fe2O3(T) (wt %)	12,11	11,89	11,35	11,79	11,99	11,58	11,93
MnO (wt %)	0,19	0,19	0,18	0,19	0,19	0,18	0,19
MgO (wt %)	6,32	6,26	6,88	6,63	6,06	6,00	6,13
CaO (wt %)	10,38	10,46	10,90	10,61	10,20	10,46	10,37
Na2O (wt %)	2,48	2,46	2,40	2,42	2,50	2,45	2,49
K2O (wt %)	0,62	0,63	0,55	0,60	0,68	0,70	0,67
P2O5 (wt %)	0,15	0,15	0,13	0,15	0,16	0,16	0,16
SUM	99,0	99,4	99,2	99,1	99,2	98,2	98,5
Cs (ppm)	0,6	0,7	0,6	0,5	0,7	1,1	0,4
Tl (ppm)	b.d.	b.d.	b.d.	b.d.	b.d.	b.d.	b.d.
Rb (ppm)	13	14	12	12	14	15	14
Ba (ppm)	211	215	180	191	209	254	200
Th (ppm)	1,6	1,5	1,1	1,3	1,9	1,4	1,5
U (ppm)	0,24	0,23	0,20	0,23	0,29	0,27	0,26
Nb (ppm)	8,3	8,1	7,1	7,6	8,4	8,4	8,8
Ta (ppm)	0,44	0,43	0,38	0,41	0,41	0,50	0,46
La (ppm)	11,03	10,77	8,96	9,89	12,56	11,46	11,53
Ce (ppm)	25,05	24,98	20,66	22,43	28,00	26,35	24,81
Pb (ppm)	7	5	4	3	5	4	3
Pr (ppm)	2,90	2,76	2,46	2,71	3,27	3,14	2,99
Mo (ppm)	1,5	1,3	1,1	1,5	1,5	0,9	1,1
Sr (ppm)	197	205	198	197	209	197	193
Nd (ppm)	14,3	13,7	12,0	13,1	15,6	15,7	14,8
Zr (ppm)	98	95	83	90	97	102	97
Hf (ppm)	2,48	2,53	2,14	2,37	2,48	2,41	2,57
Sm (ppm)	3,78	3,39	3,39	3,12	4,07	3,91	3,67
Eu (ppm)	1,04	1,09	0,96	1,03	1,11	1,13	1,10
Sn (ppm)	b.d.	0,5	b.d.	b.d.	0,7	b.d.	b.d.
Gd (ppm)	3,32	3,08	2,87	3,08	3,65	3,59	3,24
Dy (ppm)	3,89	4,02	3,35	3,68	4,08	4,10	3,95
Li (ppm)	4	5	3	4	5	2	4
Y (ppm)	26	26	23	24	28	28	27
Ho (ppm)	b.d.	b.d.	b.d.	b.d.	b.d.	b.d.	b.d.
Er (ppm)	2,42	2,28	1,98	2,27	2,26	2,36	2,46
Yb (ppm)	2,42	2,29	2,10	2,15	2,40	2,50	2,31
Lu (ppm)	0,34	0,35	0,32	0,32	0,38	0,37	0,35
Co (ppm)	33	33	32	33	33	34	34
Cr (ppm)	278	266	317	300	267	258	262
Cu (ppm)	108	99	95	100	106	106	110
Ni (ppm)	63	63	74	70	64	64	63
Sc (ppm)	39	38	38	38	37	36	38
V (ppm)	272	256	257	258	264	251	269
Zn (ppm)	94	91	86	90	95	95	94
Tb (ppm)	0,7	0,7	0,6	0,6	0,7	0,7	0,7
Tm (ppm)	0,3	0,3	0,3	0,3	0,4	0,4	0,4
S I	3,85	3,68	3,53	3,12	2,54	1,86	3,85
S II	-3,53	-2,55	-0,07	-1,44	-3,28	-2,28	-2,13
S III	2,17	2,22	1,93	1,55	2,61	2,15	1,29

Sample:	K05-86	K05-193	K05-198	K05-199	K05-200	K05-201	K05-202
Magma b./Loc.:	GS	GS	GS	GS	GS	GS	GS
Latitude (N):	-31,782386	-31,774939	-31,858596	-31,858596	-31,858596	-31,858596	-31,858596
Longitude (E):	26,301823	26,301913	26,346569	26,346569	26,346569	26,346569	26,346569
Altitude (m):	2056	2053	1418	1434	1424	1408	1419
SiO2 (wt %)	50,93	51,26	51,01	50,61	50,37	50,72	51,67
TiO2 (wt %)	1,08	1,13	1,09	1,00	1,03	1,08	1,21
Al2O3 (wt %)	14,90	14,39	14,75	15,25	14,47	14,88	15,05
Fe2O3(T) (wt %)	12,08	12,86	12,46	11,70	12,13	12,24	12,61
MnO (wt %)	0,19	0,19	0,20	0,18	0,18	0,18	0,18
MgO (wt %)	6,19	6,49	6,24	6,60	6,86	6,20	5,53
CaO (wt %)	10,19	10,24	10,15	10,77	10,45	10,51	10,00
Na2O (wt %)	2,42	2,73	2,64	2,44	2,56	2,59	2,55
K2O (wt %)	0,69	0,78	0,86	0,59	0,71	0,74	0,80
P2O5 (wt %)	0,17	0,17	0,16	0,16	0,16	0,17	0,19
SUM	98,8	100,2	99,6	99,3	98,9	99,3	99,8
Cs (ppm)	1,0	0,2	0,2	0,3	0,2	0,3	0,4
Tl (ppm)	0,2	b.d.	b.d.	b.d.	b.d.	b.d.	b.d.
Rb (ppm)	15	15	14	12	12	14	16
Ba (ppm)	270	228	230	197	207	221	231
Th (ppm)	1,4	1,5	1,5	1,1	1,3	1,6	1,7
U (ppm)	0,23	0,28	0,32	0,23	0,22	0,29	0,33
Nb (ppm)	8,1	9,3	7,9	7,1	7,1	9,0	11,0
Ta (ppm)	0,44	0,54	0,46	0,40	0,46	0,53	0,57
La (ppm)	10,91	11,55	10,79	9,19	10,21	12,50	13,98
Ce (ppm)	24,85	26,48	24,65	21,25	23,19	29,28	31,51
Pb (ppm)	5	5	5	5	4	3	3
Pr (ppm)	2,92	3,16	2,92	2,61	2,84	3,43	3,74
Mo (ppm)	1,2	2,1	1,6	1,5	1,4	1,5	1,7
Sr (ppm)	207	203	211	212	196	206	202
Nd (ppm)	14,3	15,7	14,5	12,9	13,6	16,0	18,3
Zr (ppm)	96	107	106	86	97	102	115
Hf (ppm)	2,69	2,82	2,64	2,11	2,51	2,78	3,30
Sm (ppm)	3,78	4,06	3,63	3,43	3,39	3,84	4,23
Eu (ppm)	1,07	1,11	1,10	1,00	1,08	1,26	1,40
Sn (ppm)	b.d.	0,6	0,6	0,6	b.d.	b.d.	b.d.
Gd (ppm)	3,37	3,87	3,39	3,17	3,26	3,62	4,07
Dy (ppm)	3,93	4,43	4,19	3,39	3,82	4,44	4,84
Li (ppm)	8	b.d.	11	5	b.d.	b.d.	b.d.
Y (ppm)	26	28	26	23	24	30	33
Ho (ppm)	b.d.	b.d.	b.d.	b.d.	b.d.	b.d.	b.d.
Er (ppm)	2,45	2,32	2,44	2,18	2,18	2,38	2,79
Yb (ppm)	2,32	2,55	2,48	2,06	2,22	2,44	2,70
Lu (ppm)	0,36	0,37	0,36	0,31	0,34	0,40	0,42
Co (ppm)	34	35	34	33	35	35	35
Cr (ppm)	257	321	253	283	330	265	239
Cu (ppm)	110	110	106	98	103	105	121
Ni (ppm)	64	65	62	73	71	65	52
Sc (ppm)	38	39	38	37	39	37	38
V (ppm)	271	279	261	255	270	261	274
Zn (ppm)	94	96	94	89	93	95	100
Tb (ppm)	0,7	0,7	0,6	0,6	0,6	0,6	0,8
Tm (ppm)	0,3	0,4	0,4	0,3	0,4	0,4	0,4
S I	2,98	2,36	2,68	2,98	1,46	2,50	2,54
S II	-2,48	-2,08	-2,95	-0,28	-2,46	-2,77	-3,10
S III	3,11	3,52	0,89	1,63	2,76	2,70	1,53

Sample:	K05-203	K05-204	K05-206	K05-207	K05-210	K05-211	K05-213
Magma b./Loc.:	GS	GS	GS/L7	GS/L7	GS/L9	GS/L9	GS
Latitude (N):	-31,858596	-31,858596	-31,816319	-31,817693	-31,802511	-31,802355	-31,792508
Longitude (E):	26,346569	26,346569	26,319152	26,319768	26,327109	26,327121	26,332992
Altitude (m):	1421	1430	1936	1933	1610	1606	1532
SiO2 (wt %)	51,70	51,02	50,79	50,22	51,31	51,80	51,89
TiO2 (wt %)	1,05	1,14	1,08	1,09	0,83	0,90	1,05
Al2O3 (wt %)	15,20	15,04	15,06	15,12	15,32	15,55	15,36
Fe2O3(T) (wt %)	11,71	12,56	12,32	12,22	10,74	9,85	11,80
MnO (wt %)	0,18	0,19	0,18	0,19	0,17	0,15	0,18
MgO (wt %)	6,18	6,18	6,34	6,24	7,89	6,70	6,25
CaO (wt %)	10,49	10,39	10,48	10,43	10,97	11,09	10,53
Na2O (wt %)	2,54	2,54	2,53	2,44	2,23	2,26	2,57
K2O (wt %)	0,66	0,75	0,74	0,62	0,50	0,55	0,67
P2O5 (wt %)	0,16	0,16	0,16	0,16	0,11	0,12	0,17
SUM	99,9	100,0	99,7	98,7	100,1	99,0	100,5
Cs (ppm)	0,3	0,2	0,3	0,3	0,4	0,3	0,3
Tl (ppm)	b.d.	b.d.	b.d.	b.d.	b.d.	b.d.	b.d.
Rb (ppm)	14	15	14	12	12	13	14
Ba (ppm)	203	219	211	205	162	173	217
Th (ppm)	1,4	1,6	1,4	1,4	1,6	2,1	2,0
U (ppm)	0,25	0,31	0,29	0,29	0,42	0,48	0,47
Nb (ppm)	8,8	9,7	8,9	8,9	7,0	7,8	10,2
Ta (ppm)	0,47	0,54	0,49	0,49	0,52	0,62	0,76
La (ppm)	11,04	12,17	11,85	11,88	8,45	9,07	10,90
Ce (ppm)	25,65	27,51	27,12	27,59	19,12	21,07	25,48
Pb (ppm)	4	5	3	5	b.d.	6	2
Pr (ppm)	3,02	3,34	3,23	3,26	2,22	2,48	3,00
Mo (ppm)	1,9	1,6	1,2	1,2	1,2	1,0	1,3
Sr (ppm)	200	206	200	201	184	180	204
Nd (ppm)	14,5	16,9	16,7	15,6	11,2	12,3	14,4
Zr (ppm)	98	105	101	106	77	84	100
Hf (ppm)	2,67	3,00	2,71	2,88	1,99	2,14	2,51
Sm (ppm)	3,56	3,82	3,79	3,58	2,89	3,29	3,42
Eu (ppm)	1,19	1,32	1,34	1,25	0,99	0,98	1,11
Sn (ppm)	0,5	b.d.	b.d.	b.d.	b.d.	b.d.	0,9
Gd (ppm)	3,52	3,59	3,56	3,57	2,75	3,03	3,45
Dy (ppm)	3,76	4,56	4,38	4,51	3,33	3,64	3,99
Li (ppm)	4	b.d.	b.d.	b.d.	6	5	5
Y (ppm)	27	30	29	29	22	24	27
Ho (ppm)	b.d.	b.d.	b.d.	b.d.	b.d.	b.d.	b.d.
Er (ppm)	2,47	2,49	2,53	2,44	2,17	2,25	2,48
Yb (ppm)	2,39	2,53	2,47	2,38	2,03	2,05	2,38
Lu (ppm)	0,37	0,39	0,41	0,37	0,31	0,36	0,35
Co (ppm)	33	35	34	34	33	30	34
Cr (ppm)	260	274	272	276	500	372	303
Cu (ppm)	108	108	106	108	84	85	107
Ni (ppm)	63	64	64	63	107	69	66
Sc (ppm)	38	37	38	38	34	37	37
V (ppm)	270	262	263	267	232	277	268
Zn (ppm)	94	95	94	93	83	82	93
Tb (ppm)	0,7	0,8	0,6	0,7	0,6	0,7	0,7
Tm (ppm)	0,3	0,4	0,4	0,4	0,3	0,3	0,3
S I	3,68	2,19	2,24	2,90	-1,28	-0,25	3,52
S II	-2,49	-1,03	-1,91	-1,53	4,34	3,60	-1,68
S III	1,76	1,46	1,32	1,19	0,81	1,22	3,27

Sample:	K05-214	K05-215	K05-216	K05-134	K05-135	K05-136	K05-137
Magma b./Loc.:	GS	GS	GS	CD	CD	CD	CD
Latitude (N):	-31,79252	-31,792504	-31,792276	-32,0549	-32,0549	-32,0549	-32,0548
Longitude (E):	26,332988	26,333114	26,333137	25,3592	25,3593	25,3593	25,3593
Altitude (m):	1539	1539	1546	1088	1087	1086	1086
SiO2 (wt %)	51,43	51,56	51,58	52,36	50,99	50,98	51,83
TiO2 (wt %)	1,09	1,01	1,01	1,08	1,35	1,45	1,33
Al2O3 (wt %)	14,92	15,19	15,16	15,00	14,18	14,13	14,49
Fe2O3(T) (wt %)	12,10	11,73	11,48	12,00	13,62	13,92	13,22
MnO (wt %)	0,19	0,18	0,18	0,19	0,20	0,20	0,20
MgO (wt %)	6,29	6,08	6,26	6,10	5,66	5,15	5,33
CaO (wt %)	10,35	10,45	10,37	10,07	9,71	9,45	9,69
Na2O (wt %)	2,50	2,60	2,59	2,39	2,50	2,49	2,47
K2O (wt %)	0,66	0,64	0,67	0,74	0,78	0,78	0,69
P2O5 (wt %)	0,20	0,16	0,16	0,17	0,19	0,21	0,19
SUM	99,7	99,6	99,5	100,1	99,2	98,8	99,4
Cs (ppm)	0,3	0,2	0,3	1,0	1,6	1,5	1,2
Tl (ppm)	b.d.	b.d.	b.d.	0,2	b.d.	b.d.	b.d.
Rb (ppm)	14	14	15	16	17	18	16
Ba (ppm)	218	215	257	226	226	246	230
Th (ppm)	2,4	3,5	28,2	1,9	1,6	1,9	1,8
U (ppm)	0,62	1,01	9,83	0,45	0,41	0,42	0,37
Nb (ppm)	11,0	13,4	52,7	8,6	7,7	7,7	7,5
Ta (ppm)	0,91	1,47	12,15	0,48	0,42	0,44	0,41
La (ppm)	11,72	10,87	12,71	12,21	11,45	12,23	11,86
Ce (ppm)	27,24	25,60	35,20	27,24	25,93	28,71	26,31
Pb (ppm)	4	6	8	5	7	7	6
Pr (ppm)	3,19	2,93	3,72	3,07	3,11	3,31	3,22
Mo (ppm)	1,4	1,6	1,8	1,3	1,3	1,2	1,3
Sr (ppm)	203	196	198	216	215	199	197
Nd (ppm)	16,1	15,0	17,9	15,6	15,9	17,2	16,1
Zr (ppm)	102	102	126	99	108	120	113
Hf (ppm)	2,58	2,58	2,96	2,52	2,94	2,91	2,94
Sm (ppm)	3,95	3,63	4,30	3,66	3,97	4,39	4,43
Eu (ppm)	1,14	1,13	1,30	1,07	1,30	1,32	1,29
Sn (ppm)	b.d.	0,5	0,5	b.d.	b.d.	b.d.	b.d.
Gd (ppm)	3,82	3,48	3,89	3,49	3,79	4,22	3,96
Dy (ppm)	4,48	4,00	4,02	3,88	4,62	5,05	4,56
Li (ppm)	5	4	8	8	7	8	8
Y (ppm)	28	27	27	26	31	33	31
Ho (ppm)	b.d.	b.d.	b.d.	b.d.	b.d.	1	b.d.
Er (ppm)	2,56	2,45	2,54	2,38	2,94	3,16	2,86
Yb (ppm)	2,48	2,30	2,58	2,51	2,79	3,07	2,72
Lu (ppm)	0,36	0,38	0,38	0,39	0,41	0,45	0,43
Co (ppm)	34	34	34	33	37	37	37
Cr (ppm)	269	289	363	240	183	184	172
Cu (ppm)	111	109	113	90	149	156	148
Ni (ppm)	64	66	66	43	48	46	45
Sc (ppm)	39	37	38	37	39	37	37
V (ppm)	274	260	266	245	297	289	280
Zn (ppm)	96	96	94	100	110	114	111
Tb (ppm)	0,8	0,7	0,8	0,7	0,8	0,9	0,8
Tm (ppm)	0,4	0,3	0,4	0,4	0,4	0,5	0,4
S I	3,81	4,52	3,04	-5,26	-2,54	-4,01	-2,81
S II	-3,14	-2,82	-2,49	-4,99	-1,68	-2,49	-3,33
S III	2,09	2,67	2,37	-0,42	-4,96	-5,55	-5,79

Sample:	K05-138	K05-140	K05-141	K05-142	K05-143	K05-144	K05-145
Magma b./Loc.:	CD	CD	CD	CD	CD	CD	CD
Latitude (N):	-32,0548	-31,9262	-31,9261	-31,9261	-31,9261	-31,9261	-31,7683
Longitude (E):	25,3594	25,3064	25,3065	25,3065	25,3065	25,3065	25,2127
Altitude (m):	1087	1052	1053	1037	1036	1037	1143
SiO2 (wt %)	52,05	51,30	50,50	51,40	51,67	51,58	50,59
TiO2 (wt %)	1,07	1,16	1,18	1,19	1,25	1,13	1,07
Al2O3 (wt %)	14,92	14,65	14,45	14,66	14,48	14,76	14,74
Fe2O3(T) (wt %)	12,04	12,47	12,84	12,74	13,01	12,60	12,07
MnO (wt %)	0,19	0,19	0,20	0,20	0,20	0,19	0,18
MgO (wt %)	6,11	6,04	6,00	5,88	5,88	6,08	6,20
CaO (wt %)	9,86	9,79	9,61	9,75	9,77	9,79	10,08
Na2O (wt %)	2,29	2,32	2,28	2,29	2,34	2,19	2,30
K2O (wt %)	0,70	0,80	0,68	0,80	0,75	0,73	0,76
P2O5 (wt %)	0,17	0,17	0,17	0,17	0,18	0,17	0,17
SUM	99,4	98,9	97,9	99,1	99,5	99,2	98,2
Cs (ppm)	0,9	0,6	0,7	1,0	0,9	0,8	0,4
Tl (ppm)	0,2	b.d.	b.d.	0,2	0,2	0,2	b.d.
Rb (ppm)	17	17	16	19	22	18	16
Ba (ppm)	217	227	193	222	216	215	218
Th (ppm)	1,8	2,0	1,7	2,2	2,7	2,0	1,9
U (ppm)	0,45	0,43	0,40	0,46	0,53	0,44	0,47
Nb (ppm)	8,6	8,5	7,8	8,9	8,9	9,2	9,3
Ta (ppm)	0,43	0,47	0,45	0,47	0,54	0,46	0,54
La (ppm)	11,84	11,40	11,24	12,86	13,33	12,49	13,79
Ce (ppm)	27,01	26,38	25,53	29,04	30,04	28,02	29,42
Pb (ppm)	5	6	5	7	6	3	3
Pr (ppm)	3,26	3,18	3,05	3,32	3,51	3,29	3,35
Mo (ppm)	1,4	2,0	1,8	1,8	1,7	1,9	1,2
Sr (ppm)	204	201	202	205	193	204	199
Nd (ppm)	15,7	15,8	15,1	16,7	17,2	16,2	15,9
Zr (ppm)	100	103	97	108	113	103	97
Hf (ppm)	2,58	2,69	2,48	2,98	2,98	2,61	2,53
Sm (ppm)	3,71	3,77	3,79	4,37	4,49	4,02	3,47
Eu (ppm)	1,11	1,06	1,21	1,24	1,26	1,19	1,17
Sn (ppm)	b.d.	0,8	0,9	0,8	1,0	0,7	1,1
Gd (ppm)	3,37	3,50	3,50	3,76	4,24	3,71	3,54
Dy (ppm)	3,93	4,12	4,36	4,83	5,08	4,15	4,25
Li (ppm)	9	6	11	7	8	7	29
Y (ppm)	26	28	29	31	33	29	29
Ho (ppm)	b.d.	b.d.	b.d.	b.d.	1	b.d.	b.d.
Er (ppm)	2,56	2,60	2,53	2,95	2,92	2,53	2,36
Yb (ppm)	2,46	2,66	2,71	2,79	2,88	2,64	2,41
Lu (ppm)	0,39	0,40	0,42	0,42	0,44	0,40	0,36
Co (ppm)	32	33	34	33	35	33	33
Cr (ppm)	250	239	229	226	217	242	313
Cu (ppm)	91	104	111	106	130	92	94
Ni (ppm)	42	45	46	44	46	43	46
Sc (ppm)	37	37	37	36	39	37	37
V (ppm)	239	249	259	253	277	236	246
Zn (ppm)	99	101	104	102	106	101	97
Tb (ppm)	0,7	0,7	0,7	0,8	0,8	0,7	0,6
Tm (ppm)	0,4	0,4	0,4	0,4	0,4	0,4	0,4
S I	-5,87	-4,84	-5,67	-5,83	-3,54	-6,18	-4,79
S II	-5,45	-4,44	-3,65	-3,41	-4,44	-4,75	-4,76
S III	-1,58	-2,75	-3,84	-3,15	-5,77	-2,63	-0,35

Sample:	K05-146	K05-147	K05-148	K05-149	K05-150	K05-151	K05-152
Magma b./Loc.:	CD	CD	CD	CD	CD	CD	CD
Latitude (N):	-31,7683	-31,7683	-31,7684	-31,7684	-31,5525	-31,5525	-31,5527
Longitude (E):	25,2127	25,2126	25,2126	25,2125	25,0827	25,0827	25,0827
Altitude (m):	1143	1147	1149	1147	1206	1207	1207
SiO2 (wt %)	51,35	51,41	50,45	49,81	51,10	50,59	51,37
TiO2 (wt %)	1,14	1,15	1,15	1,12	1,14	1,22	1,22
Al2O3 (wt %)	14,64	14,96	14,40	14,22	14,65	14,34	14,59
Fe2O3(T) (wt %)	12,56	12,35	12,46	12,39	12,65	13,24	13,21
MnO (wt %)	0,19	0,19	0,19	0,19	0,19	0,20	0,20
MgO (wt %)	6,17	5,94	6,10	6,01	6,22	6,32	6,24
CaO (wt %)	9,97	9,83	10,09	9,95	10,03	9,93	9,69
Na2O (wt %)	2,35	2,27	2,40	2,34	2,34	2,46	2,28
K2O (wt %)	0,77	0,72	0,76	0,79	0,80	0,82	0,75
P2O5 (wt %)	0,18	0,17	0,17	0,17	0,17	0,17	0,17
SUM	99,3	99,0	98,2	97,0	99,3	99,3	99,7
Cs (ppm)	0,4	0,4	0,4	0,4	0,5	0,3	0,3
Tl (ppm)	b.d.	0,2	b.d.	b.d.	b.d.	b.d.	b.d.
Rb (ppm)	15	16	14	15	18	15	16
Ba (ppm)	227	219	224	222	234	230	233
Th (ppm)	2,0	1,8	2,1	1,8	2,1	1,8	2,1
U (ppm)	0,52	0,36	0,42	0,46	0,48	0,46	0,40
Nb (ppm)	9,4	7,9	7,9	7,0	8,0	8,7	8,6
Ta (ppm)	0,51	0,42	0,47	0,49	0,49	0,49	0,50
La (ppm)	13,69	11,69	13,30	12,49	13,22	12,82	12,76
Ce (ppm)	29,87	25,59	27,77	26,22	28,35	26,82	27,93
Pb (ppm)	2	5	6	3	1	3	6
Pr (ppm)	3,51	3,09	3,44	3,10	3,29	3,15	3,17
Mo (ppm)	1,2	2,1	0,7	0,5	0,6	0,8	2,0
Sr (ppm)	206	214	205	197	207	233	215
Nd (ppm)	16,6	15,0	16,7	15,2	15,2	15,2	16,4
Zr (ppm)	106	97	104	102	105	102	107
Hf (ppm)	2,67	2,40	2,46	2,52	2,62	2,52	2,69
Sm (ppm)	3,81	3,74	3,73	3,18	3,82	3,75	4,02
Eu (ppm)	1,26	1,10	1,21	1,21	1,19	1,17	1,24
Sn (ppm)	0,9	0,8	1,0	1,1	0,7	0,8	0,8
Gd (ppm)	3,56	3,47	3,73	3,56	3,44	3,59	3,82
Dy (ppm)	4,55	4,13	4,33	3,98	4,06	4,45	4,35
Li (ppm)	14	8	14	10	6	9	11
Y (ppm)	30	27	28	27	29	28	31
Ho (ppm)	b.d.	b.d.	b.d.	b.d.	b.d.	b.d.	b.d.
Er (ppm)	2,58	2,59	2,41	2,36	2,43	2,38	2,78
Yb (ppm)	2,66	2,44	2,47	2,35	2,38	2,40	2,78
Lu (ppm)	0,38	0,40	0,37	0,32	0,38	0,37	0,44
Co (ppm)	35	33	34	34	33	34	34
Cr (ppm)	258	240	255	241	243	255	247
Cu (ppm)	104	105	104	101	96	110	111
Ni (ppm)	46	44	45	45	44	47	46
Sc (ppm)	38	36	37	36	37	39	38
V (ppm)	248	245	244	244	250	261	257
Zn (ppm)	102	99	99	98	97	100	102
Tb (ppm)	0,7	0,7	0,7	0,6	0,6	0,6	0,7
Tm (ppm)	0,4	0,4	0,4	0,4	0,4	0,4	0,4
S I	-4,92	-4,79	-4,84	-5,78	-5,77	-3,79	-4,70
S II	-4,51	-3,76	-3,96	-3,58	-3,94	-2,91	-3,89
S III	-3,85	-2,81	-2,91	-3,66	-2,38	-2,59	-3,50

Sample:	K05-153	K05-154	K05-155	K05-156	K05-157	K05-158	K05-159
Magma b./Loc.:	CD	CD	GVD	GVD	GVD	GVD	GVD
Latitude (N):	-31,5527	-31,5527	-31,9754	-31,9754	-31,9754	-31,9752	-31,9009
Longitude (E):	25,0827	25,0827	26,2203	26,2203	26,2201	26,2200	26,1639
Altitude (m):	1208	1209	1290	1291	1291	1288	1225
SiO2 (wt %)	51,11	51,35	51,20	50,83	51,08	51,40	50,23
TiO2 (wt %)	1,07	1,07	1,29	1,20	1,27	1,23	1,30
Al2O3 (wt %)	14,72	14,75	14,38	14,40	14,37	14,39	14,06
Fe2O3(T) (wt %)	11,95	11,95	13,89	13,43	13,76	13,22	13,80
MnO (wt %)	0,18	0,18	0,21	0,20	0,21	0,21	0,20
MgO (wt %)	6,23	6,43	5,78	5,82	5,82	5,90	5,64
CaO (wt %)	10,07	10,07	10,38	10,62	10,28	10,34	10,50
Na2O (wt %)	2,24	2,30	2,38	2,41	2,32	2,43	2,56
K2O (wt %)	0,74	0,77	0,41	0,36	0,38	0,45	0,40
P2O5 (wt %)	0,17	0,17	0,16	0,15	0,16	0,16	0,16
SUM	98,5	99,0	100,1	99,4	99,7	99,7	98,9
Cs (ppm)	0,3	0,3	0,6	0,4	0,5	1,1	0,4
Tl (ppm)	b.d.	b.d.	b.d.	b.d.	b.d.	b.d.	b.d.
Rb (ppm)	14	16	11	9	10	11	8
Ba (ppm)	213	216	171	152	164	171	189
Th (ppm)	1,9	2,1	1,4	1,2	1,3	1,4	1,4
U (ppm)	0,43	0,49	0,30	0,29	0,28	0,31	0,33
Nb (ppm)	8,8	9,0	6,6	6,1	6,0	6,2	6,4
Ta (ppm)	0,47	0,54	0,33	0,33	0,33	0,35	0,33
La (ppm)	13,22	15,67	9,53	8,66	9,24	9,39	10,13
Ce (ppm)	28,39	30,33	21,76	20,72	21,26	22,00	22,63
Pb (ppm)	6	4	8	5	5	5	3
Pr (ppm)	3,29	3,42	2,62	2,54	2,58	2,68	2,75
Mo (ppm)	0,6	1,0	1,6	1,5	1,8	1,5	0,5
Sr (ppm)	198	194	185	186	190	184	186
Nd (ppm)	15,8	17,3	13,9	13,3	13,9	13,8	13,9
Zr (ppm)	104	100	97	92	96	97	97
Hf (ppm)	2,58	2,79	2,45	2,31	2,53	2,45	2,43
Sm (ppm)	3,80	3,82	3,72	3,63	3,81	3,83	3,76
Eu (ppm)	1,14	1,19	1,24	1,32	1,32	1,32	1,18
Sn (ppm)	0,8	0,9	0,6	0,6	0,6	0,7	0,9
Gd (ppm)	3,33	3,66	3,88	3,78	4,00	3,86	3,68
Dy (ppm)	4,31	4,47	4,65	4,52	4,29	4,58	4,42
Li (ppm)	13	6	12	10	13	12	8
Y (ppm)	28	30	31	30	30	30	30
Ho (ppm)	b.d.	b.d.	b.d.	b.d.	b.d.	b.d.	1
Er (ppm)	2,42	2,55	2,83	2,69	2,83	2,96	2,54
Yb (ppm)	2,49	2,67	2,66	2,58	2,77	2,70	2,70
Lu (ppm)	0,39	0,36	0,40	0,39	0,43	0,43	0,38
Co (ppm)	33	33	36	36	37	37	39
Cr (ppm)	234	253	184	174	172	170	184
Cu (ppm)	97	96	150	137	150	155	147
Ni (ppm)	44	44	55	59	57	56	58
Sc (ppm)	38	39	40	39	40	41	39
V (ppm)	249	245	310	299	310	315	303
Zn (ppm)	98	97	105	101	102	105	108
Tb (ppm)	0,7	0,7	0,7	0,7	0,7	0,8	0,7
Tm (ppm)	0,4	0,4	0,4	0,4	0,4	0,4	0,4
S I	-4,71	-4,61	2,38	2,89	3,06	2,78	0,95
S II	-4,73	-5,64	1,70	2,84	1,71	0,34	1,78
S III	-2,80	-2,93	-8,93	-8,37	-8,28	-8,00	-8,48

Sample:	K05-160	K05-161	K05-162	K05-163	K05-164	K05-165	K05-166
Magma b./Loc.:	GVD	GVD	GVD	GVD	GVD	GVD	GVD
Latitude (N):	-31,9010	-31,9009	-31,9009	-31,8402	-31,8402	-31,8402	-31,8400
Longitude (E):	26,1639	26,1640	26,1640	26,1327	26,1326	26,1328	26,1327
Altitude (m):	1229	1230	1232	1273	1277	1278	1270
SiO2 (wt %)	50,56	51,05	50,20	50,45	50,54	50,93	50,84
TiO2 (wt %)	1,25	1,30	1,22	1,26	1,26	1,23	1,21
Al2O3 (wt %)	14,08	14,34	14,03	14,07	14,17	14,58	14,06
Fe2O3(T) (wt %)	13,40	13,96	13,37	13,44	13,52	13,47	13,16
MnO (wt %)	0,20	0,21	0,20	0,20	0,20	0,20	0,20
MgO (wt %)	5,85	5,85	5,67	5,80	5,76	5,92	5,75
CaO (wt %)	10,38	10,29	10,54	10,49	10,43	10,52	10,47
Na2O (wt %)	2,35	2,31	2,40	2,41	2,47	2,41	2,42
K2O (wt %)	0,56	0,54	0,52	0,59	0,58	0,56	0,56
P2O5 (wt %)	0,16	0,16	0,16	0,17	0,16	0,16	0,16
SUM	98,8	100,0	98,3	98,9	99,1	100,0	98,8
Cs (ppm)	0,5	0,5	0,5	0,3	0,4	0,4	0,5
Tl (ppm)	b.d.	0,2	b.d.	b.d.	b.d.	b.d.	b.d.
Rb (ppm)	11	12	10	12	13	12	12
Ba (ppm)	170	177	174	203	198	180	184
Th (ppm)	1,3	1,4	1,3	1,3	1,4	1,2	1,4
U (ppm)	0,31	0,26	0,35	0,30	0,36	0,28	0,37
Nb (ppm)	6,2	6,0	5,8	5,7	6,2	5,7	6,4
Ta (ppm)	0,35	0,36	0,37	0,34	0,36	0,32	0,38
La (ppm)	9,82	9,29	9,39	9,57	10,10	8,80	9,73
Ce (ppm)	21,61	21,26	20,38	21,28	22,12	21,04	22,20
Pb (ppm)	5	5	b.d.	3	b.d.	4	2
Pr (ppm)	2,73	2,54	2,66	2,63	2,74	2,51	2,68
Mo (ppm)	0,3	1,5	0,5	b.d.	0,3	1,4	0,4
Sr (ppm)	172	188	179	183	185	187	178
Nd (ppm)	13,5	14,4	13,4	13,8	13,8	12,1	14,2
Zr (ppm)	101	95	98	97	97	92	97
Hf (ppm)	2,27	2,54	2,28	2,41	2,48	2,41	2,49
Sm (ppm)	3,41	3,88	3,75	3,66	3,89	3,67	3,57
Eu (ppm)	1,24	1,18	1,11	1,12	1,20	1,21	1,15
Sn (ppm)	0,8	0,8	1,2	0,8	0,7	0,7	0,9
Gd (ppm)	3,51	3,86	3,39	3,55	3,65	3,23	3,65
Dy (ppm)	4,56	4,37	4,31	4,44	4,71	4,33	4,59
Li (ppm)	3	9	22	7	4	7	3
Y (ppm)	30	30	29	30	31	29	30
Ho (ppm)	b.d.	b.d.	b.d.	b.d.	b.d.	b.d.	b.d.
Er (ppm)	2,48	2,67	2,41	2,44	2,41	2,54	2,49
Yb (ppm)	2,76	2,69	2,54	2,58	2,60	2,62	2,45
Lu (ppm)	0,39	0,42	0,36	0,35	0,40	0,39	0,36
Co (ppm)	38	37	37	38	38	36	38
Cr (ppm)	180	178	197	181	185	189	193
Cu (ppm)	154	151	147	156	151	152	150
Ni (ppm)	57	57	59	57	58	58	58
Sc (ppm)	41	40	40	41	41	42	40
V (ppm)	316	311	305	318	311	318	308
Zn (ppm)	103	104	103	104	102	101	103
Tb (ppm)	0,7	0,8	0,7	0,7	0,7	0,7	0,6
Tm (ppm)	0,4	0,4	0,4	0,4	0,4	0,4	0,4
S I	2,79	2,67	2,97	3,56	3,75	5,07	3,24
S II	1,07	0,64	1,83	0,47	1,45	-0,10	0,35
S III	-8,88	-7,90	-8,72	-9,06	-8,93	-7,44	-8,37

Sample:	K04C-53	K04C-54	K04C-55	K04C-56	K04C-62	K04K-04	K04K-05
Magma b./Loc.:	L1	L1	L1	L1	L1	L1	L1
Latitude (N):	-31,8617	-31,8618	-31,8616	-31,8618	-31,8614	-31,8168	-31,8160
Longitude (E):	26,1578	26,1578	26,1575	26,1570	26,1569	26,1975	26,1980
Altitude (m):	1215	1227	1239	1253	1255	1434	1428
SiO2 (wt %)	50,43	50,17	49,82	49,95	52,07	49,54	50,58
TiO2 (wt %)	0,99	0,92	0,83	0,88	1,15	0,83	1,02
Al2O3 (wt %)	15,38	15,89	16,30	16,23	14,71	15,80	16,01
Fe2O3(T) (wt %)	10,64	10,24	10,27	10,73	11,28	10,15	10,60
MnO (wt %)	0,16	0,16	0,16	0,16	0,18	0,16	0,16
MgO (wt %)	7,04	7,04	7,67	7,88	5,78	8,30	6,34
CaO (wt %)	10,69	10,41	10,40	10,23	10,49	10,41	10,68
Na2O (wt %)	2,51	2,46	2,32	2,41	2,56	2,37	2,51
K2O (wt %)	0,44	0,45	0,41	0,40	0,51	0,40	0,51
P2O5 (wt %)	0,14	0,13	0,12	0,12	0,17	0,12	0,15
SUM	98,4	97,9	98,3	99,0	98,9	98,1	98,6
Cs (ppm)	0,9	0,7	0,4	0,5	1,1	0,4	0,4
Tl (ppm)	b.d.	b.d.	b.d.	b.d.	b.d.	b.d.	b.d.
Rb (ppm)	9	9	8	8	10	8	10
Ba (ppm)	165	159	138	148	188	135	162
Th (ppm)	1,4	1,1	0,8	1,0	2,3	1,1	1,8
U (ppm)	0,25	0,21	0,15	0,20	0,32	0,19	0,24
Nb (ppm)	7,5	6,9	6,8	5,8	8,8	6,1	7,7
Ta (ppm)	0,35	0,41	0,32	0,31	0,49	0,32	0,37
La (ppm)	8,29	7,51	6,66	7,15	10,12	6,73	7,94
Ce (ppm)	18,73	16,72	15,06	15,98	22,84	14,86	18,16
Pb (ppm)	3	5	5	4	3	5	3
Pr (ppm)	2,32	2,10	1,76	1,94	2,69	1,76	2,06
Mo (ppm)	1,1	0,9	0,9	0,8	1,0	0,8	1,0
Sr (ppm)	218	234	227	241	221	216	245
Nd (ppm)	11,5	10,5	9,2	9,5	13,2	9,3	10,7
Zr (ppm)	70	61	55	55	80	61	70
Hf (ppm)	1,74	1,48	1,35	1,44	1,97	1,45	1,78
Sm (ppm)	3,24	2,53	2,66	2,82	3,64	2,41	3,02
Eu (ppm)	1,02	0,97	0,92	0,99	1,25	0,83	1,03
Sn (ppm)	b.d.	b.d.	b.d.	b.d.	3,5	0,6	0,7
Gd (ppm)	2,83	2,65	2,32	2,48	3,45	2,45	2,85
Dy (ppm)	3,32	3,14	2,92	3,10	3,99	2,79	3,43
Li (ppm)	9	6	4	4	6	3	5
Y (ppm)	23	21	19	20	27	18	21
Ho (ppm)	b.d.	b.d.	b.d.	b.d.	b.d.	b.d.	b.d.
Er (ppm)	2,10	1,84	1,65	1,84	2,46	1,68	2,05
Yb (ppm)	2,03	1,78	1,72	1,84	2,43	1,64	1,95
Lu (ppm)	0,32	0,24	0,28	0,28	0,36	0,25	0,30
Co (ppm)	33	33	34	34	33	35	31
Cr (ppm)	477	422	440	384	361	487	336
Cu (ppm)	93	83	80	84	100	78	94
Ni (ppm)	113	123	145	145	60	170	82
Sc (ppm)	34	30	28	28	37	29	33
V (ppm)	255	216	204	203	268	201	237
Zn (ppm)	83	80	79	82	87	80	82
Tb (ppm)	0,6	0,6	0,4	0,5	0,7	0,5	0,6
Tm (ppm)	0,3	0,3	0,2	0,3	0,4	0,2	0,3
S I	2,52	2,50	3,42	1,41	0,81	3,93	2,18
S II	10,07	10,04	10,01	9,63	6,49	11,42	6,52
S III	5,64	6,60	6,06	4,00	3,92	6,08	3,60

Sample:	K04A-06	K04A-07	K04A-05	K04A-08	K04A-09	K04A-10	K04-C57
Magma b./Loc.:	L2	L2	L2	L2	L2	L2	L2
Latitude (N):	-31,8887	-31,8925		-31,8891	-31,8882	-31,8888	-31,8871
Longitude (E):	26,1920	26,2018		26,1970	26,1967	26,1934	26,1720
Altitude (m):	1362	1509		1401	1380	1375	1303
SiO2 (wt %)	50,55	49,83	49,00	49,16	50,21	51,27	50,34
TiO2 (wt %)	0,97	0,93	0,90	0,85	0,77	0,86	0,93
Al2O3 (wt %)	15,28	15,26	15,18	15,21	15,99	14,71	15,46
Fe2O3(T) (wt %)	11,31	10,93	10,64	10,31	9,91	11,00	11,16
MnO (wt %)	0,18	0,17	0,16	0,16	0,16	0,19	0,17
MgO (wt %)	6,97	7,50	7,33	7,04	6,56	6,13	7,14
CaO (wt %)	10,66	10,82	10,84	10,65	11,22	10,57	11,06
Na2O (wt %)	2,51	2,46	2,37	2,28	2,33	2,47	2,23
K2O (wt %)	0,46	0,45	0,43	0,44	0,39	0,46	0,42
P2O5 (wt %)	0,14	0,12	0,12	0,12	0,10	0,11	0,12
SUM	99,0	98,5	97,0	96,2	97,6	97,8	99,0
Cs (ppm)	2,2	0,6	0,4	0,3	0,4	0,2	0,7
Tl (ppm)	b.d.	b.d.	b.d.	b.d.	b.d.	b.d.	b.d.
Rb (ppm)	23	10	7	7	7	9	7
Ba (ppm)	160	150	146	139	130	226	156
Th (ppm)	1,9	0,8	0,8	0,7	0,8	0,8	0,7
U (ppm)	0,66	0,21	0,18	0,17	0,16	0,16	0,19
Nb (ppm)	7,3	5,2	5,2	4,4	4,3	4,5	4,5
Ta (ppm)	0,48	0,30	0,26	0,29	0,26	0,29	0,29
La (ppm)	9,25	6,77	6,87	6,55	6,13	6,89	6,64
Ce (ppm)	20,63	16,11	15,68	15,26	14,53	15,15	15,60
Pb (ppm)	2	4	4	4	3	4	4
Pr (ppm)	2,61	1,97	2,00	1,86	1,83	1,95	1,93
Mo (ppm)	1,0	0,8	0,6	0,7	0,9	0,6	0,8
Sr (ppm)	194	202	200	180	191	194	191
Nd (ppm)	12,7	9,9	11,6	10,3	9,5	10,2	10,4
Zr (ppm)	85	78	76	74	71	71	77
Hf (ppm)	1,90	1,77	1,80	1,74	1,62	1,80	1,71
Sm (ppm)	3,89	2,94	2,66	2,61	2,70	2,84	2,55
Eu (ppm)	1,10	0,89	0,95	0,94	0,93	0,96	0,86
Sn (ppm)	b.d.	b.d.	b.d.	b.d.	b.d.	b.d.	b.d.
Gd (ppm)	3,18	2,57	2,64	2,69	2,59	2,71	2,73
Dy (ppm)	4,12	3,55	3,72	3,31	3,10	3,45	3,40
Li (ppm)	b.d.	b.d.	2	12	2	2	2
Y (ppm)	27	23	24	21	21	24	23
Ho (ppm)	b.d.	b.d.	b.d.	b.d.	b.d.	b.d.	b.d.
Er (ppm)	2,13	1,76	1,98	1,97	1,73	2,12	1,97
Yb (ppm)	2,26	1,82	1,92	1,87	1,82	2,13	1,74
Lu (ppm)	0,32	0,32	0,28	0,26	0,28	0,31	0,29
Co (ppm)	35	35	36	34	31	35	35
Cr (ppm)	345	402	400	384	258	115	368
Cu (ppm)	103	92	96	94	87	149	96
Ni (ppm)	92	112	117	103	80	61	105
Sc (ppm)	35	34	33	33	34	39	33
V (ppm)	254	240	232	234	240	275	240
Zn (ppm)	89	86	86	85	79	89	88
Tb (ppm)	0,6	0,5	0,5	0,5	0,5	0,5	0,5
Tm (ppm)	0,3	0,3	0,3	0,3	0,3	0,3	0,3
S I	-1,83	0,19	1,08	0,42	3,15	9,66	-0,47
S II	6,37	8,20	9,91	6,10	5,47	-1,78	8,23
S III	-3,77	-0,18	-1,87	-1,19	-2,24	-8,52	-2,49

Sample:	K05-52	K05-54	K05-55	K05-56	K05-57	K05-58	K05-60
Magma b./Loc.:	L3	L3	L3	L3	L3	L3	L3
Latitude (N):	-31,9886	-31,9884	-31,9885	-31,9886	-31,9887	-31,9887	-31,9888
Longitude (E):	26,2196	26,2197	26,2197	26,2198	26,2199	26,2199	26,2201
Altitude (m):	1245	1242	1248	1246	1249	1248	1251
SiO2 (wt %)	50,67	50,78	50,68	50,80	50,61	51,26	50,16
TiO2 (wt %)	0,94	0,90	0,91	0,91	0,89	0,94	0,94
Al2O3 (wt %)	15,36	15,31	15,37	15,57	15,71	15,62	15,35
Fe2O3(T) (wt %)	11,34	10,96	11,18	11,14	11,24	11,30	11,34
MnO (wt %)	0,17	0,17	0,18	0,18	0,17	0,17	0,17
MgO (wt %)	6,95	6,72	6,97	7,05	7,37	7,09	7,02
CaO (wt %)	10,94	10,71	10,90	10,75	11,08	10,82	10,92
Na2O (wt %)	2,37	2,31	2,34	2,36	2,35	2,37	2,36
K2O (wt %)	0,56	0,58	0,58	0,59	0,55	0,67	0,59
P2O5 (wt %)	0,14	0,14	0,14	0,14	0,14	0,15	0,14
SUM	99,4	98,6	99,2	99,5	100,1	100,4	99,0
Cs (ppm)	1,3	1,5	0,4	1,1	0,9	0,4	0,9
Tl (ppm)	0,2	b.d.	b.d.	b.d.	b.d.	b.d.	b.d.
Rb (ppm)	14	14	12	13	12	13	11
Ba (ppm)	175	173	180	179	167	188	185
Th (ppm)	1,5	1,4	1,2	1,2	2,0	1,3	1,2
U (ppm)	0,31	0,26	0,26	0,23	0,32	0,26	0,24
Nb (ppm)	6,9	7,3	6,8	6,8	6,6	7,5	6,9
Ta (ppm)	0,36	0,37	0,38	0,34	0,39	0,39	0,36
La (ppm)	9,36	9,63	9,55	9,19	9,29	10,07	8,93
Ce (ppm)	21,67	22,08	21,42	20,92	21,29	22,58	19,42
Pb (ppm)	6	8	5	7	7	5	b.d.
Pr (ppm)	2,60	2,59	2,53	2,44	2,47	2,73	2,30
Mo (ppm)	1,1	1,3	1,2	1,2	1,1	0,9	1,4
Sr (ppm)	206	199	202	202	206	216	211
Nd (ppm)	13,0	12,5	13,0	12,3	12,5	13,3	11,7
Zr (ppm)	84	90	85	82	79	86	80
Hf (ppm)	2,20	2,18	2,12	2,03	1,89	2,34	1,87
Sm (ppm)	3,00	3,19	3,22	3,02	3,10	3,22	2,94
Eu (ppm)	1,01	0,98	1,02	1,00	0,98	1,10	0,89
Sn (ppm)	b.d.	b.d.	b.d.	b.d.	b.d.	b.d.	1,6
Gd (ppm)	2,97	3,04	3,03	2,81	2,80	3,03	2,54
Dy (ppm)	3,36	3,51	3,47	3,54	3,47	3,56	3,16
Li (ppm)	12	8	5	8	7	8	7
Y (ppm)	24	23	23	22	22	24	21
Ho (ppm)	b.d.	b.d.	b.d.	b.d.	b.d.	b.d.	b.d.
Er (ppm)	2,21	2,14	2,08	2,05	2,07	2,26	1,99
Yb (ppm)	2,22	2,23	2,18	2,08	2,06	2,26	2,00
Lu (ppm)	0,32	0,32	0,34	0,29	0,30	0,33	0,30
Co (ppm)	34	33	34	33	33	33	33
Cr (ppm)	306	303	312	295	292	284	293
Cu (ppm)	91	89	89	89	90	93	90
Ni (ppm)	84	81	83	84	85	79	81
Sc (ppm)	36	35	36	36	36	37	36
V (ppm)	246	243	242	238	236	250	243
Zn (ppm)	85	91	88	92	89	88	88
Tb (ppm)	0,6	0,6	0,6	0,6	0,6	0,6	0,6
Tm (ppm)	0,3	0,3	0,3	0,3	0,3	0,3	0,3
S I	1,14	0,20	1,58	0,16	-0,67	1,52	0,70
S II	3,29	0,26	0,56	-0,21	0,35	-0,34	1,64
S III	0,92	2,23	0,36	0,99	-0,57	1,01	1,29

Sample:	K05-61	K05-184	K05-185	K05-187	K05-188	K05-21	K05-22
Magma b./Loc.:	L3	s1	s1	s1	s1	d5	d5
Latitude (N):	-31,9888	-31,9779	-31,9803	-31,9416	-31,9419	-31,8978	-31,8978
Longitude (E):	26,2201	26,2713	26,2726	26,2490	26,2487	26,3700	26,3699
Altitude (m):	1252	1353	1362	1419	1425	1298	1365
SiO2 (wt %)	50,53	50,56	50,68	49,73	49,72	53,01	52,60
TiO2 (wt %)	0,91	0,95	0,89	0,98	0,88	1,36	1,38
Al2O3 (wt %)	15,44	15,58	15,34	14,77	15,63	14,72	14,61
Fe2O3(T) (wt %)	11,24	11,43	10,71	11,38	10,84	10,98	11,28
MnO (wt %)	0,18	0,18	0,17	0,18	0,16	0,18	0,17
MgO (wt %)	7,08	7,53	7,21	7,33	7,45	5,69	6,10
CaO (wt %)	10,72	10,99	10,86	10,92	11,16	9,39	9,44
Na2O (wt %)	2,37	2,62	2,27	2,46	2,41	2,47	2,55
K2O (wt %)	0,57	0,45	0,11	0,48	0,43	0,77	0,79
P2O5 (wt %)	0,14	0,13	0,12	0,12	0,11	0,22	0,22
SUM	99,2	100,4	98,4	98,3	98,8	98,8	99,1
Cs (ppm)	1,3	0,2	0,5	0,2	0,1	0,7	0,8
Tl (ppm)	b.d.	b.d.	b.d.	b.d.	b.d.	0,2	0,2
Rb (ppm)	13	7	3	8	7	17	16
Ba (ppm)	181	154	76	159	142	263	259
Th (ppm)	1,5	b.d.	b.d.	b.d.	b.d.	1,8	1,8
U (ppm)	0,24	0,18	0,17	0,19	0,16	0,36	0,35
Nb (ppm)	6,7	5,0	5,4	5,2	4,5	5,7	5,1
Ta (ppm)	0,32	0,26	0,26	0,29	0,24	0,39	0,25
La (ppm)	10,2	6,9	7,8	7,1	5,7	11,4	11,9
Ce (ppm)	24,1	15,7	17,0	16,6	14,1	26,0	26,4
Pb (ppm)	6	0	5	4	5	7	5
Pr (ppm)	2,70	1,90	2,11	2,10	1,82	3,08	3,15
Mo (ppm)	1,5	0,3	2,1	1,7	1,7	1,3	1,4
Sr (ppm)	211	199	193	197	198	192	206
Nd (ppm)	13,5	10,3	10,8	11,5	9,0	15,1	14,6
Zr (ppm)	82	78	78	79	71	96	94
Hf (ppm)	2,10	1,58	1,72	1,82	1,68	2,40	2,51
Sm (ppm)	3,17	2,75	3,19	3,24	2,56	3,97	3,93
Eu (ppm)	1,10	1,01	1,05	1,11	0,81	1,23	1,27
Sn (ppm)	0,5	0,6	0,5	b.d.	b.d.	0,6	0,5
Gd (ppm)	3,07	2,83	2,99	2,85	2,65	3,92	3,77
Dy (ppm)	3,45	3,45	3,82	3,59	3,08	4,46	4,07
Li (ppm)	16	b.d.	11	7	b.d.	11	10
Y (ppm)	23	23	25	24	20	28	28
Ho (ppm)	b.d.	b.d.	b.d.	b.d.	b.d.	b.d.	b.d.
Er (ppm)	2,12	1,91	2,02	2,04	1,80	2,46	2,47
Yb (ppm)	2,04	2,00	2,13	2,23	1,87	2,52	2,35
Lu (ppm)	0,30	0,27	0,31	0,31	0,31	0,35	0,34
Co (ppm)	33	35	34	34	34	33	33
Cr (ppm)	271	403	345	442	447	247	276
Cu (ppm)	90	101	102	94	83	35	35
Ni (ppm)	81	100	99	96	103	14	14
Sc (ppm)	36	36	35	37	33	31	31
V (ppm)	243	260	252	262	234	248	255
Zn (ppm)	87	87	85	84	80	94	96
Tb (ppm)	0,6	0,5	0,6	0,5	0,5	0,7	0,7
Tm (ppm)	0,3	0,3	0,3	0,3	0,3	0,4	0,4
S I	0,71	0,74	1,39	0,42	-0,79	-22,64	-27,26
S II	-0,73	7,37	8,59	8,41	9,07	4,51	5,61
S III	2,56	-1,32	-2,84	-0,45	0,05	1,75	1,11

Sample:	K05-23	K05-28	%
Magma b./Loc.:	d5	d5	3 x STD
Latitude (N):	-31,8982	-31,9016	
Longitude (E):	26,3698	26,3743	
Altitude (m):	1364	1368	
SiO2 (wt %)	52,95	53,11	
TiO2 (wt %)	1,32	1,40	
Al2O3 (wt %)	14,71	14,62	
Fe2O3(T) (wt %)	11,20	11,24	
MnO (wt %)	0,17	0,18	
MgO (wt %)	6,32	5,92	
CaO (wt %)	9,35	9,48	
Na2O (wt %)	2,50	2,50	
K2O (wt %)	0,88	0,50	
P2O5 (wt %)	0,22	0,23	
SUM	99,6	99,2	
Cs (ppm)	0,4	0,6	0,085
Tl (ppm)	0,2	b.d.	0,064
Rb (ppm)	17	11	0,700
Ba (ppm)	252	238	1,273
Th (ppm)	2,0	2,1	1,527
U (ppm)	0,35	0,34	0,021
Nb (ppm)	5,5	5,1	1,973
Ta (ppm)	0,25	0,29	0,042
La (ppm)	12,0	11,7	0,361
Ce (ppm)	26,5	25,9	0,445
Pb (ppm)	6	5	2,503
Pr (ppm)	3,21	3,08	0,064
Mo (ppm)	1,4	1,5	1,421
Sr (ppm)	199	210	0,270
Nd (ppm)	15,0	15,5	0,212
Zr (ppm)	95	93	6,512
Hf (ppm)	2,52	2,51	0,127
Sm (ppm)	4,08	3,99	0,042
Eu (ppm)	1,23	1,32	0,042
Sn (ppm)	b.d.	b.d.	0,700
Gd (ppm)	3,81	3,75	0,042
Dy (ppm)	4,13	4,37	0,021
Li (ppm)	9	16	0,267
Y (ppm)	29	27	0,148
Ho (ppm)	b.d.	b.d.	0,636
Er (ppm)	2,54	2,46	0,021
Yb (ppm)	2,47	2,47	0,064
Lu (ppm)	0,34	0,38	0,021
Co (ppm)	34	33	0,814
Cr (ppm)	290	275	0,018
Cu (ppm)	36	36	2,546
Ni (ppm)	14	14	0,424
Sc (ppm)	30	31	1,026
V (ppm)	242	256	0,000
Zn (ppm)	97	95	1,697
Tb (ppm)	0,7	0,7	0,064
Tm (ppm)	0,4	0,4	0,636
S I	-28,08	-25,42	
S II	4,15	6,42	
S III	-0,99	1,69	

These analyses have been completed at the University of London, Royal Holloway using inductively coupled plasma - atomic emission spectrometry (ICP-AES) and - mass spectrometry (ICP-MS).

The analytical precision for major elements is 1% for Si, AL, Fe, Mg and Ca and 2% for Na, K, Ti, P and Mn. The analytical precisions and the standard deviations for the measured traces elements are directly reported from communicated values by the commercial laboratory of London.

Sample:	K04C-38	K04C-39	K04C-27	K04C-28	K04C-29	K04C-06	%
Magma b./Loc.:	MS	MS	MS/L4a	MS/L4a	MS/L4a	MS	STD
Latitude (N):	-31,9756	-31,9793	-31,9967	-31,9968	-31,9969	-31,9346	
Longitude (E):	26,2678	26,2673	26,2763	26,2764	26,2765	26,3875	
Altitude (m):	1353	1314	1601	1594	1582	1271	
SiO2 (wt %)	52,69	51,36	51,78	51,41	52,94	51,59	0,09
TiO2 (wt %)	1,13	0,90	0,99	0,78	1,19	0,99	0,80
Al2O3 (wt %)	15,17	16,01	15,52	15,85	14,05	15,59	0,44
Fe2O3(T) (wt %)	12,23	10,84	11,37	11,00	13,44	11,79	0,11
MnO (wt %)	0,19	0,17	0,18	0,17	0,21	0,18	0,00
MgO (wt %)	6,25	7,44	7,00	7,35	5,83	6,89	0,35
CaO (wt %)	10,21	10,92	10,80	11,32	9,38	10,44	0,15
Na2O (wt %)	2,16	2,31	2,18	2,16	2,36	2,12	0,40
K2O (wt %)	0,77	0,45	0,43	0,37	0,61	0,49	0,00
P2O5 (wt %)	0,19	0,13	0,13	0,09	0,15	0,13	6,29
L.O.I	0,03	0,06	0,17	0,22	0,46	0,25	0,00
SUM	101,0	100,6	100,6	100,7	100,6	100,5	0,06
Rb (ppm)	18	10	10	7	11	10	4,09
Nb (ppm)	8	7	6	5	9	7	6,42
Sr (ppm)	194	190	188	199	206	195	0,80
Zr (ppm)	111	80	79	53	92	78	1,68
Y (ppm)	30	24	27	20	32	27	4,25
Co (ppm)	48	47	51	50	57	53	1,20
Cr (ppm)	266	411	429	538	96	431	1,70
Cu (ppm)	117	96	104	90	140	108	0,86
Ni (ppm)	58	117	102	110	49	97	1,26
V (ppm)	299	261	279	279	352	288	1,80
Zn (ppm)	97	82	91	89	119	96	1,65

Sample:	K04C-07	K04C-09	K04C-48	K04C-66	K04C-67	K04C-68	%
Magma b./Loc.:	MS	MS	MS	GVS	GVS	GVS	STD
Latitude (N):	-31,9351	-31,9352	-31,9801	-31,867096	-31,865938	-31,865758	
Longitude (E):	26,3878	26,3875	26,2668	26,232899	26,23678	26,236905	
Altitude (m):	1272	1269	1275	1453	1436	1437	
SiO2 (wt %)	51,52	52,92	51,63	52,06	51,73	51,37	0,09
TiO2 (wt %)	0,85	1,39	0,94	1,05	1,05	1,05	0,80
Al2O3 (wt %)	15,86	13,86	15,89	15,36	15,49	15,35	0,44
Fe2O3(T) (wt %)	10,87	14,07	11,22	11,95	11,88	11,94	0,11
MnO (wt %)	0,17	0,21	0,18	0,19	0,20	0,19	0,00
MgO (wt %)	7,34	5,58	7,33	6,49	6,50	6,26	0,35
CaO (wt %)	11,03	9,20	10,82	10,45	10,40	10,49	0,15
Na2O (wt %)	2,13	2,26	2,16	2,22	2,29	2,27	0,40
K2O (wt %)	0,40	0,67	0,42	0,46	0,24	0,29	0,00
P2O5 (wt %)	0,12	0,21	0,12	0,14	0,16	0,15	6,29
L.O.I	0,29	0,36	0,26	0,59	1,05	0,71	0,00
SUM	100,6	100,7	101,0	101,0	101,0	100,1	0,06
Rb (ppm)	8	14	11	14	5	6	4,09
Nb (ppm)	6	9	7	9	8	7	6,42
Sr (ppm)	196	193	192	212	232	213	0,80
Zr (ppm)	67	120	79	106	110	112	1,68
Y (ppm)	20	39	25	30	28	29	4,25
Co (ppm)	50	54	51	53	54	53	1,20
Cr (ppm)	466	111	408	281	255	262	1,70
Cu (ppm)	100	157	97	110	112	113	0,86
Ni (ppm)	112	42	113	72	72	70	1,26
V (ppm)	262	346	274	322	292	300	1,80
Zn (ppm)	83	113	89	101	104	104	1,65

Sample:	K04C-40	K04C-41	K04C-42	K04C-43	K04C-44	K04C-45	%
Magma b./Loc.:	GVS	GVS	GVS	GVS	GVS	GVS	STD
Latitude (N):	-31,863297	-31,870807	-31,87087	-31,870931	-31,870288	-31,8708	
Longitude (E):	26,297931	26,307636	26,30759	26,30744	26,306951	26,30705	
Altitude (m):	1635	1684	1693	1700	1736	1751	
SiO2 (wt %)	52,70	51,70	52,08	52,20	51,78	51,98	0,09
TiO2 (wt %)	1,07	1,01	1,06	1,05	1,17	0,99	0,80
Al2O3 (wt %)	15,70	15,65	15,54	15,73	15,39	15,88	0,44
Fe2O3(T) (wt %)	12,17	11,82	11,92	11,88	12,06	11,50	0,11
MnO (wt %)	0,19	0,18	0,19	0,18	0,19	0,19	0,00
MgO (wt %)	6,18	6,23	6,38	6,30	6,58	6,45	0,35
CaO (wt %)	10,34	10,55	10,44	10,43	10,51	10,65	0,15
Na2O (wt %)	2,25	2,14	2,27	2,25	2,14	2,28	0,40
K2O (wt %)	0,70	0,64	0,72	0,71	0,67	0,65	0,00
P2O5 (wt %)	0,17	0,15	0,14	0,17	0,14	0,13	6,29
L.O.I	0,09	0,26	0	0,17	0,15	0,24	0,00
SUM	101,6	100,3	100,7	101,1	100,8	100,9	0,06
Rb (ppm)	16	14	16	15	17	16	4,09
Nb (ppm)	11	8	9	9	9	8	6,42
Sr (ppm)	202	201	201	198	197	207	0,80
Zr (ppm)	102	102	108	102	109	99	1,68
Y (ppm)	30	27	30	28	31	28	4,25
Co (ppm)	49	50	48	48	50	48	1,20
Cr (ppm)	276	281	277	273	298	281	1,70
Cu (ppm)	109	102	112	106	120	106	0,86
Ni (ppm)	66	69	66	67	67	66	1,26
V (ppm)	299	291	286	292	331	284	1,80
Zn (ppm)	97	93	96	94	93	93	1,65
Sample:	K04C-46	K04C-47	K04C-12	K04C-13	K04C-14	K04C-15	%
Magma b./Loc.:	GVS	GVS	GVS	GVS	GVS	GVS	STD
Latitude (N):	-31,863094	-31,863633	-31,987903	-31,987828	-31,987908	-31,987926	
Longitude (E):	26,302794	26,302487	26,287726	26,287925	26,287948	26,28803	
Altitude (m):	1687	1668	1439	1456	1455	1456	
SiO2 (wt %)	52,09	51,66	52,39	51,98	52,06	51,94	0,09
TiO2 (wt %)	1,08	1,05	1,06	1,03	1,06	1,02	0,80
Al2O3 (wt %)	15,50	15,44	15,54	15,32	15,51	15,46	0,44
Fe2O3(T) (wt %)	11,99	11,83	12,11	12,13	12,14	11,89	0,11
MnO (wt %)	0,19	0,19	0,19	0,19	0,19	0,19	0,00
MgO (wt %)	6,22	6,25	6,24	6,36	6,28	6,38	0,35
CaO (wt %)	10,35	10,37	10,33	10,45	10,33	10,45	0,15
Na2O (wt %)	2,19	2,19	2,24	2,19	2,22	2,18	0,40
K2O (wt %)	0,74	0,65	0,72	0,68	0,72	0,71	0,00
P2O5 (wt %)	0,17	0,17	0,15	0,15	0,16	0,16	6,29
L.O.I	0,1	0,71	0,06	0,06	0,1	0,12	0,00
SUM	100,6	100,5	101,0	100,5	100,8	100,5	0,06
Rb (ppm)	17	16	15	14	16	15	4,09
Nb (ppm)	10	9	8	7	8	7	6,42
Sr (ppm)	200	208	202	198	199	201	0,80
Zr (ppm)	107	108	102	94	102	100	1,68
Y (ppm)	28	29	28	27	27	28	4,25
Co (ppm)	48	49	48	48	48	47	1,20
Cr (ppm)	270	271	282	293	275	296	1,70
Cu (ppm)	108	101	105	107	108	102	0,86
Ni (ppm)	64	69	64	68	62	66	1,26
V (ppm)	296	294	304	295	303	293	1,80
Zn (ppm)	95	98	96	95	93	92	1,65

Sample:	K04C-23	K04C-24	K04C-25	K04C-26	K04C-30	K04C-31	%
Magma b./Loc.:	GVS	GVS	GVS	GVS	GVS	GVS	STD
Latitude (N):	-31,994224	-31,9948	-31,996589	-31,996694	-31,977376	-31,977632	
Longitude (E):	26,272432	26,273533	26,276351	26,276502	26,268863	26,269036	
Altitude (m):	1692	1692	1614	1604	1364	1377	
SiO2 (wt %)	51,69	52,02	52,09	52,03	52,02	52,23	0,09
TiO2 (wt %)	0,95	0,98	1,06	1,06	1,01	1,05	0,80
Al2O3 (wt %)	15,87	15,68	15,45	15,61	15,55	15,67	0,44
Fe2O3(T) (wt %)	11,43	11,57	12,01	12,01	11,73	12,00	0,11
MnO (wt %)	0,18	0,19	0,18	0,18	0,18	0,18	0,00
MgO (wt %)	6,51	6,67	6,30	6,13	6,41	6,28	0,35
CaO (wt %)	10,73	10,67	10,43	10,36	10,49	10,38	0,15
Na2O (wt %)	2,19	2,18	2,30	2,30	2,17	2,24	0,40
K2O (wt %)	0,63	0,67	0,65	0,68	0,70	0,71	0,00
P2O5 (wt %)	0,13	0,14	0,18	0,17	0,15	0,17	6,29
L.O.I	0,09	0	0,22	0,43	0,03	0	0,00
SUM	100,4	100,8	100,9	101,0	100,4	100,9	0,06
Rb (ppm)	13	17	12	16	14	16	4,09
Nb (ppm)	7	8	9	8	7	7	6,42
Sr (ppm)	208	204	201	201	200	201	0,80
Zr (ppm)	90	102	102	97	98	102	1,68
Y (ppm)	25	27	29	29	25	25	4,25
Co (ppm)	47	48	49	49	47	47	1,20
Cr (ppm)	329	306	266	246	287	266	1,70
Cu (ppm)	95	103	111	105	101	103	0,86
Ni (ppm)	75	71	67	65	68	64	1,26
V (ppm)	293	280	294	294	284	294	1,80
Zn (ppm)	90	90	93	100	91	94	1,65
Sample:	K04C-32	K04C-33	K04C-34	K04C-35	K04C-36	K04C-37	%
Magma b./Loc.:	GVS	GVS	GVS	GVS	GVS	GVS	STD
Latitude (N):	-31,977263	-31,977133	-31,977148	-31,977014	-31,975615	-31,974794	
Longitude (E):	26,268909	26,268842	26,26871	26,268636	26,270141	26,26674	
Altitude (m):	1368	1364	1355	1343	1332	1420	
SiO2 (wt %)	52,20	51,93	52,21	52,19	52,41	52,16	0,09
TiO2 (wt %)	0,99	1,02	0,85	0,96	1,05	0,97	0,80
Al2O3 (wt %)	15,64	15,49	15,97	15,68	15,60	15,63	0,44
Fe2O3(T) (wt %)	11,60	12,36	11,32	11,75	12,05	11,86	0,11
MnO (wt %)	0,19	0,19	0,18	0,18	0,19	0,19	0,00
MgO (wt %)	6,79	6,45	6,77	6,28	6,29	6,43	0,35
CaO (wt %)	10,71	10,52	10,95	10,46	10,45	10,43	0,15
Na2O (wt %)	2,16	2,16	2,10	2,15	2,18	2,33	0,40
K2O (wt %)	0,64	0,66	0,57	0,69	0,68	0,67	0,00
P2O5 (wt %)	0,13	0,16	0,12	0,15	0,17	0,15	6,29
L.O.I	0	0	0,03	0,13	0	0	0,00
SUM	101,1	100,9	101,1	100,6	101,1	100,8	0,06
Rb (ppm)	15	15	12	14	15	16	4,09
Nb (ppm)	7	7	6	7	9	7	6,42
Sr (ppm)	198	200	207	206	204	204	0,80
Zr (ppm)	99	93	79	91	101	98	1,68
Y (ppm)	28	26	22	28	30	26	4,25
Co (ppm)	48	50	46	50	49	48	1,20
Cr (ppm)	315	306	276	319	282	295	1,70
Cu (ppm)	103	104	93	106	112	101	0,86
Ni (ppm)	69	70	67	74	67	66	1,26
V (ppm)	295	312	283	282	298	300	1,80
Zn (ppm)	90	95	85	104	95	91	1,65

Sample:	K04C-52	K04K-01	K04K-02	K04K-07	K04K-08	K04K-09	%
Magma b./Loc.:	GVS	MVS	MVS	MVS	MVS	MVS	STD
Latitude (N):	-31,996094	-31,851324	-31,825099	-31,820648	-31,820721	-31,820822	
Longitude (E):	26,282938	26,220757	26,211922	26,195939	26,196055	26,196004	
Altitude (m):	1564	1657	1488	1555	1562	1572	
SiO2 (wt %)	52,08	51,94	51,40	52,08	51,98	52,32	0,09
TiO2 (wt %)	1,04	0,99	0,92	1,05	1,05	1,06	0,80
Al2O3 (wt %)	15,93	15,29	15,60	15,46	15,46	15,49	0,44
Fe2O3(T) (wt %)	11,84	12,10	11,46	12,19	12,04	12,20	0,11
MnO (wt %)	0,18	0,19	0,18	0,19	0,19	0,19	0,00
MgO (wt %)	6,26	6,78	7,11	6,30	6,32	6,34	0,35
CaO (wt %)	10,48	10,66	11,06	10,40	10,37	10,41	0,15
Na2O (wt %)	2,21	2,10	2,11	2,16	2,25	2,20	0,40
K2O (wt %)	0,71	0,63	0,59	0,70	0,70	0,71	0,00
P2O5 (wt %)	0,16	0,16	0,12	0,15	0,15	0,15	6,29
L.O.I	0	0,02	0,2	0	0	0	0,00
SUM	100,9	100,9	100,8	100,7	100,5	101,1	0,06
Rb (ppm)	15	15	15	15	17	15	4,09
Nb (ppm)	7	8	7	9	8	8	6,42
Sr (ppm)	206	206	212	200	203	200	0,80
Zr (ppm)	102	94	83	100	100	96	1,68
Y (ppm)	26	28	25	29	30	26	4,25
Co (ppm)	48	51	51	48	49	50	1,20
Cr (ppm)	280	392	398	272	290	288	1,70
Cu (ppm)	103	109	96	103	115	109	0,86
Ni (ppm)	67	75	81	64	66	68	1,26
V (ppm)	286	310	303	302	298	305	1,80
Zn (ppm)	96	96	89	98	94	97	1,65
Sample:	K04K-10	K04K-11	K04K-12	K04K-13	K04K-14	K04K-15	%
Magma b./Loc.:	MVS	MVS	MVS	MVS	MVS	MVS	STD
Latitude (N):	-31,820895	-31,820991	-31,821118	-31,821386	-31,821403	-31,821591	
Longitude (E):	26,195964	26,195937	26,196166	26,195943	26,195978	26,195927	
Altitude (m):	1575	1579	1587	1600	1609	1611	
SiO2 (wt %)	52,22	52,07	51,67	52,17	52,12	52,30	0,09
TiO2 (wt %)	0,99	1,02	0,92	0,92	0,82	1,05	0,80
Al2O3 (wt %)	15,73	16,02	15,58	15,86	15,41	15,81	0,44
Fe2O3(T) (wt %)	11,65	11,48	12,20	11,58	11,27	11,84	0,11
MnO (wt %)	0,18	0,18	0,20	0,19	0,19	0,18	0,00
MgO (wt %)	6,51	6,04	6,45	6,56	6,75	6,08	0,35
CaO (wt %)	10,65	10,54	10,73	10,75	10,79	10,32	0,15
Na2O (wt %)	2,20	2,44	2,19	2,19	2,25	2,32	0,40
K2O (wt %)	0,66	0,70	0,58	0,61	0,60	0,76	0,00
P2O5 (wt %)	0,13	0,16	0,13	0,14	0,10	0,16	6,29
L.O.I	0	0,06	0,05	0,07	0	0,11	0,00
SUM	100,9	100,7	100,7	101,0	100,3	100,9	0,06
Rb (ppm)	16	16	13	12	13	17	4,09
Nb (ppm)	8	8	8	7	7	7	6,42
Sr (ppm)	205	210	207	199	209	199	0,80
Zr (ppm)	97	96	88	83	83	106	1,68
Y (ppm)	27	26	27	23	23	29	4,25
Co (ppm)	49	45	49	46	47	46	1,20
Cr (ppm)	320	250	346	267	290	248	1,70
Cu (ppm)	105	94	103	90	89	106	0,86
Ni (ppm)	69	60	60	62	66	60	1,26
V (ppm)	300	289	312	281	294	279	1,80
Zn (ppm)	93	91	91	87	86	92	1,65

Sample:	K04K-16	K04K-17	K04K-18	K04K-19	K04K-20	K04K-21	%
Magma b./Loc.:	MVS	MVS	MVS	MVS	MVS	MVS	STD
Latitude (N):	-31,821928	-31,841542	-31,847869	-31,847753	-31,847637	-31,847504	
Longitude (E):	26,196009	26,195615	26,201906	26,206881	26,206876	26,206646	
Altitude (m):	1621	1612	1734	1646	1657	1670	
SiO2 (wt %)	51,98	52,12	51,70	52,00	51,74	51,48	0,09
TiO2 (wt %)	1,06	0,99	1,01	1,02	0,96	0,96	0,80
Al2O3 (wt %)	15,58	15,95	15,54	15,56	15,41	15,00	0,44
Fe2O3(T) (wt %)	12,03	11,67	11,67	12,09	11,80	11,97	0,11
MnO (wt %)	0,18	0,18	0,18	0,19	0,19	0,19	0,00
MgO (wt %)	6,23	6,20	6,68	6,37	6,82	6,95	0,35
CaO (wt %)	10,34	10,57	10,65	10,49	10,72	10,80	0,15
Na2O (wt %)	2,22	2,26	2,18	2,19	2,33	2,05	0,40
K2O (wt %)	0,71	0,67	0,65	0,68	0,63	0,61	0,00
P2O5 (wt %)	0,17	0,15	0,14	0,16	0,14	0,15	6,29
L.O.I	0,08	0,16	0,03	0,12	0	0,09	0,00
SUM	100,6	100,9	100,4	100,9	100,7	100,3	0,06
Rb (ppm)	15	16	17	15	15	13	4,09
Nb (ppm)	7	7	7	7	7		6,42
Sr (ppm)	197	204	209	210	211	201	0,80
Zr (ppm)	98	90	100	96	90	85	1,68
Y (ppm)	28	27	30	26	25	26	4,25
Co (ppm)	47	48	48	50	50	50	1,20
Cr (ppm)	260	274	332	298	348	366	1,70
Cu (ppm)	105	101	106	104	105	98	0,86
Ni (ppm)	65	65	73	69	76	80	1,26
V (ppm)	286	288	302	300	305	298	1,80
Zn (ppm)	95	92	92	98	92	93	1,65

Sample:	K04K-23	K04K-24	K04K-25	K04K-26	K04K-27	K04K-27	%
Magma b./Loc.:	MVS	MVS	MVS	MVS	MVS	MVS	STD
Latitude (N):	-31,847572	-31,847618	-31,847837	-31,846034	-31,846576	-31,846576	
Longitude (E):	26,206302	26,206043	26,205289	26,20958	26,216795	26,216795	
Altitude (m):	1694	1707	1711	1631	1646	1645,65	
SiO2 (wt %)	51,67	51,72	52,18	51,77	51,80	51,73	0,09
TiO2 (wt %)	0,99	1,00	0,99	1,00	1,01	1,00	0,80
Al2O3 (wt %)	15,43	15,52	15,29	15,47	15,15	15,56	0,44
Fe2O3(T) (wt %)	11,74	11,67	11,99	11,84	12,02	11,92	0,11
MnO (wt %)	0,18	0,18	0,20	0,19	0,19	0,19	0,00
MgO (wt %)	6,70	6,79	6,82	6,49	6,59	6,56	0,35
CaO (wt %)	10,59	10,63	10,63	10,55	10,49	10,63	0,15
Na2O (wt %)	2,12	2,20	2,12	2,19	2,21	2,18	0,40
K2O (wt %)	0,66	0,66	0,65	0,68	0,69	0,63	0,00
P2O5 (wt %)	0,17	0,13	0,14	0,14	0,12	0,14	6,29
L.O.I	0,11	0,03	0,15	0,18	0,06	0,14	0,00
SUM	100,4	100,5	101,2	100,5	100,3	100,7	0,06
Rb (ppm)	15	17	15	17	16	15	4,09
Nb (ppm)	8	8	7	7	9	8	6,42
Sr (ppm)	194	203	200	201	203	197	0,80
Zr (ppm)	93	99	87	101	96	90	1,68
Y (ppm)	27	27	24	27	29	24	4,25
Co (ppm)	49	49	50	49	52	49	1,20
Cr (ppm)	328	323	345	305	354	301	1,70
Cu (ppm)	97	104	105	107	109	101	0,86
Ni (ppm)	75	75	77	71	73	70	1,26
V (ppm)	284	306	299	289	303	296	1,80
Zn (ppm)	92	91	97	94	97	96	1,65

Sample:	K04K-28	K04K-29	K04K-30	K04K-31	K04K-32	K04K-33	%
Magma b./Loc.:	MVS	MVS	MVS	MVS	MVS	MVS	STD
Latitude (N):	-31,847568	-31,834978	-31,833031	-31,839595	-31,837295	-31,837377	
Longitude (E):	26,216467	26,198255	26,205633	26,232880	26,235059	26,232203	
Altitude (m):	1653	1580	1601	1580.52	1588.45	1591.34	
SiO2 (wt %)	51,95	51,61	52,39	51,92	51,78	52,16	0,09
TiO2 (wt %)	1,03	1,05	1,03	1,08	1,04	0,98	0,80
Al2O3 (wt %)	15,88	15,43	15,48	15,72	15,45	15,68	0,44
Fe2O3(T) (wt %)	11,65	12,17	12,04	11,97	11,96	11,64	0,11
MnO (wt %)	0,18	0,19	0,19	0,19	0,19	0,19	0,00
MgO (wt %)	6,36	6,32	6,31	6,08	6,26	6,27	0,35
CaO (wt %)	10,51	10,43	10,34	10,23	10,48	10,44	0,15
Na2O (wt %)	2,23	2,20	2,25	2,32	2,28	2,30	0,40
K2O (wt %)	0,69	0,70	0,71	0,73	0,69	0,70	0,00
P2O5 (wt %)	0,17	0,17	0,16	0,16	0,15	0,14	6,29
L.O.I	0,12	0,02	0,17	0,1	0,04	0,1	0,00
SUM	100,8	100,3	101,1	100,5	100,3	100,6	0,06
Rb (ppm)	16	14	17	16	15	16	4,09
Nb (ppm)	7	8	9	9	8	8	6,42
Sr (ppm)	202	207	212	207	201	205	0,80
Zr (ppm)	97	101	102	106	97	102	1,68
Y (ppm)	28	28	28	33	27	29	4,25
Co (ppm)	47	48	48	50	47	48	1,20
Cr (ppm)	289	260	254	279	264	258	1,70
Cu (ppm)	103	108	106	114	100	105	0,86
Ni (ppm)	69	65	61	60	64	62	1,26
V (ppm)	286	292	292	296	297	292	1,80
Zn (ppm)	92	95	95	101	94	93	1,65
Sample:	K04K-34	K04K-35	K04K-36	K04K-37	K04K-38	K04K-39	%
Magma b./Loc.:	MVS	MVS	MVS	MVS	MVS	MVS	STD
Latitude (N):	-31,844804	-31,845305	-31,826017	-31,826477	-31,841271	-31,850484	
Longitude (E):	26,227736	26,229411	26,230976	26,234055	26,218479	26,221734	
Altitude (m):	1587.25	1576.44	1674.01	1695.40	1656.47	1668.00	
SiO2 (wt %)	51,96	52,09	51,61	51,54	51,71	51,84	0,09
TiO2 (wt %)	1,03	1,03	0,99	0,97	0,96	1,04	0,80
Al2O3 (wt %)	15,24	15,48	15,43	15,57	15,80	15,61	0,44
Fe2O3(T) (wt %)	11,95	11,96	11,78	11,40	12,24	11,81	0,11
MnO (wt %)	0,19	0,19	0,18	0,18	0,19	0,19	0,00
MgO (wt %)	6,48	6,32	6,65	6,51	6,67	6,76	0,35
CaO (wt %)	10,41	10,54	10,70	10,63	10,72	10,60	0,15
Na2O (wt %)	2,21	2,18	2,14	2,23	2,12	2,36	0,40
K2O (wt %)	0,70	0,67	0,67	0,66	0,59	0,67	0,00
P2O5 (wt %)	0,15	0,16	0,16	0,14	0,12	0,15	6,29
L.O.I	0,16	0,12	0,05	0,19	0	0	0,00
SUM	100,5	100,7	100,4	100,0	101,1	101,0	0,06
Rb (ppm)	17	15	16	17	13	15	4,09
Nb (ppm)	8	7	8	8	8	9	6,42
Sr (ppm)	206	205	200	206	203	201	0,80
Zr (ppm)	104	97	96	96	86	101	1,68
Y (ppm)	30	26	27	28	26	27	4,25
Co (ppm)	50	48	48	48	50	49	1,20
Cr (ppm)	282	251	341	319	320	320	1,70
Cu (ppm)	113	103	97	107	101	106	0,86
Ni (ppm)	67	64	77	74	74	74	1,26
V (ppm)	293	308	283	289	303	302	1,80
Zn (ppm)	97	93	92	91	94	94	1,65

Sample:	K04K-40	K04K-41	K04K-42	K04K-43	K04K-44	K04K-45	%
Magma b./Loc.:	MVS	MVS	MVS	MVS	MVS	MVS	STD
Latitude (N):	-31.852338	-31.855888	-31,8201087	-31,8235045	-31,8245638	-31,8281289	
Longitude (E):	26.220092	26.217240	26,2179908	26,216669	26,2176725	26,2241824	
Altitude (m):	1671.37	1684.82	1462.04	1497.85	1524	1545	
SiO2 (wt %)	52,13	52,03	52,03	51,63	51,42	51,92	0,09
TiO2 (wt %)	1,03	1,01	1,03	0,82	0,91	0,94	0,80
Al2O3 (wt %)	15,71	15,54	15,89	16,43	15,60	16,15	0,44
Fe2O3(T) (wt %)	11,80	11,82	11,64	10,45	11,33	11,32	0,11
MnO (wt %)	0,19	0,19	0,18	0,17	0,18	0,18	0,00
MgO (wt %)	6,32	6,60	6,25	6,96	6,83	6,35	0,35
CaO (wt %)	10,40	10,53	10,53	11,33	10,80	10,70	0,15
Na2O (wt %)	2,26	2,20	2,26	2,19	2,22	2,28	0,40
K2O (wt %)	0,71	0,67	0,72	0,57	0,60	0,66	0,00
P2O5 (wt %)	0,17	0,15	0,16	0,11	0,12	0,12	6,29
L.O.I	0,18	0	0,09	0,03	0,55	0	0,00
SUM	100,9	100,7	100,8	100,7	100,6	100,6	0,06
Rb (ppm)	16	18	16	12	16	17	4,09
Nb (ppm)	8	8	9	6	8	7	6,42
Sr (ppm)	200	197	203	208	202	212	0,80
Zr (ppm)	98	102	103	80	87	92	1,68
Y (ppm)	27	29	28	21	23	56	4,25
Co (ppm)	47	49	48	45	48	47	1,20
Cr (ppm)	281	286	284	338	309	308	1,70
Cu (ppm)	103	108	101	84	102	101	0,86
Ni (ppm)	67	66	69	81	71	71	1,26
V (ppm)	286	297	302	274	300	285	1,80
Zn (ppm)	94	93	95	79	89	91	1,65
Sample:	K04K-46	K04K-47	K04K-48	K04K-49	K04K-06	K04C-01	%
Magma b./Loc.:	MVS	MVS	MVS	MVS	L1	s1	STD
Latitude (N):	-31,8324564	-31,8338917	-31,8363638	-31,8395138	-31,8168	-31,9754	
Longitude (E):	26,223367	26,2262388	26,2262002	26,2155426	26,1975	26,2718	
Altitude (m):	1526	1528	1542	1599	1440	1335	
SiO2 (wt %)	52,56	52,19	51,75	52,24	52,27	51,42	0,09
TiO2 (wt %)	1,15	0,99	1,03	1,08	1,05	0,94	0,80
Al2O3 (wt %)	16,04	15,74	15,59	15,70	16,51	15,82	0,44
Fe2O3(T) (wt %)	11,75	11,58	11,96	11,98	10,96	11,17	0,11
MnO (wt %)	0,18	0,18	0,19	0,19	0,17	0,17	0,00
MgO (wt %)	5,50	6,10	6,26	6,01	6,40	7,12	0,35
CaO (wt %)	10,01	10,45	10,45	10,24	10,02	10,92	0,15
Na2O (wt %)	2,48	2,30	2,24	2,26	2,38	2,13	0,40
K2O (wt %)	0,81	0,71	0,71	0,75	0,72	0,44	0,00
P2O5 (wt %)	0,16	0,14	0,18	0,19	0,18	0,13	6,29
L.O.I	0,17	0,11	0,08	0,13	0,64	0,52	0,00
SUM	100,8	100,5	100,4	100,8	101,3	100,8	0,06
Rb (ppm)	18	16	18	17	18	13	4,09
Nb (ppm)	8	7	7	7	9	6	6,42
Sr (ppm)	214	209	204	208	247	193	0,80
Zr (ppm)	111	100	93	104	77	77	1,68
Y (ppm)	30	28	26	29	23	23	4,25
Co (ppm)	46	47	48	49	47	50	1,20
Cr (ppm)	178	220	275	252	222	518	1,70
Cu (ppm)	119	108	102	110	93	101	0,86
Ni (ppm)	50	58	64	63	87	112	1,26
V (ppm)	295	294	297	302	270	273	1,80
Zn (ppm)	97	92	94	99	89	90	1,65

Sample:	KO4-AA11	KO4 AA-12	KO4 AA-13	KO4 AA-14	KO4 AA-15	KO4 AA-16	%
Magma b./Loc.:	GVS	GVS	GVS	GVS	GVS	GVS	STD
Latitude (N):							
Longitude (E):							
Altitude (m):							
SiO2 (wt %)	52,64	52,31	52,02	51,44	51,57	52,03	0,09
TiO2 (wt %)	1,05	0,97	0,92	0,93	0,95	0,96	0,80
Al2O3 (wt %)	16,07	15,28	16,20	15,57	15,36	16,09	0,44
Fe2O3(T) (wt %)	11,83	11,80	10,99	11,41	11,67	11,16	0,11
MnO (wt %)	0,19	0,19	0,17	0,18	0,18	0,18	0,00
MgO (wt %)	5,71	6,42	6,65	6,98	7,13	6,58	0,35
CaO (wt %)	10,09	10,37	10,86	10,89	10,81	10,76	0,15
Na2O (wt %)	2,34	2,18	2,23	2,14	2,12	2,26	0,40
K2O (wt %)	0,73	0,71	0,64	0,60	0,61	0,64	0,00
P2O5 (wt %)	0,16	0,16	0,15	0,13	0,13	0,15	6,29
L.O.I	0,10	0,19	0,11	0	0,02	0,09	0,00
SUM	100,9	100,6	100,9	100,3	100,6	100,9	0,06
Rb (ppm)	12	16	14	15	16	15	4,09
Nb (ppm)	9	7	7	6	8	6	6,42
Sr (ppm)	231	198	207	198	196	206	0,80
Zr (ppm)	98	101	90	89	87	88	1,68
Y (ppm)	29	26	24	21	22	24	4,25
Co (ppm)	47	48	45	48	49	46	1,20
Cr (ppm)	193	269	346	362	384	341	1,70
Cu (ppm)	111	98	83	92	95	91	0,86
Ni (ppm)	49	63	77	81	84	76	1,26
V (ppm)	311	280	273	274	286	286	1,80
Zn (ppm)	95	94	85	89	92	89	1,65
Sample:	KO4 AA-17	KO4 AA-19	KO4 AA-20	KO4 AA-21	KO4 AA-22	KO4 AA-23	%
Magma b./Loc.:	GVS	GVS	GVS	GVS	GVS	GVS	STD
Latitude (N):							
Longitude (E):							
Altitude (m):							
SiO2 (wt %)	51,82	51,75	52,24	52,47	52,19	51,43	0,09
TiO2 (wt %)	1,01	0,98	0,97	1,01	1,10	0,93	0,80
Al2O3 (wt %)	15,87	15,85	16,38	15,89	15,72	16,01	0,44
Fe2O3(T) (wt %)	11,66	11,44	11,33	11,61	12,11	11,29	0,11
MnO (wt %)	0,18	0,18	0,18	0,19	0,19	0,17	0,00
MgO (wt %)	6,44	6,71	6,11	5,86	5,94	6,51	0,35
CaO (wt %)	10,64	10,88	10,55	10,39	10,23	10,85	0,15
Na2O (wt %)	2,18	2,18	2,28	2,32	2,31	2,20	0,40
K2O (wt %)	0,68	0,63	0,67	0,76	0,74	0,62	0,00
P2O5 (wt %)	0,15	0,14	0,17	0,17	0,17	0,14	6,29
L.O.I	0,15	0	0,1	0,12	0	0,11	0,00
SUM	100,8	100,7	101,0	100,8	100,7	100,3	0,06
Rb (ppm)	17	14	16	15	13	13	4,09
Nb (ppm)	7	6	6	7	9	7	6,42
Sr (ppm)	204	207	212	211	203	205	0,80
Zr (ppm)	96	93	98	101	100	88	1,68
Y (ppm)	25	26	27	28	28	25	4,25
Co (ppm)	45	47	45	45	48	46	1,20
Cr (ppm)	296	317	278	250	247	312	1,70
Cu (ppm)	102	95	96	105	109	93	0,86
Ni (ppm)	69	74	65	57	61	72	1,26
V (ppm)	277	278	278	275	294	277	1,80
Zn (ppm)	90	87	91	95	98	87	1,65

Sample:	KO4 AA-24	KO4 AA-25	KO4 AA-26	KO4 AA-27	KO4 AA-28	K04C-02	%
Magma b./Loc.:	P 18	P 18	P 18	P 18	P 18	s1	STD
Latitude (N):						-31,9741	
Longitude (E):						26,2734	
Altitude (m):						1333	
SiO2 (wt %)	51,28	51,71	52,02	51,92	51,69	51,07	0,09
TiO2 (wt %)	0,97	0,99	0,97	0,99	0,92	0,94	0,80
Al2O3 (wt %)	15,88	15,54	15,40	15,68	15,84	15,64	0,44
Fe2O3(T) (wt %)	11,40	11,81	11,92	11,72	11,44	11,10	0,11
MnO (wt %)	0,18	0,19	0,19	0,18	0,18	0,18	0,00
MgO (wt %)	6,92	6,90	6,97	6,39	6,60	7,32	0,35
CaO (wt %)	11,09	10,72	10,65	10,64	10,87	11,11	0,15
Na2O (wt %)	2,10	2,05	2,06	2,19	2,15	2,05	0,40
K2O (wt %)	0,58	0,64	0,64	0,70	0,63	0,13	0,00
P2O5 (wt %)	0,14	0,15	0,14	0,17	0,14	0,12	6,29
L.O.I	0	0,06	0,15	0	0	0,94	0,00
SUM	100,5	100,8	101,1	100,6	100,5	100,6	0,06
Rb (ppm)	14	15	15	14	14	n.d	4,09
Nb (ppm)	6	7	8	7	7	6	6,42
Sr (ppm)	201	200	195	207	205	227	0,80
Zr (ppm)	82	87	89	97	88	79	1,68
Y (ppm)	24	25	26	24	24	25	4,25
Co (ppm)	47	47	50	46	46	53	1,20
Cr (ppm)	355	351	341	276	326	433	1,70
Cu (ppm)	95	98	100	105	94	106	0,86
Ni (ppm)	80	76	82	66	74	121	1,26
V (ppm)	293	299	297	276	276	260	1,80
Zn (ppm)	88	92	92	90	87	91	1,65
Sample:	K04C-03	K04C-04	K04C-05	K04C-10	K04C-51	K04C-59	%
Magma b./Loc.:	s1	s1	d1	d2	s2	d3	STD
Latitude (N):	-31,9741	-31,9741	-31,9117	-31,7909	-31,9984	-31,8591	
Longitude (E):	26,2738	26,2738	26,1131	26,2331	26,2808	26,1693	
Altitude (m):	1324	1324	1226	1359	1470	1243	
SiO2 (wt %)	51,51	51,31	51,83	51,45	51,78	51,83	0,09
TiO2 (wt %)	0,94	0,94	1,00	0,97	1,04	1,04	0,80
Al2O3 (wt %)	15,90	15,91	15,17	15,43	15,74	15,39	0,44
Fe2O3(T) (wt %)	10,53	11,19	11,04	10,83	11,89	11,90	0,11
MnO (wt %)	0,16	0,18	0,18	0,32	0,19	0,19	0,00
MgO (wt %)	6,88	7,10	7,23	6,98	6,17	6,40	0,35
CaO (wt %)	11,12	10,94	10,73	10,83	10,61	10,50	0,15
Na2O (wt %)	2,08	2,06	2,22	2,07	2,09	2,24	0,40
K2O (wt %)	0,12	0,23	0,39	0,35	0,37	0,67	0,00
P2O5 (wt %)	0,11	0,15	0,14	0,13	0,16	0,16	6,29
L.O.I	1,42	0,92	0,73	1,44	0,83	0,4	0,00
SUM	100,8	100,9	100,7	100,8	100,9	100,7	0,06
Rb (ppm)	b.d.	5	8	7	5	16	4,09
Nb (ppm)	5	5	7	7	7	8	6,42
Sr (ppm)	267	233	225	234	209	206	0,80
Zr (ppm)	76	73	82	77	107	107	1,68
Y (ppm)	24	23	26	26	29	30	4,25
Co (ppm)	51	53	51	54	53	50	1,20
Cr (ppm)	469	450	426	436	263	277	1,70
Cu (ppm)	104	99	98	98	107	111	0,86
Ni (ppm)	111	120	89	109	70	69	1,26
V (ppm)	283	271	271	254	297	307	1,80
Zn (ppm)	93	92	98	93	100	99	1,65

Sample:	K04C-60	K04C-49	K04C-50	%
Magma b./Loc.:	d3	d4	d4	STD
Latitude (N):	-31,8591	-31,9990	-31,9990	
Longitude (E):	26,1693	26,2816	26,2816	
Altitude (m):	1243	1421	1421	
SiO2 (wt %)	52,14	49,45	51,02	0,09
TiO2 (wt %)	1,05	1,03	1,02	0,80
Al2O3 (wt %)	15,65	17,58	16,38	0,44
Fe2O3(T) (wt %)	11,79	11,84	11,56	0,11
MnO (wt %)	0,19	0,14	0,20	0,00
MgO (wt %)	6,30	6,01	5,96	0,35
CaO (wt %)	10,59	7,65	10,34	0,15
Na2O (wt %)	2,15	2,43	2,21	0,40
K2O (wt %)	0,62	0,53	0,59	0,00
P2O5 (wt %)	0,16	0,17	0,16	6,29
L.O.I	0,8	3,69	1,35	0,00
SUM	101,4	100,5	100,8	0,06
Rb (ppm)	15	12	11	4,09
Nb (ppm)	9	9	8	6,42
Sr (ppm)	209	349	223	0,80
Zr (ppm)	113	113	106	1,68
Y (ppm)	30	34	28	4,25
Co (ppm)	49	59	53	1,20
Cr (ppm)	255	211	210	1,70
Cu (ppm)	117	116	110	0,86
Ni (ppm)	71	90	84	1,26
V (ppm)	296	387	307	1,80
Zn (ppm)	97	114	103	1,65

These analyses have been completed by standard XRF techniques at the University of Bergen (Norway).